Site directed mutagenesis of the E. coli MDH structural gene with an aim to improving EMIT

Murray, James Hamer

Award date:
1993

Awarding institution:
University of Bath

SITE DIRECTED MUTAGENESIS OF THE *E.COLI* MDH STRUCTURAL GENE WITH AN AIM TO IMPROVING EMIT.

Submitted by James Hamer Murray

for the degree of Ph.D. of the

University of Bath 1993.

James Hamer Murray.

ProQuest LLC
789 East Eisenhower Parkway
P.O. Box 1346
Ann Arbor, MI 48106-1346

ACKNOWLEDGEMENTS.

I would like to thank my supervisor, Dr. Paul Towner and industrial supervisor Dr. Andrew Garman for their help and encouragement throughout the project. Thanks are also due to the people in the "middle " and molecular graphics labs notably, Dr. P Harris and Dr. J Pedersen for their help and support during my Ph. D. I would also like to thank Dr. R Eisenthal for his assistance with the enzyme kinetics and Dr. K.-D. Entian for the *Escherichia coli* strain W945T1-2 and malate dehydrogenase clone. This project has been jointly funded by the SERC and ICI Diagnostics.

ABSTRACT.

An attempt was made to improve the sensitivity and efficiency of the Enzyme Multiplied Immumoassay Technique by introducing a specific cysteine residue into *Escherichia coli* malate dehydrogenase to act as a unique ligand coupling site. The structural gene encoding dimeric *Escherichia coli* malate dehydrogenase encodes three reduced cysteines per identical subunit at residues 109, 113 and 251. Initial attempts to produce a malate dehydrogenase devoid of cysteines by site directed mutagenesis were unsuccessful.

Conserved substitution of cysteine to serine were made to the codons at positions 113 and 109, singly and in tandem to produce two mutant malate dehydrogenases. The gene encoding the single substitution of cysteine 113 (pUC113S) when expressed in an *Escherichia coli* strain which is devoid of malate dehydrogenase, produced a malate dehydrogenase which was comparable in activity to that observed for wild type *Escherichia coli* malate dehydrogenase. The gene encoding substitutions to cysteines 109 and 113 (pUC109S/113S), resulted in low levels of expressed malate dehydrogenase with a specific activity of only 5% of the wild type.

Amino acid sequence alignment of malate dehydrogenases and analysis of the crystal structure of porcine cytoplasmic malate dehydrogenase indicated that arginine 81, glycine 84 and leucine 90 of the βDαD surface loop would be solvent accessible in the *Escherichia coli* malate dehydrogenase. Substitution of these residues to cysteine resulted in the absence of malate dehydrogenase activity.

Model building of the *Escherichia coli* malate dehydrogenase using the porcine malate dehydrogenase as a template indicated that threonine 64 and serine 222 were suitable sites for substitution to cysteine. Expression of the malate dehydrogenase with threonine 64 substituted for cysteine resulted in a low level of the malate

dehydrogenase in the cell-extract and a specific activity similar to that observed for the wild type malate dehydrogenase. The Km for coenzyme and substrate (oxaloacetate) for this mutant was similar to that observed for the wild type malate dehydrogenase. Attempts to derivatize the introduced cysteine with DTNB were unsuccessful.

Expression of malate dehydrogenase with serine 222 substituted for cysteine (222C) resulted in similar levels of expression as that observed for wild type. However, 222C malate dehydrogenase had a specific activity of only 3.5% of that observed for the wild type enzyme with an increased Km for substrate (oxaloacetate) of 0.94 mM as opposed to 0.04 mM. Attempts to derivatize the introduced thiol groups resulted in a decrease in the activity of the enzyme in excess of 95% making this enzyme unsuitable for use in the Enzyme Multiplied Immunoassay Technique.

CONTENTS.

		Page
Title.		I
Acknowledgements.		II
Abstract.		III
CHAPTER ONE: INTRODUCTION.		
1.1	**Recombinant DNA technology.**	1
1.2.	**The enzyme multiplied immunoassay technique (EMIT).**	2
1.3	**Malate dehydrogenase.**	6
1.4	**Aims of the project.**	8
1.5	**Homology modelling of *E.coli* MDH.**	10
1.6	**The *E.coli* MDH.**	11
1.6.1	*E. coli* MDH structural gene.	11
1.6.2	Comparison of the secondary, tertiary and quaternary structures of *E.coli* and porcine cytoplasmic MDH.	14
1.6.3	Binding of coenzyme and substrate in the active site of MDH.	18
1.7	**The action of MDH in catalysis.**	20
1.8	**Derivatization of MDH.**	23
1.9	**Substitution of codons in the MDH gene.**	25
1.10	**Purification of *E.coli* MDH.**	26
CHAPTER TWO: MATERIALS, EQUIPMENT AND METHODS.		
2.1	**Materials.**	29
2.2	**Equipment.**	30

2.3 ***E.coli* Strains and Culture conditions.** 31

2.4 **General reagents.** 32

2.5 **General Methods.** 33

2.5.1 Quantification of DNA. 33

2.5.2 Extraction of DNA with organic solvents. 33

2.5.2.1 Phenol/Chloroform extraction of DNA. 33

2.5.2.2 Diethyl ether extraction of DNA. 33

2.5.3. Precipitation of DNA using ethanol or isopropanol. 34

2.5.3.1 Precipitation of DNA using ethanol. 34

2.5.3.2 Precipitation of DNA using isopropanol. 34

2.5.4 Purification of DNA on "mini" spun columns. 34

2.5.4.1 Sepharose CL6-B spun columns. 34

2.5.4.2 Sephadex G-25 and G-50 spun columns. 35

2.5.5 Agarose gel electrophoresis. 35

2.5.6 Isolation of DNA from agarose gels. 36

2.5.6.1 Freeze-squeeze. 36

2.5.6.2 Geneclean. 36

2.5.7 Restriction digestion of DNA. 37

2.5.8 Ligation of DNA. 37

2.5.9 End-fill of recessed 3' end of DNA. 37

2.6 **DNA Methods.** 38

2.6.1 Manipulation of *E.coli* cultures. 38

2.6.2 Preparation of *E.coli* competent cells. 38

2.6.3 Transformation of *E.coli* competent cells with plasmid and RF M13 DNA. 39

2.6.3.1 Transformation of *E.coli* TG1 and W945T1-2 cells with Plasmid DNA. 39

2.6.3.2 Transformation of *E.coli* TG1 with RF M13 DNA. 39

2.6.4 Preparation of phage stocks. 39

2.6.5 Small scale preparation of plasmid and RF M13 DNA. 40

2.6.5.1 Plasmid DNA. 40

2.6.5.2 RF M13 DNA. 40

2.6.6 Large scale preparation of plasmid and RF M13 DNA. 41

2.6.6.1 Plasmid DNA. 41

2.6.6.2 RF M13 DNA. 42

2.6.7 Preparation of single stranded M13 DNA template. 42

2.6.7.1 Small scale preparation of template DNA. 42

2.6.7.2 Large scale preparation of template DNA. 43

2.6.8 Purification of DNA using a Nensorb column. 44

2.6.9 Purification of DNA using a Qiagen column. 44

2.6.10 Caesium chloride equilibrium density gradient centrifugation. 45

2.6.11 Preparation of oligonucleotides. 46

2.6.11.1 Design of oligonucleotides. 46

2.6.11.2 Synthesis and purification of oligonucleotides. 46

2.6.11.3 5' End labelling of oligonucleotides with T4 Polynucleotide Kinase. 47

2.6.11.4 Determination of size and purity of oligonucleotide. 47

2.6.12 Sequencing of DNA. 48

2.6.13 Polyacrylamide gel electrophoresis (sequencing gel). 49

2.6.14 Site directed mutagenesis of the *E.coli* MDH gene. 50

2.6.14.1 Mutagenesis of the *E.coli* MDH gene using the Amersham Oligonucleotide-directed *in vitro* mutagenesis system. 50

2.6.14.2 Mutagenesis of the *E.coli* MDH gene using the PCR. 51

2.6.15 Colony hybridisation. 51

2.7 Expression and purification of MDH. 53

2.7.1 Expression and purification of plasmid encoded MDH. 53

2.7.1.1 Preparation of Procion red H3-B/CL6-B matrix. 53

2.7.1.2 Preparation of modified Sepharose CL6-B matrix containing thiol groups. 54

2.7.2 Preparation of cell-free extracts of plasmid encoded MDH. 55
2.7.2.1 Small scale preparation of cell-free extract. 55
2.7.2.2 Large scale preparation of cell-free extract. 56
2.7.3 Purification of MDH. 57
2.7.3.1 Method I. 57
2.7.3.2 Purification of *E.coli* MDH by precipitation of proteins with ammonium sulphate. 57
2.7.3.3 Purification of *E.coli* MDH by Procion red/CL6-B affinity chromatography. 58
2.7.3.4 Purification of *E.coli* MDH using modified Sepharose CL6-B matrix containing thiol groups. 58
2.7.4 Estimation of protein concentration. 58
2.7.5 SDS-polyacrylamide gel electrophoresis. 59
2.7.6 Determination of the properties of wild type and mutant MDH. 60
2.7.7 Derivatization of MDH with DTNB and N-ethylmaleimide. 60
2.7.7.1 Derivatization of MDH with DTNB. 60
2.7.7.2 Derivatization of MDH with N-ethylmaleimide. 60
2.7.8 Iso-electric focussing of MDH. 62
2.8 **Homology modelling of *E.coli* MDH.** 62

CHAPTER THREE: PURIFYING *E.COLI* WILD TYPE MDH.

3.1 **Introduction.** 65
3.2.1 Purification of *E.coli* MDH using ammonium sulphate. 65
3.2.2 Purification of *E.coli* MDH by Procion red H3-B affinity chromatography. 66
3.2.3 Purification of pUCWT MDH. 66
3.3 **Discussion.** 70

CHAPTER FOUR: SUBSTITUTION OF ENDOGENOUS CYSTEINES IN *E.COLI* WILD TYPE MDH.

4.1	**Introduction.**	71
4.2.1	Substitution of the cysteine 113 codon (113S).	71
4.2.2	Screening for the mutation in the codon for cysteine 113 (113S).	73
4.2.3	Purification of pUC113S MDH.	73
4.3.1	Substitution of the codons for cysteines 109 and 113 (109S/113S).	79
4.3.2	Screening for the substitutions in the codons for cysteine 109 and 113 (109S/113S).	79
4.3.3	Purification of pUC109S/113S.	82
4.4.1	Substitution of the cysteine codons 109, 113 and 251 (109S/113S/251S).	82
4.4.2	Screening for the substitutions for the codons of cysteines 109, 113 and 251 (109S/113S/251S).	87
4.5.1	Substitution of the cysteine codon 251 (251S).	91
4.6	**Discussion.**	91

CHAPTER FIVE: SUBSTITUTION OF CYSTEINES INTO THE *E.COLI* MDH βD/αD SURFACE LOOP.

5.1	**Introduction.**	97
5.2.1	Substitution of the codons for arginine 81, glycine 84 and leucine 90.	97
5.2.2	Screening for the substitutions in the codons for arginine 81, glycine 84 and leucine 90.	99
5.2.3	Purification of pUC109S/113S/81C, pUC109S/113S/84C and pUC109S/113S/90C MDHs.	99
5.3	**Discussion.**	103

CHAPTER SIX: HOMOLOGY MODELLING OF *E.COLI* MDH.

6.1 **Amino acid sequence alignment.** 106

6.2 ***E.coli* MDH model.** 109

6.3 **Identification of suitable residues for substitution to cysteine.** 114

6.4 **Appraisal of the of model.** 115

6.5 **Discussion.** 122

CHAPTER SEVEN: SUBSTITUTION OF THREONINE 64 AND SERINE 222 FOR CYSTEINES IN *E.COLI* WILD TYPE MDH.

7.1 **Introduction.** 123

7.2.1 Screening for the substitution in the codon for threonine 64 (64C). 123

7.2.2 Purification of pUC64C MDH. 128

7.3.1 Screening for the substitutions of the codon for serine 222 (222C). 128

7.3.2 Purification of pUC222C MDH. 133

7.4 **Derivatization of MDH.** 133

7.5 **Kinetic studies on wild type, mutant 64C and 222C MDHs.** 141

7.6.1 Increasing the yield of mutant 222C MDH. 145

7.6.2 Screening for the substitution in 222C. 145

7.6.3 Purification of pMEX222C MDH. 150

7.7 **Discussion.** 150

7.7.1 Substitution of threonine 64 to cysteine. 152

7.7.2 Conclusion. 153

7.7.3 Substitution of serine 222 to cysteine. 154

7.7.4 Conclusion. 158

CHAPTER EIGHT: IMPLICATIONS OF RESULTS ON EMIT.

8.1 **Implications of results on EMIT.** 159

References. 161

Abbreviations. 170

Appendix A : Restriction endonucleases with restriction endonuclease recognition sites. 174

Appendix B: Restriction map of pUC19 and location of restriction endonuclease sites. 175

Appendix C: Sense and anti-sense codon table. 176

Appendix D: Table of oligonucleotides. 177

Appendix E: Properties of Amino acids. 180

Appendix F: Ammonium sulphate addition table. 183

CHAPTER ONE:

INTRODUCTION.

(1.1) Recombinant DNA technology.

Gene cloning, whereby a fragment of DNA to be cloned is inserted into a circular DNA molecule called a vector to produce a recombinant DNA molecule, has led to extraordinary advances in molecular biology and biochemistry. The recombinant DNA molecule when inserted into host cells multiplies to produce numerous copies of itself (cloned gene). When the inserted DNA fragment encodes a protein, the host can often be made to produce the protein in large quantities.

Techniques have been developed which enable manipulation of the DNA insert and subsequent modification of the expressed protein. Until recently these techniques have been primarily used for the elucidation of the structure and function relationship of residues in proteins. For example Wilks *et al*, (1992) replaced a surface polypeptide loop in lactate dehydrogenase with longer and shorter polypeptides and ascertained the effect of substitution upon catalysis. This technique is now being employed in such diverse fields as protein purification, biosensors and therapeutic proteins. Persson *et al*, (1990) incorporated cysteines into glucose dehydrogenase enabling rapid purification from cell-extracts using thiol-affinity chromatography. Bülow and Mosbach, (1991) have developed polyfunctional enzymes via gene fusion. The gene encoding human insulin, which is responsible for controlling blood glucose level, has been synthesised and expressed in *Escherichia coli* (*E.coli*) (Goedall *et al*, 1979). This has enabled the production of large amounts of insulin suitable for the treatment of diabetes mellitus. It is now feasible to design and express monoclonal antibodies with defined antigen specificity which has been determined by manipulation of the gene sequence encoding the antibody variable domain polypeptide sequence (Winter and Milstein, 1991). Antibodies have also been "humanised" whereby epitopes on the

antibody surface which are recognised as "foreign" by the recipient of the antibody are removed to produce a non-immunogenic antibody (Sandhu, 1992). Diagnostic assays often require enzymes. Enzymes such as DNA polymerase which is used in the polymerase chain reaction (PCR) are produced via recombinant DNA technology, and have been modified to improve their efficiency by gene manipulation. Some enzymes like malate dehydrogenase (MDH), lysozyme and glucose-6-phosphate dehydrogenase have been used in enzyme "linked" assays where the enzyme activity forms an intimate part of the assay. These enzymes although produced using recombinant DNA have not been optimised for use in the enzyme "linked" assay. Optimisation using recombinant DNA technology could significantly improve the performance of these assays.

(1.2) **The enzyme multiplied immunoassay technique (EMIT).**

Radio immunoassay (RIA) and enzyme immunoassay (EIA) have been successfully used to detect and quantify many drugs and metabolites in biological fluids and tissues (Table 1.1). The disadvantage of RIA products are the short shelf life and the problems of storage and disposal of radio-chemiclal wast. In general EIA products have a longer shelf life, with storage and disposal conditions being less stringent.

A novel type of EIA is the homogeneous EMIT assay (Van Weemen and Schuurs, 1971). In this assay the ligand is covalently bound to an enzyme such that the enzyme retains activity. However, when an antibody recognising both free and bound ligand interacts with the covalently bound ligand, the enzyme is inhibited (Fig 1.1). In the assay, the analyte (free ligand) to be tested is mixed with modified enzyme, and incubated with sufficient antibody to just inhibit the enzyme in the absence of free ligand (Fig 1.2). Free ligand competes with the enzyme for the limited amount of antibody, reducing the amount of antibody available for inactivation of the enzyme. Enzyme activity remaining will then be proportional to the amount of free ligand in the

Assay	Analyte	Limit of Sensitivity	Source	Reference
RIA	Barbiturates, Methadone, Methaqualone, Benzoylecgonine	~3 μmol	Urine	Cleeland *et al*, 1976
RIA	Thyrotropin	0.01 fmol	Serum	Odell *et al*, 1986
RIA	Adenosine	6.25 fmol	Blood	Lindel *et al*, 1992
RIA	Deoxycytidine kinase	0.16 pmol	Cytosolic tissue	Kawasaki *et al*, 1992
EIA	6β-Hydroxycortisol	14 fmol	Serum/urine	Zhiri *et al*, 1986
EIA	Immunoglobulin G	40 pmol	Serum	Papadea *et al*, 1985
EIA	Morphine	2 pmol		Rowley *et al*, 1975
EIA	Theophylline	2.5 μmol		Chang *et al*, 1982

Table 1.1: Some applications of RIA and EIA.

Fig 1.1: The basis of the EMIT assay.

(1) Formation of the enzyme-ligand complex does not inhibit enzyme activity.

(2) and (3) introduction of the ligand specific antibody inhibited enzyme activity.

Fig 1.2: The EMIT assay.

(1) In the assay sufficient antibody was used to just inhibit the enzyme.

(2) Addition of free ligand (analyte), competed with enzyme bound ligand for the limited amount of antibody.

Fig 1.1

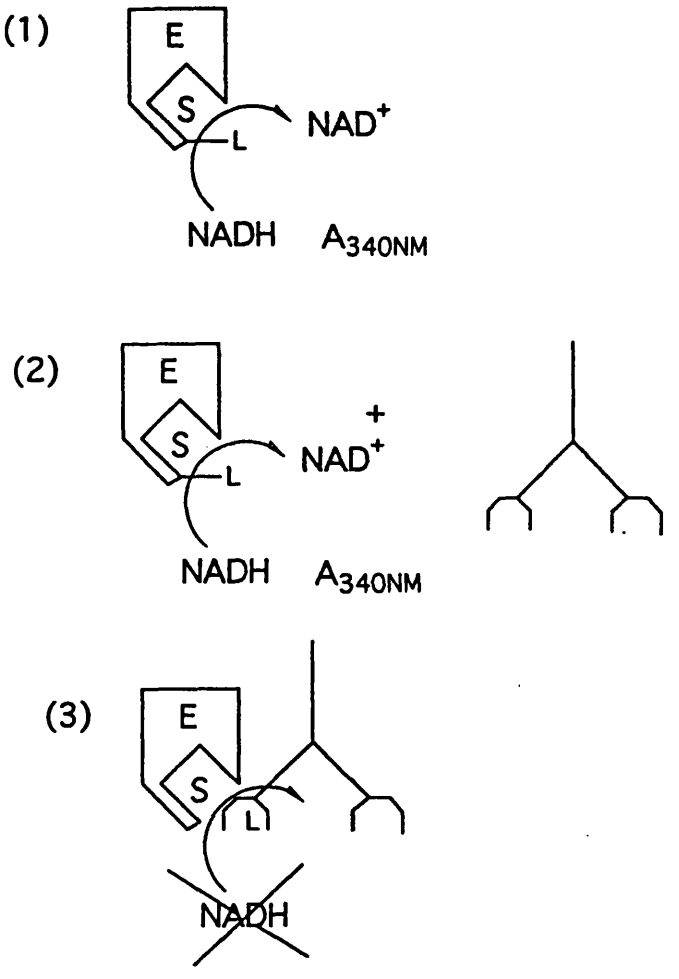
(1)
E
S
L
NAD+
NADH
A340NM
(2)
E
S
L
+
NAD+
NADH
A340NM
(3)
E
S
L
NADH

Fig 1.2

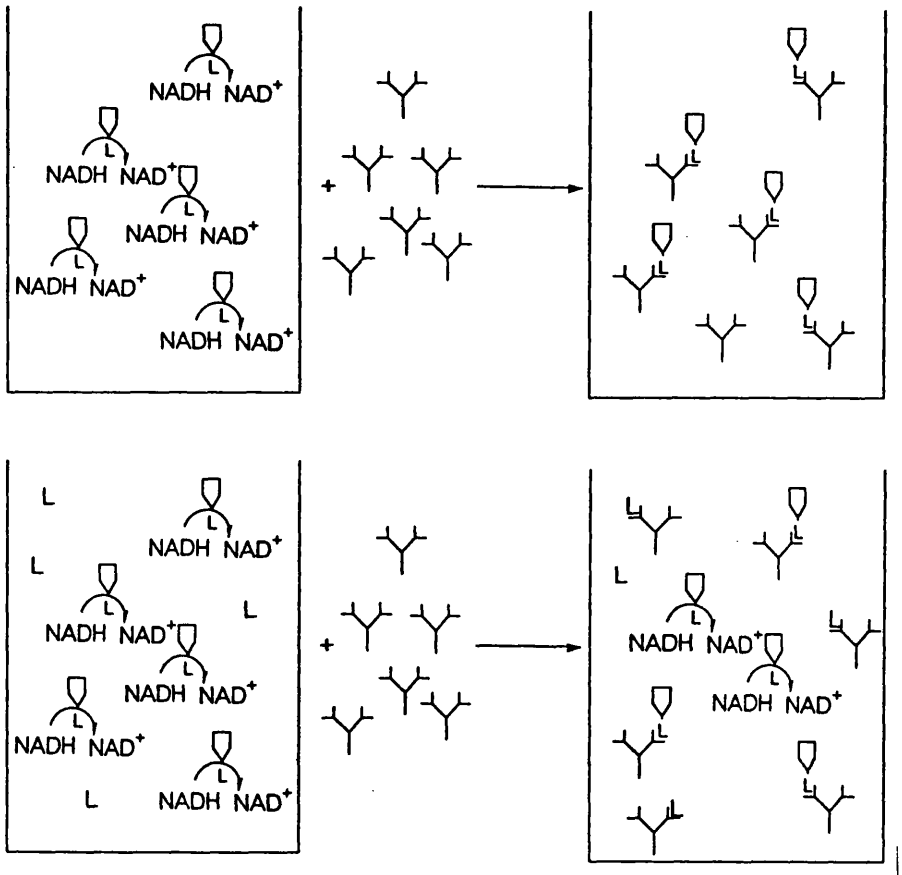
(1)
NADH NAD+
(2)
NADH NAD+

sample (Voller *et al,* 1978). It has been proposed that inactivation of the ligand-enzyme complex with antibody could be due to steric interference by the antibody, inhibition of conformational change required for enzyme function, or antibody induced conformational change of the enzyme (Rowley *et al,* 1975).

Porcine NAD-dependent mitochondrial malate dehydrogenase and bacterial glucose-6-phosphate dehydrogenase (*Leuconostoc mesenteroides*) have been widely used in the ligand-enzyme complex (Chang *et al,* 1982; Rowley *et al,* 1975), because of their high stability (extending the shelf-life of the EMIT assay kit), ease of purification and the ability to detect pmol quantities of active enzyme via spectroscopy at 340nm. However, even with attachment of up to 26 ligands per enzyme, only partial inactivation of the enzyme in the ligand-enzyme complex with excess antibody was achieved (Rowley *et al,* 1975).

The decrease in the activity of the complex has been attributed to the binding of a single antibody to a specific ligand (Rowley *et al,* 1975). However, the ligand may not be in a strategically important position on the enzyme for complete inactivation and incomplete inactivation reduces the sensitivity of the EMIT assay. An excess of ineffective ligands bound to the enzyme requires an excess of antibody to cause inactivation of the enzyme and reduces the sensitivity and efficiency of the assay. Ideally a unique ligand bound to the enzyme which is capable of complete inactivation of the enzyme upon formation of the antibody-ligand-enzyme complex would provide maximum sensitivity and efficiency in the EMIT assay..

(1.3) **Malate dehydrogenase.**

MDH catalyses the inter-conversion of L-malate and oxaloacetate, using nicotinamide adenine dinucleotide (NAD) as a coenzyme. Eukaryotes possess dimeric mitochondrial and cytoplasmic MDH, and in certain cases glyoxysomal MDH, while eubacteria possess a single form, with varying numbers of identical subunits. With a few exceptions, the size of all forms of subunit are between 30,000 and 35,000 Daltons.

All eukaryotic and eubacterial MDHs have the same reaction mechanism; transferring a hydride ion to and from the 4 position of the A face of the nicotinamide ring (Davies *et al,* 1972; Noyes *et al,* 1974). The MDHs can be characterised *in vitro* by the type and extent of their allosteric regulation. High concentrations of L-malate stimulate the production of oxaloacetate in mitochondrial MDH, while high concentrations of oxaloacetate inhibit the production of L- malate. Cytoplasmic MDH is inhibited to a lesser extent by the effect of high concentrations of oxaloacetate (Bernstein *et al,* 1978; Datta *et al,* 1985), but exhibits greater inhibition with high concentrations of L-malate (Kitto and Kaplan, 1966). Citrate has a dual effect on the enzyme, acting as an activator and an inhibitor of the enzyme in the direction $NAD^+ \rightarrow NADH$, depending on the substrate concentration (Gelpi *et al,* 1992). At high concentrations of NAD^+ MDH activity is enhanced with citrate, however when the NAD^+ concentration is low citrate acts as an inhibitor. Eubacteria appear to mirror some of the characteristics of eukaryotes, showing marked allosteric inhibition, possibly reflecting the control mechanism in a non-compartmentalised system (Sanwal, 1969). Examples of allosteric inhibition in eukaryotic and eubacterial MDH are shown (Table 1.2).

Immunological cross-reactivity tests on dimeric and tetrameric MDHs suggests that there are common antigens (Smith and Sundaram, 1988) (Table 1.3). However, cross-reactivity was only observed between partially denatured MDHs of different

Species	Inhibitors	References
Chicken mitochondrial	oxaloacetate	Kito and Kaplan, 1966
Chicken Cytoplasmic	L-malate	Kito and Kaplan, 1966
Porcine mitochondrial	oxaloacetate and citrate.	Gelpi *et al*, 1992
Porcine Cytoplasmic	L-malate	Kitto and Kaplan, 1966
E.coli	NADH, oxaloacetate, ATP, ADP and AMP.	Sanwal, 1969
Thermoleophilum alba NM	oxaloacetate	Novotny and Perry, 1990
Methanothermus fervidus	oxaloacetate.	Honika *et al*, 1990
Coccochloris peniocystis	oxaloacetate, citrate, ATP, and CoA.	Norman and Colman, 1991

Table 1.2: Inhibitors of eukaryotic and eubacterial MDHs.

Antibodies raised against.	Antibodies tested against.	Cross-reactivity (Native)	Cross-reactivity (Partially denatured)	Reference
Dimer	Dimer	√	√	Smith and Sundaram, 1988
Dimer	Tetramer	X	√	
Tetramer	Tetramer	√	√	
Tetramer	Dimer	X	√	

Table 1.3: Immunological cross-reactivity of dimeric and tetrameric MDHs.

Table 1.3 indicates that immunological cross-reactivity was only observed between partially denatured MDHs of different oligomeric forms.

oligomeric forms (Smith and Sundaram, 1988). This suggests that greater primary structure homology exists within the dimeric and tetrameric forms than between the dimeric and tetrameric forms.

Mitochondrial, cytoplasmic and glyoxysomal MDHs form part of a complex interactive compartmentalised system (Fig 1.3). There is evidence to suggest that MDH exists as a multi-enzyme cluster in eukaryotes and eubacteria (Barnes and Weitzman, 1986; Beeckmans and Kanarek, 1981; Robinson *et al,* 1987), with other tricarboxylic acid cycle (TCA) enzymes and aspartate aminotransferase. Cytoplasmic and mitochondrial MDHs have been found associated with fumarase, citrate synthase and aspartate aminotransferase (Beeckmans and Kanarek, 1981; Robinson *et al,* 1987). *E.coli* MDH has been isolated in a multi-enzyme cluster with fumarase, citrate synthase, aconitase and isocitrate dehydrogenase (Barnes and Weitzman, 1986). The standard free energy of the conversion of oxaloacetate to L-malate with NADH as a coenzyme lies in favour of L-malate formation. It is believed that the formation of the TCA enzyme complex drives MDH in the direction of oxaloacetate, by facilitating the transfer of oxaloacetate from MDH to citrate synthase (Beeckmans and Kanarek, 1981).

(1.4) **Aims of the project.**

The initial objective was to prepare a genetically modified enzyme suitable for modification, and eventual use in the EMIT assay. *E.coli* MDH was chosen, as it has a similar structure and properties to porcine mitochondrial MDH, and the gene encoding the structural protein was available and could be expressed in *E.coli* MDH^- strains (Vogel *et al,* 1987).

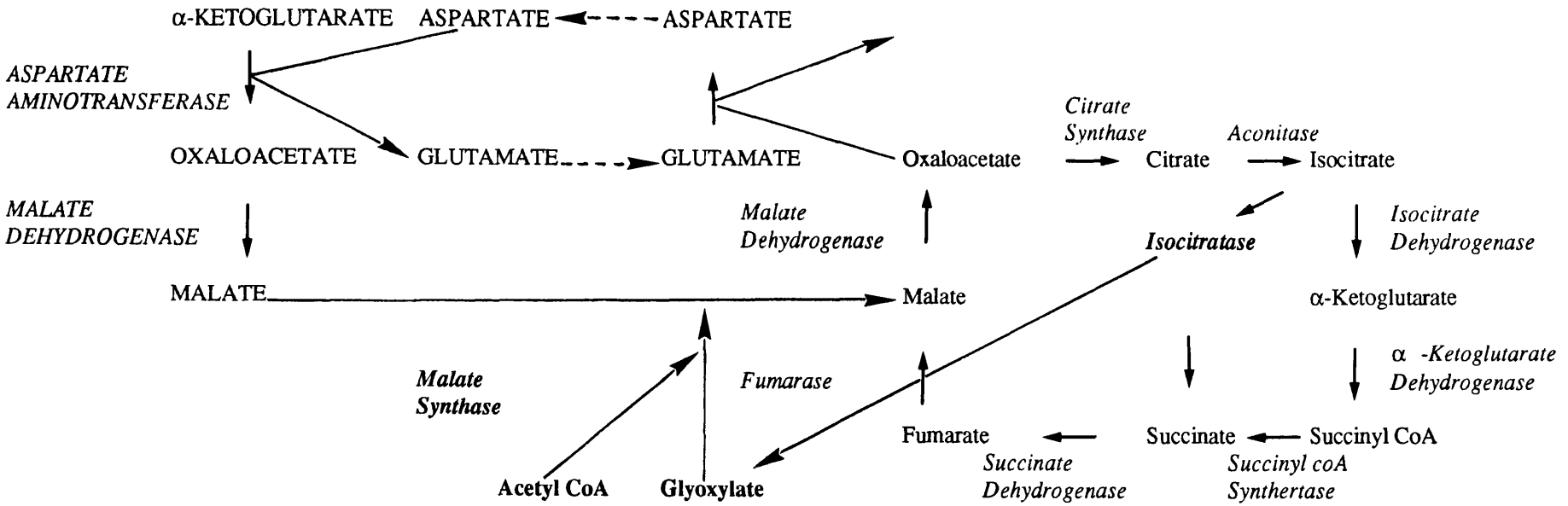

Fig 1.3: Schematic representation of the interaction between the TCA cycle, glyoxylate cycle and the aspartate-malate Shuttle.

Enzymes are indicated in italics,bold indicates glyoxylate cycle, uppercase aspartate-malate shuttle and lower case indicates TCA cycle.

(1.5) **Homology modelling of *E.coli* MDH.**

To identify potential sites on the *E.coli* MDH surface to allow attachment of ligands it was necessary to determine the three dimensional (3D) co-ordinates of solvent exposed residues. A homology model was built of the *E.coli* MDH using the porcine cytoplasmic MDH structure as a template. The crystal structure of porcine cytoplasmic holo-MDH (enzyme with coenzyme) had been determined and the 3D co-ordinates deposited into the Brookhaven protein data bank (Birktoft *et al*, 1989; Roderick and Banaszak, 1986). A crystal structure of *E.coli* apo-MDH (enzyme with substrate analogue) has recently been published, since the work described here was carried out. Comparison of the *E.coli* crystal structure with porcine MDH confirmed that the secondary, tertiary and quaternary structures were homologous (Hall *et al*, 1992). However greater structural homology was observed between *E.coli* and mitochondrial MDHs (root mean square (RMS) deviation of *E.coli* and mitochondrial MDH polypeptide backbone was 0.76Å), than between *E.coli* and cytoplasmic MDHs (RMS deviation 1.88Å). The core structures of these proteins displayed the greatest homology, while surface turns were less homologous (Hall *et al*, 1992). The greater deviation between the *E.coli* and cytoplasmic MDH structures can be attributed to lower sequence identity; *E.coli* and mitochondrial MDH have a sequence identity of 55%, whereas *E.coli* and cytoplasmic MDH have a sequence identity of approximately 20%. Although porcine mitochondrial MDH was a better candidate as a template structure for modelling, the 3D co-ordinates had not been deposited into the Brookhaven protein data bank and therefore were not available for use.

(1.6) **The *E.coli* MDH.**

(1.6.1) *E. coli* MDH structural gene.

The deduced amino acid sequences of *E.coli* MDH structural genes have been obtained by three groups (McAlister-Henn *et al,* 1987; Nicholls *et al,* 1989; Vogel *et al,* 1987). The sequences are in agreement, except for the insertion of a cytosine at position +910 which would cause a frame-shift at amino acid position 305 (W) and lead to a change in the carboxy terminal from WAKSSILSN COOH to LGEEFVNK COOH (Fig 1.4). However, this deviation is a sequence artefact since the clone with which I was provided had the extra base, contrary to the literature source and the group providing the clone (Vogel *et al,* 1987). This gene encodes all 312 residues of a single polypeptide subunit of 32,500 Daltons containing three reduced cysteines at residues 109, 113 and 251. A ribosome binding site 5'AGGA is located six nucleotides upstream of the ATG initiation codon of Met 1. Promoter regions -10 promoter (5'TAAGGT) and -35 promoter (5'TTGTAA) are located at nucleotide positions -57 to -52 and -70 to -65 respectively. Vogel *et al,* (1987) has proposed that the G nucleotide, 44 base pairs upstream of the ATG initiation codon corresponds to the transcription initiation site. The 5'TTTTTTGTTTT at nucleotide positions 980 to 990 preceded by G and C residues indicates a *rho* termination site (Vogel *et al,* 1987).

E.coli MDH^- strain W945T1-2 has a mutation within the regulatory gene controlling MDH expression. This regulatory gene has been mapped to the histidine operon. The strain spontaneously reverts with a frequency of 10^{-6} to 10^{-8} (Courtright and Henning, 1970). However, growth of *E.coli* on glucose minimal medium under anaerobic conditions suppresses the TCA cycle and the subsequent production of chromosomally encoded MDH (Gray *et al,* 1966). Therefore, anaerobic growth of *E.coli* W945T1-2 on glucose minimal media will prevent the expression of MDH in revertants, thus

-340 -330 -320 -310 -300 -290 -280 -270

*agtgaatt CGAGCTCGGT ACCCGGGGAT CCTCTAGAGT CGACCTGCAG GCATGCAAGC TT*gcaaattc tgcttaaaag

-260 -250 -240 -230 -220 -210 -200 -190 -180 -170 -160 -150 -140

taaattaatt gttatcaaat tgatgttgtt ttggctgaac ggtagggtat atgtcaccac ctgttggaat gttgcgctaa tgcataagcg actgttaatt acgtaagtta ggttcctgat tacggcaatt

-130 -120 -110 -100 -90 -80 -70 -60 -50 -40 -30 -20 -10

aaatgcataa acgctaaatt gcgtgactac acattcttga ga**tgtggtca ttgtaa**acgg caattttgtg gat**taaggt**c gcggca**g**cgg agcaacatat cttagtttat caatataata **agga**tttagg

10 20 30 40 50 60 70 80 90 100

ATG AAA GTC GCA GTC CTC GGC GCT GCT GGC GGT ATT GGC CAG GCG CTT GCA CTA CTG TTA AAA ACC CAA CTG CCT TCA GGT TCA GAA CTC TCT CTG TAT GAT ATC GCT
M K V A V L G A A G G I G Q A L A L L L K T Q L P S G S E L S L Y D I A
1 10 20 30

110 120 130 140 150 160 170 180 190 200 210

CCA GTG ACT CCC GGT GTG GCT GTC GAT CTG AGC CAT ATC CCT ACT GCT GTG AAA ATC AAA GGT TTT TCT GGT GAA GAT GCG ACT CCG GCG CTG GAA GGC CGA GAT GTC
P V T P G V A V D L S H I P T A V K I L G F S G E D A T P A L E G R D V
40 50 60 70

220 230 240 250 260 270 280 290 300 310 320

GTT CTT ATC TCT GCA GGC GTA CGG CGT AAA CCG GGT ATG GAT CGT TCC GAC CTG TTT AAC GTT AAC GCC GGC ATC GTG AAA AAC CTG GTA CAG CAA GTT GCG AAA ACC
V L I S A G V R R K P G M D R S D L F N V N A G I V K N L V Q Q V A K T
80 90 100

330 340 350 360 370 380 390 400 410 420 430

TGC CCG AAA GCG TGC ATT GGT AAT ATC ACT AAC CCG GTT AAC ACC ACA GTT GCA ATT GCT GCT GAA GTG CTG AAA AAA GCC GGT GTT TAT GAC AAA AAC AAA CTG TTC
C P K A C I G N I T N P V N T T V A I A A E V L K K A G V Y D K N K L F
110 120 130 140

440 450 460 470 480 490 500 510 520 530 540

GGC GTT ACC ACG CTG GAT ATC ATT CGT TCC AAC ACC TTT GTT GCG GAA CTG AAA GGC AAA CAG CCA GGC GAA GTT GAA GTG CCG GTT ATT GGC GGT CAC TCT GGT GTT
G V T T L D I I R S N T P V A E L K G K Q P G E V E V P V I G G H S G V
150 160 170 180

550 560 570 580 590 600 610 620 630 640

ACC ATT CTG CCG CTG CTG TCA CAG GTT CCT GGC GTT AGT TTT ACC GAG CAG GAA GTG GCT GAT CTG ACC AAA CGC ATC CAG AAC GCG GGT ACT GAA GTG GTT GAA GCG
T I L P L L S Q V P G V S P T E Q E V A D L T K R I Q N A G T E V V E A
190 200 210

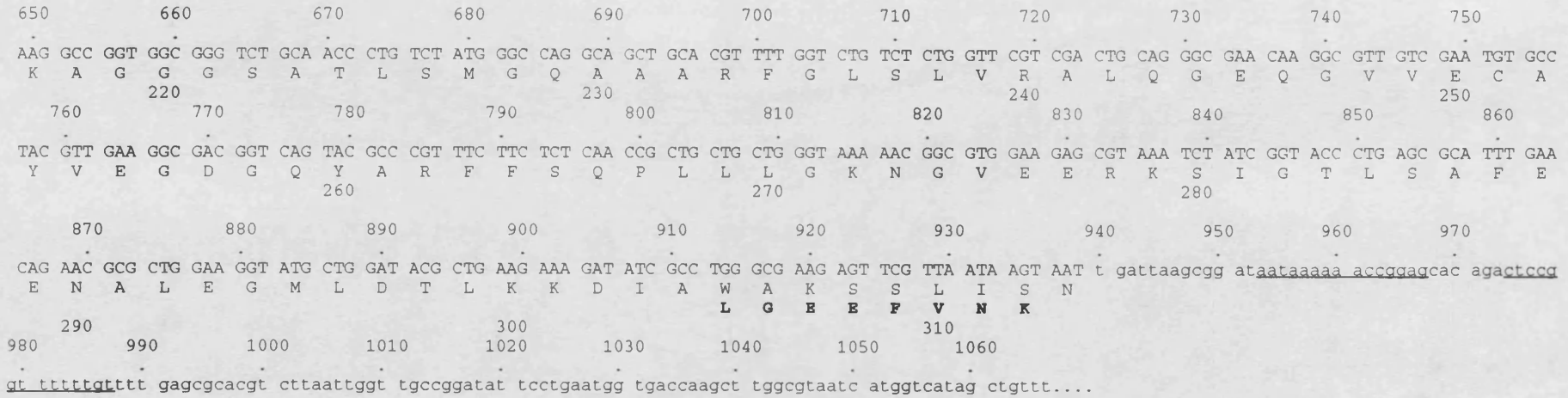

Fig 1.4: The nucleotide sequence of a single subunit of the *E.coli* MDH gene.

The nucleotide sequence of the 1344 bp DNA fragment containing the MDH structural gene encoding 312 residues and part of pUC19 polylinker (italics, -279 to -338). Uppercase letters (1 to 939) indicate coding region. Below each codon is the single letter amino acid code (uppercase). Amino acid sequence deviation is depicted in bold. Bold lowercase indicates the putative -10 and -35 promoter recognition sites. *RBS* is the ribosome binding site. **g** and ***rho*** are the transcription initiation site and putative termination site.

enabling expression of plasmid encoded MDH without contamination from endogenous MDH.

(1.6.2) Comparison of the secondary, tertiary and quaternary structures of *E.coli* and porcine cytoplasmic MDH.

The underlying organisation of *E.coli* and porcine cytoplasmic dimeric MDHs are similar, with the subunits being divided into a coenzyme-binding domain and catalytic domain. The coenzyme-binding domaine, consists of the N-terminal half of the polypeptide chain. In the *E.coli* (Fig 1.5) and porcine MDHs these are residues 1-150. The main structural motif of this domain in *E.coli* MDH is a centrally located six-stranded parallel β-sheet (β-sheet I) flanked by five α-helices (Birktoft *et al,* 1989; Birktoft *et al,* 1989b; Hall *et al,* 1992) (Fig 1.6). The C-terminal half of the polypeptide chain (*E.coli* residues 151-312 (Fig 1.5); porcine residues 151-332) is the catalytic domain (Birktoft and Banaszak, 1983). The predominant structural features are two anti-parallel β-sheets (β-sheets II and III) (Fig 1.6). Beta sheets II and III are interspersed with five α-helices (Birktoft *et al,* 1989; Hall *et al,* 1992).

Minor deviations are apparent between the *E.coli* and porcine MDHs in the length of the polypeptide chain in the surface turn motif segments which connect the α-helices and β-strands structures and the initiation and termination points of the joining turns. Beta-Sheet I consists of β-strands βA to βF and is flanked on one side by α-helices αB, αC and αC' and on the other by αDE and α1F. Beta-Sheet I displays a degree of right handed twist. All the β-strands and α-helices in the nucleotide binding domain with the exception of βC and αDE (which are located on the surface of the protein), are buried within the interior of the protein. A turn motif of seven residues between αB and βB in the porcine MDH (Birktoft *et al,* 1989b) is diminished (three residues) in *E.coli* MDH (Hall *et al,* 1992).

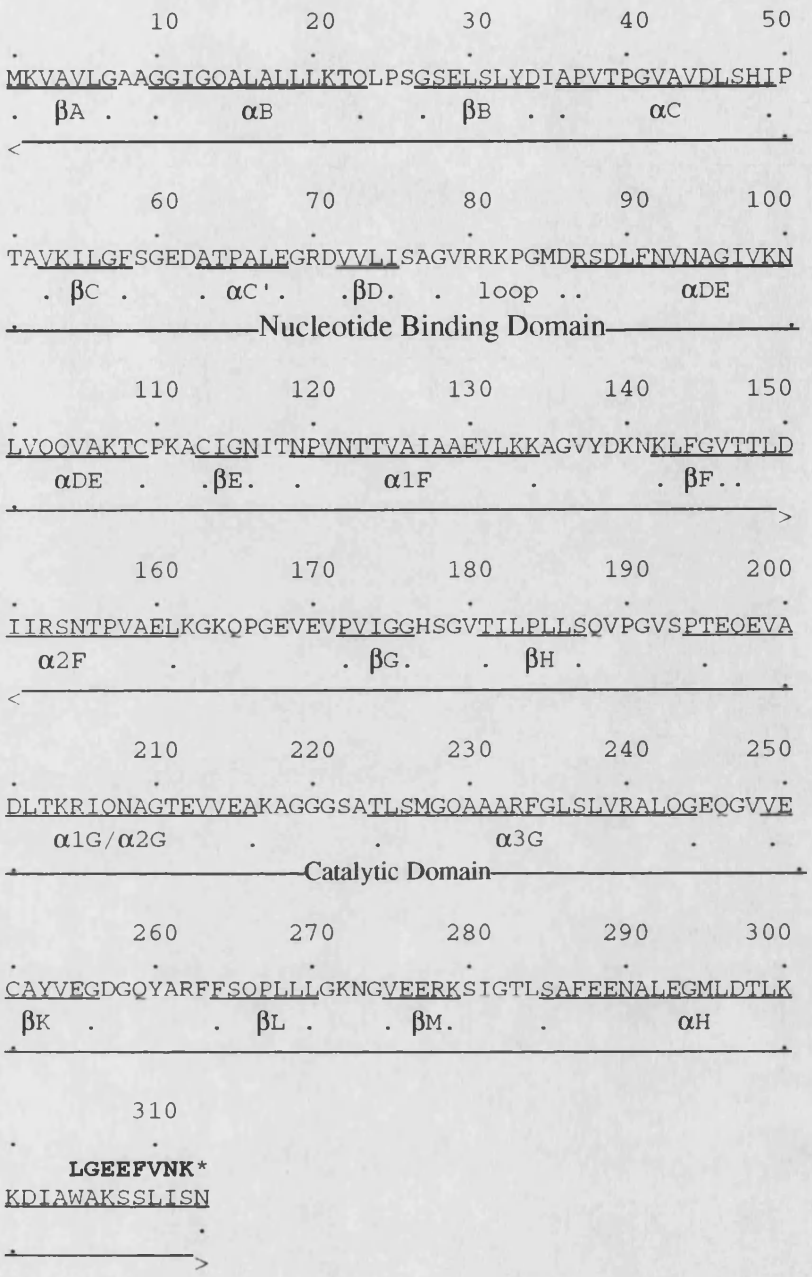

Fig 1.5: The deduced amino acid sequence of a single subunit of *E.coli* MDH. Sequence and secondary Structure based on that obtained by Hall *et al*, (1992) and Vogel *et al*, (1987). Nomenclature for secondary structure description follow the system adopted for LDHs and MDHs (Rossmann *et al*, 1975). Elements of secondary structure are indicated with β indicating β-strand and α signifying α-helix. Bold lettering indicates deviation in sequence.

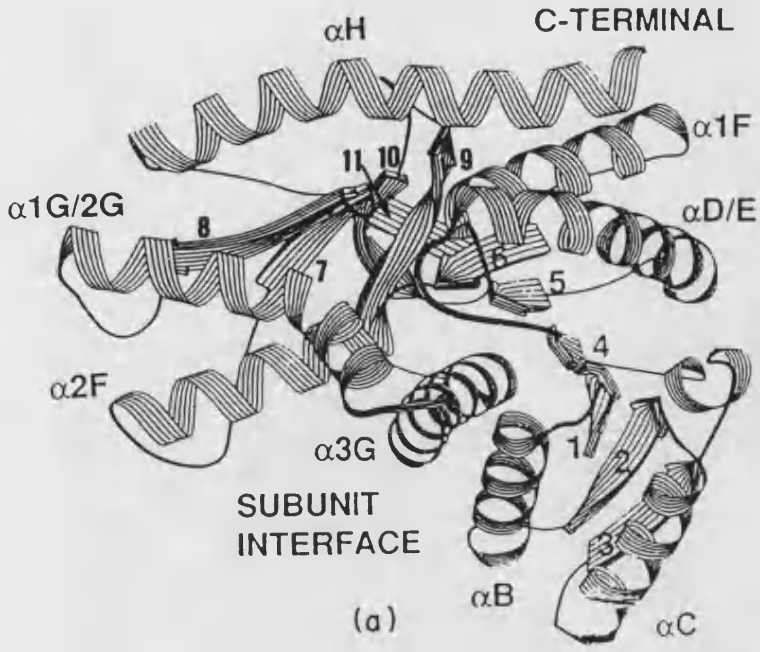

Fig 1.6: Schematic representation of the secondary and tertiary structure of *E.coli* MDH subunit.

The portion of the structure represented by arrows are β-strands, and coiled ribbons signify α-helices. Parallel β-sheet I (β-strands A to F) is indicated by numbering 1 to 6. Anti-parallel β-sheet II (β-strands G and H) is indicated by numbering 7 and 8. Anti-parallel β-sheet III(β-strands K, L and M) is indicated by numbering 9 to 11. Reproduced from Hall *et al*, (1992).

Beta-Sheet II is made up of two anti-parallel β-strands, βG and βH. This sheet has a degree of right handed twist greater than that observed in β-sheet I. Beta strand G and βH are connected by a hairpin turn which points into the interior of the protein. This turn forms part of the active site and contains a histidine which is important in catalysis (*E.coli* residue 177; porcine residue 180). Beta-Sheet II is connected to the nucleotide binding domain by α-helix α2F and to β-Sheet III by α-helix α1G/α2G. This α-helix (α1G/α2G) is located on the surface of the MDH.

Beta-sheet III consists of three anti-parallel β-strands, βK, βL and βM and is positioned between β-sheets I and II. Beta-Sheet III has a twist of approximately 90° and is flanked by two α-helices at its initiation (α3G) and termination (αH). Beta strand M and αH are solvent exposed as are the turn motifs connecting the β-strands. Porcine MDH has a turn situated between α3G and βK of six residues (Birktoft *et al*, 1989b) which is only three residues in *E.coli* MDH (Hall *et al*, 1992).

The crystal structures indicate that the subunit:subunit interactions differ between *E.coli* and porcine cytoplasmic MDHs (Birktoft *et al*, 1989; Hall *et al*, 1992). Bleile *et al*, (1977) has demonstrated that at low pH (pH <5.0) the structurally homologous porcine mitochondrial MDH dissociates into monomers, whereas porcine cytoplasmic MDH did not. It was concluded that a histidine at the mitochondrial MDH subunit inter-face was responsible for this acid dissociation. The mitochondrial MDH was also shown to be more susceptible to dissociation into its monomers at low concentrations (0.2 μ M). This is due to different residues at the subunit interface contributing to subunit:subunit stability and is manifest in the crystallographic symmetry observed at the subunit interfaces. Porcine MDH displays approximately two fold rotational symmetry at the subunit interface whereas *E.coli* has exact symmetry through the same axis (Birktoft *et al*, 1989; Hall *et al*, 1992). In *E.coli*, MDH subunit:subunit interactions are through polar and non-polar contacts. Alpha helix B interacts with α3G and with αB of the other subunit, αC interacts with the

amino terminal portion of α2F and the carboxy terminal of α3G. Polar and non-polar interactions between subunits in porcine MDH are between different elements of the secondary structure. Alpha helix B, αC and α2G of one subunit interact with αB, αC and α2G of the other subunit. Alpha helix 2F of one subunit interacts with αC of the other subunit.

(1.6.3) Binding of coenzyme and substrate in the active site of MDH.

Citrate has a similar structure to L-malate, differing only by the addition of a methyl carboxyl group, as indicated below.

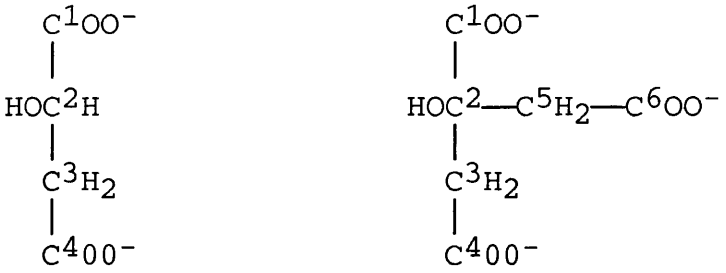

Malate Citrate

Citrate acts as an analogue, hydrogen bonding to the putative active site residues in MDH (Hall *et al*, 1992). Substrate specificity is thought to arise through the conformation of the substrate binding site and through hydrogen bonding (Clarke *et al*, 1987; Hall *et al*, 1992). Modelling of L-malate in the substrate binding site of *E.coli* MDH using the co-ordinates of citrate as a template, suggests that specificity is partly brought about by hydrogen bonding with arginine residues (Hall *et al*, 1992). The terminal guanidino nitrogens of arginine 153 are thought to hydrogen bond with the C^1 carboxyl moiety of L-malate and the Epsilon (ε) nitrogen of arginine 81 is thought to hydrogen bond with the C^4 carboxyl moiety (Fig 1.7). However Clarke *et al*, (1987) and Nicholls *et al*, (1992) have proposed that the C^4 carboxy moiety interacts with arginine 81 terminal guanidino nitrogens. The C^2 hydroxyl moiety of L-malate is within hydrogen bonding distance of the ε nitrogen of arginine 87 (Fig 1.7). Clarke *et*

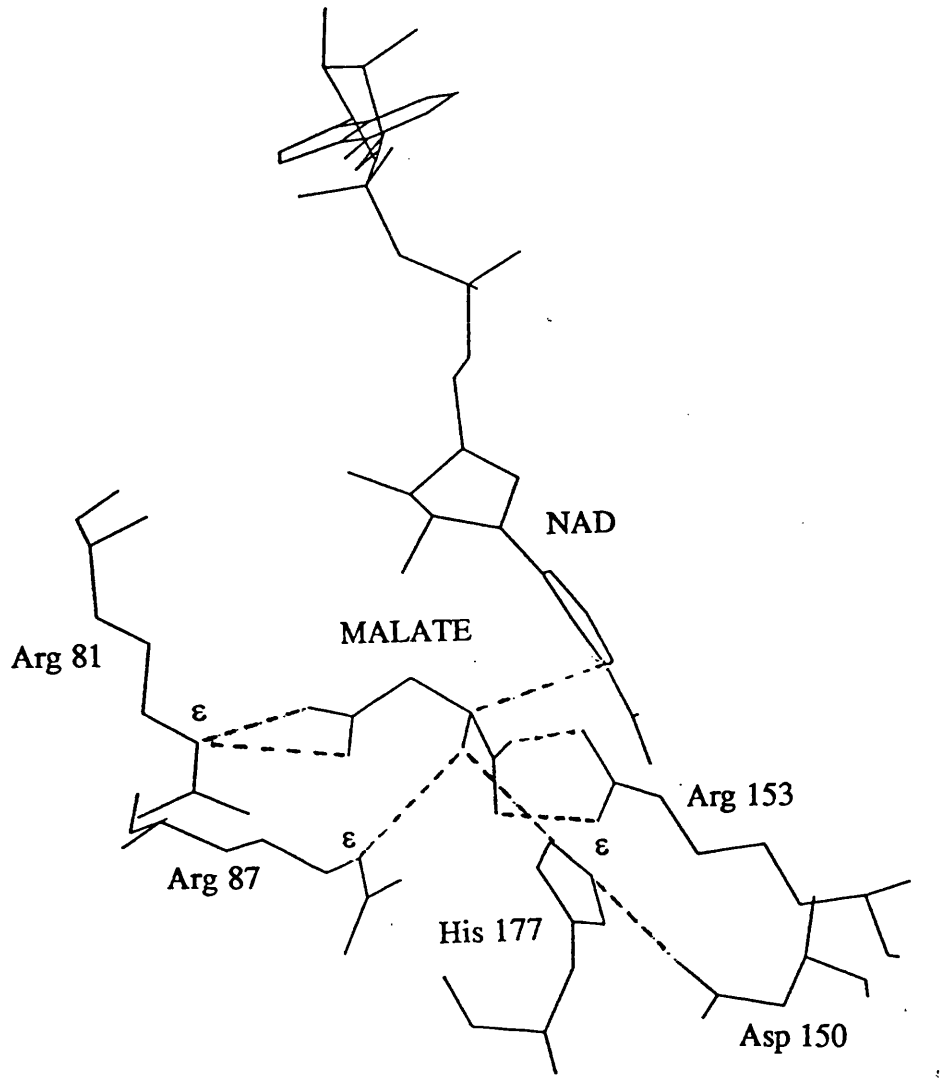

Fig 1.7: Proposed hypothetical ternary model of *E.coli* MDH active site.

Proposed ternary model of *E.coli* MDH active site of Hall *et al* (1992). Residues and atoms involved in hydrogen bonding of substrate are labelled. Stippled lines indicate hydrogen bond.

al, (1987) has shown that the homologous substrate binding site of lactate dehydrogenase (LDH) can be modified to alter the substrate specificity from pyruvate/lactate (R = $-CH_3$) to oxaloacetate/L-malate (R = $-CH_2-C^4OO^-$) by increasing the volume of the substrate binding site. Greater specificity was obtained for oxaloacetate/malate when an arginine homologous to *E.coli* MDH arginine 81 was introduced into the βD/αD loop. This residue was capable of hydrogen bonding with the C^4 carboxyl moiety. Comparison of the active sites of *E.coli* apo-MDH and porcine holo-MDH indicated that the citrate and nicotinamide ring of the NAD are in close proximity of each other (Birktoft *et al*, 1989b; Hall *et al*, 1992). This observation has been substantiated by comparison of the crystal structures of LDH binding substrate analogues and coenzyme (Grau *et al*, 1981; Abad-Zapatero *et al*, 1987). NAD is thought to interact with the coenzyme binding site in an extended conformation (Webb *et al*, 1973). The nicotinamide and purine ring of the coenzyme are stabilised through hydrophobic interactions with the active site, while the ribose and phosphate moieties are stabilised through hydrogen bonding (Birktoft *et al*, 1989). Hydrogen bonding between the carboxamide group of the nicotinamide ring and the coenzyme binding pocket is thought to provide the stereospecificity of MDH for NAD (Rossmann *et al*, 1975) (Fig 1.8).

(1.7) **The action of MDH in catalysis.**

MDH exhibits a compulsory ordered binding mechanism in the forward and reverse directions, with the coenzyme binding first followed by the substrate (Raval and Wolfe, 1962; Silversteine and Sulebelele 1969). The nicotinamide ring of NAD and substrate are thought to be in close proximity to an essential histidine and aspartate which have been implicated in the hydride transfer reaction in dehydrogenase catalysis in the active site (Birktoft and Banaszak, 1983). Evidence for the importance of these residues comes from several observations. Sequence alignments of LDH and MDH indicate that these residues are invariant (Birktoft *et al*, 1982). The crystal structure of

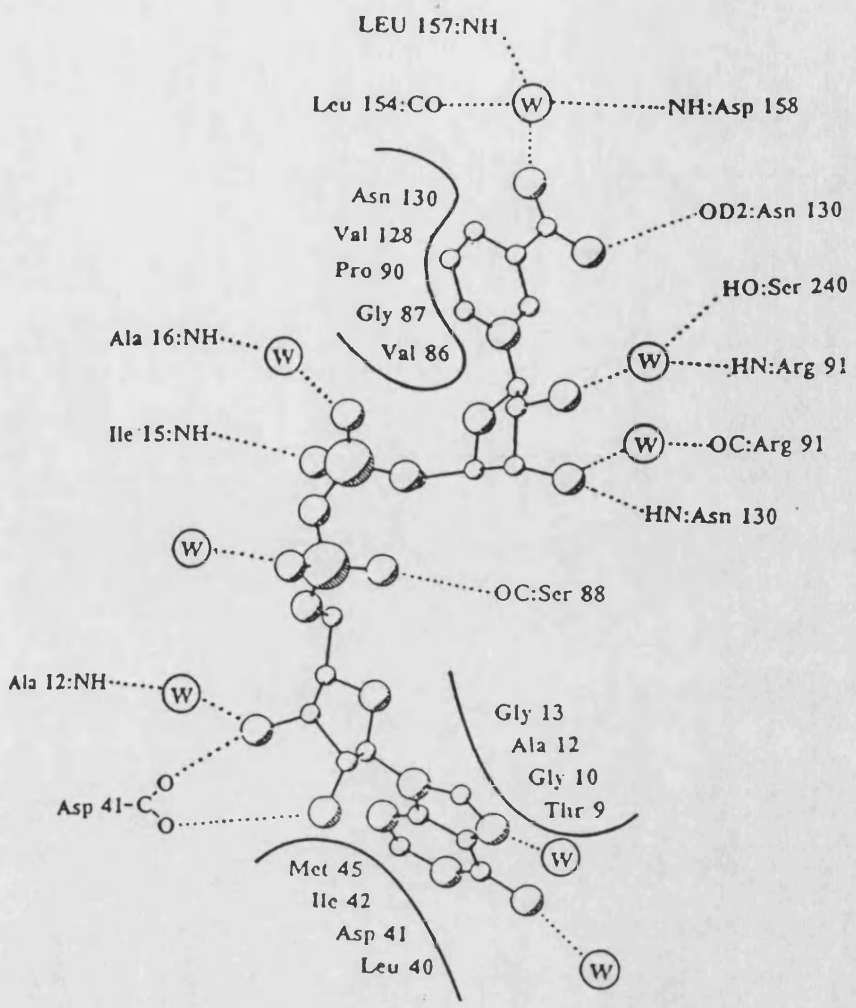

Fig 1.8: Conformation of NAD in the porcine cytoplasmic coenzyme binding site.

Residues which participate in hydrophobic binding areas are shown schematically. Atoms that participate in direct and indirect hydrogen bonding are shown in stippled lines. O Indicates hydrogen bonded water molecules.

Reproduced from Birktoft *et al*, (1989).

all MDHs so far characterised, indicate the presence of histidine and aspartate in the putative active site (Birktoft and Banaszak, 1982; Hall *et al*, 1992; Roderick and Banaszak, 1986). MDH can be inactivated by diethyl pyrocarbonate, a histidine specific reagent in a 1:1 stoichiometry. Enzyme inactivation is prevented in the presence of substrate or coenzyme indicating that the histidine residue is in the active site (Holbrook *et al*, 1974; Ijiama *et al*, 1986). Substitution of the aspartate of the histidine-aspartate pair, to a non hydrogen bonding neutral residue, alters catalysis in dehydrogenases (Clarke *et al*, 1988). Modelling studies have indicated that introduction of the coenzyme into the binding site does not significantly alter the conformation of the enzyme (Hall *et al*, 1992). Introduction of the substrate into the catalytic site, and associated hydrogen bonding with the C^1 carboxy moiety of arginine (*E.coli* residue 153), initiates a conformational change in the enzyme. The βD/αD loop, which is solvent exposed in the holoenzyme complex (*E.coli* residues 76 to 86), collapses over the active site, shielding it from solvent molecules, and initiates contact of arginine 81 (*E.coli*) with the C^4 carboxy of the substrate (Fig 1.7) (Hall *et al*, 1992; Trommer and Glöggler, 1979). Simultaneously, the imidazole ring of histidine 177 is thought to move towards the C^2 hydroxy moiety of the substrate allowing hydrogen bonding to occur. This results in the C^2 carbon developing a partial positive charge, and hydrogen bonding between the C^2 carbon and position four of the nicotinamide ring (Bernstein and Everse, 1978; Birktoft and Banaszak, 1983; Hall *et al*, 1992). A localisation of the positive charge at position four of the nicotinamide ring results in the formation of NAD^+ and L-malate, whereas a localisation of the positive charge on the imidazole ε nitrogen leads to NADH and oxaloacetate. Binding of the coenzyme in the coenzyme binding site is both non-stoichiometric as well as non-equivalent (Weininger *et al*, 1977), with the binding of coenzyme in one subunit inhibiting the binding of coenzyme in the second subunit. It has been proposed that α-helices α2G and α3G which form part or the catalytic site and subunit interface, influence the binding of the coenzyme (Hall *et al*, 1992). Binding of the coenzyme in the coenzyme

binding site causes a movement of these helices which inhibits binding of the of coenzyme in the second subunit via the subunit interface.

(1.8) **Derivatization of MDH.**

The project required that a unique coupling residue be placed on the surface of each subunit of *E.coli* MDH. Although lysine, arginine (amino groups), aspartate and glutamate (carboxyl groups) can de derivatized (Månsson and Mosbach, 1992), they are all unsuitable for derivatization as they are abundant (20% of the *E.coli* MDH residues) and are solvent accessible (Bordo and Argos, 1991). The reduced cysteines in *E.coli* MDH on the other hand are not solvent accessible (Murphey *et al*, 1967) and cannot be derivatized. Introduction of a solvent accessible cysteine in the MDH would therefore allow specific ligand attachment. Three common coupling reagents can be used to covalently bind a ligand to cysteine; the maleimides, alkyl halides and pyridyl disulphides (Fig 1.9). The pK of cysteine is 8.3 and at alkaline pH (pH>7.0) can undergo nucleophilic attack with the coupling reagents.

The presence of substituted solvent accessible cysteines can be ascertained by monitoring the change in an absorbance of a reporter molecule upon covalent attachment to thiols. N-Ethylmaleimide undergoes nucleophilic addition in a similar manner as described above (Fig 1.9) (Portis *et al*, 1983). Unbound N-ethylmaleimide has an absorbance at 305nm. The reaction of the N-ethylmaleimide with the thiol group can be monitored by measuring the decrease in absorbance at 305nm. However the low absorbance of N-ethylmaleimide (E_{305nm} = 620 $cm^{-1}M^{-1}$) and interference due to the absorbance of phenylalanine, tyrosine and tryptophan in proteins, monitoring coupling is impractical. Dithionitrobenzoate (DTNB) (Ellman, 1959) reacts with thiol groups in a similar manner as pyridyl disulfide (Fig 1.9). Reaction of DTNB with thiols releases thionitrobenzoate anion (TNB) which has a high absorbance at 412nm (E_{412nm} = 136000 $cm^{-1}M^{-1}$). The coupling of DTNB to thiols can be monitored by

Coupling reagent	Method of covalent coupling
Maleimides	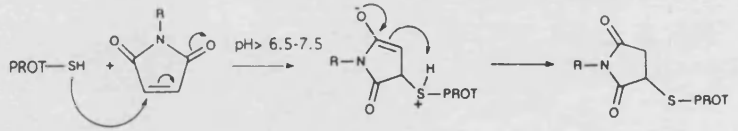
Alkyle halides	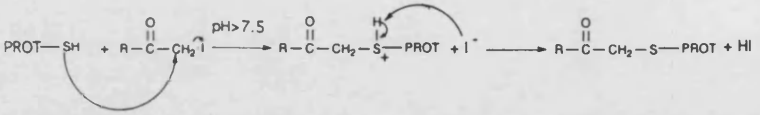
Pyridyl disulphides	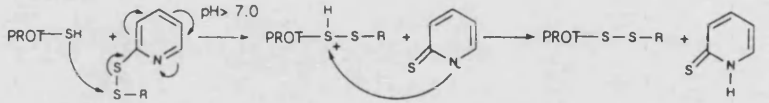
N-Ethylmaleimide	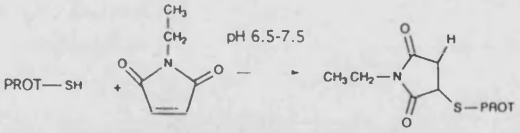
Dithionitrobenzoate	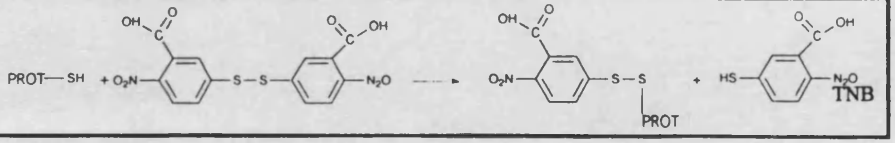

Fig 1.9: Covalent coupling of ligands to cysteines.

The conditions for covalent coupling of ligands to cystines are indicated above. TNB is Thionitrobenzoate anion and PROT-SH is cysteine in protein.

the formation of the TNB anion as no absorbance by the protein is observed at this wavelength.

(1.9) **Substitution of codons in the MDH gene.**

Two strategies can be employed in the mutation of genes; random mutagenesis and site-directed mutagenesis.

With random mutagenesis nucleotides are substituted randomly or semi-randomly. Common methods of generating random mutations include the use of chemical mutagens, ultraviolet light, ionising radiation and mutator strains of *E.coli* (Neidhardt *et al,* 1988; Winnacker, 1987). However random mutagenesis is unsuitable, because the project requires that the codons of specific residues determined by homology modelling are substituted.

Site-directed mutagenesis requires specific replacement of a small number of bases. An oligonucleotide spanning the region to be altered is synthesised containing the altered (mismatched) bases. Flanking perfect match sequence serves to precisely align the substituted bases, and the remainder of the strand is synthesised enzymatically, using either the Klenow fragment of DNA Polymerase I or PCR. Strategies for oligonucleotide directed mutagenesis can be divided into two categories based on the form of the template: single stranded templates derived from filamentous phage vector such as M13 and double stranded templates from plasmid vector. In both systems the oligonucleotide is annealed to a single stranded template. An oligonucleotide, the sequence of which is complimentary to the DNA molecule to be mutagenised, apart from one or several specific and pre-determined base changes is hybridised to its complimentary sequence of a clone of single stranded template DNA. The oligonucleotide serves as a primer for *in vitro* enzymatic DNA synthesis (using the

Klenow fragment of DNA Polymerase I) all or part of the template DNA to form a double stranded heteroduplex (Winnacker, 1987).

However this method of mutagenesis has the disadvantage that large amounts of template DNA are required for mutagenesis. The efficiency of mutation is low (40%) (Winnacker, 1987) and the entire vector has to be sequenced.

Mutagenesis using PCR mutagenesis has superseded the above for site-directed mutagenesis (Reidhaar-Olson and Sauer, 1988; Saiki *et al*, 1988). PCR amplification involves two oligonucleotide primers similar to those described above that flank a double stranded DNA segment to be amplified. Repeated cycles of heat denaturation of the DNA, annealing of the primers followed by extension of the annealed primers with thermostable DNA Polymerase. These primers hybridise to opposite strands of the target DNA so that synthesis by the Polymerase proceeds across the region between the primers doubling the amount of that DNA segment. Each successive round of target DNA replication doubles the amount of DNA synthesised in the previous cycle. Therefore primers nucleotide mismatches will be replicated with target DNA replication. This technique has the advantage that small amounts of double stranded target DNA can be used in a single step procedure. If the cassette mutagenesis method is employed (Reidhaar-Olson and Sauer, 1988), only the PCR product has to be checked for spurious mutations. This and the single mutagenesis step greatly decreases the time that a mutant can be generated.

(1.10) **Purification of *E.coli* MDH.**

Traditionally *E.coli* MDH has been purified to homogeneity using ammonium sulphate saturation precipitation of proteins followed by chromatography on DEAE-cellulose (Fernely *et al*, 1981; Murphey *et al*, 1967). With the advent of affinity chromatography MDH has been purified in a single step, using NAD^+ as the affinity

ligand (Wright and Sundaram, 1979). These techniques are however relatively expensive, and have been replaced by dye affinity chromatography. The triazinyl dye Procion red H3-B has been covalently linked to agarose by the formation of an ether link between the triazine ring of the dye and the agarose hydroxyl groups (Atkinson *et al*, 1982) (Fig 1.10). Bacterial MDH has been purified by elution from a Procion red chromatography matrix with salt and in its ternary complex by elution with NAD^+ and L-malate (Smith *et al*, 1982).

An alternative approach has been the use of thiol-affinity chromatography (Axen *et al*, 1975) (Fig 1.10). Modified galactokinase and glucose dehydrogenase incorporating a cysteine affinity tag have been purified by thiol-affinity chromatography (Persson *et al*, 1988; Persson *et al*, 1990). This technique would enable rapid purification of MDH with a solvent accessible reduced cysteine.

Matrix	Reaction
Procion Red/CL6-B	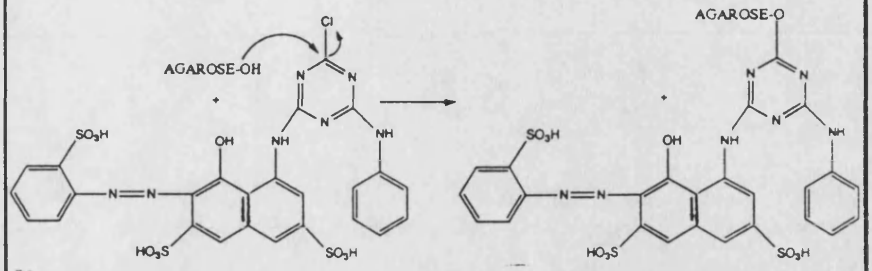
Thiol group/CL6-B	(1) AGAROSE-OH + 1-Chloro-2, 3-epoxypropane → AGAROSE-O-CH2-CH-CH2-O (2) AGAROSE-O-CH2-CH-CH2 + Na2+S2O3 2- + H2O → AGAROSE-O-CH2-CH(OH)CH2-S2O3 Na + Na OH (3) AGAROSE-O-CH2-CH(OH)CH2-S2O3 Na —DTT→ AGAROSE-O-CH2-CH(OH)CH2-SH

Fig 1.10: Preparation of chromatography matrices.

CHAPTER TWO:

MATERIALS, EQUIPMENT AND METHODS.

(2.1) **Materials.**

Vectors pUC19 and M13mp19, restriction endonucleases, DNA modifying enzymes and Lambda DNA - *Hind* III and *Pst* I molecular size markers were from Northumbria Biologicals Ltd., Cramlington, UK and Pharmacia LKB Ltd., Milton Keynes UK.

Agar, tryptone and yeast extract were from Difco, Michigan, USA. L-Leucine, L-Threonine, L-Tryptophan, Thiamine, Ampicillin and Streptomycin,were from Sigma, Poole, UK. IPTG and X-gal were from Northumbria Biologicals Ltd.

Nensorb™ nucleic acid purification cartridges were from DuPont, Stevenage, UK. Qiagen plasmid purification kits were from Diagen, Dusseldorf, Germany. Quickseal™ centrifuge tubes were from Beckman Instruments Inc., Palo Alto, USA. Agarose (normal and low melting point), was from Sigma. Sepharose CL6-B was from Pharmacia LKB Ltd. Distilled Phenol was purchased from Rathburn Chemicals Ltd., Walkerburn, UK.

[α-^{32}P]dATP (5000 Ci/mmol), [γ-^{32}P] ATP (3000 Ci/mmol) and [α-^{35}S]dATP (1000 Ci/mmol) was from NEN, Stevenage, UK. Hybond™-N hybridisation membrane and Oligonucleotide-directed *in vitro* mutagenesis kits were from Amersham International. Electran grade acrylamide; TEMED; Silane A-140 adhesion promoter and Dimethyldichlorosilane solution were from BDH. Oligodeoxyribonucleotide sequencing primers and probes were synthesised on an Applied Biosystems 381A DNA synthesiser (Applied Biosystems, Foster city, USA) or were obtained from Andrew Garman at Imperial Chemical Industries, UK.

Sequenase™ kits were from United States Biochemical Corporation, Ohio, USA. X-ray film was from Fuji photo film company, Japan.

Brij 58 was purchased from Aldrich Chemical company Ltd., UK. Visking dialysis membrane 3-20/32 was from Medicell International Ltd., London, UK. Protein molecular weight standards were from Pharmacia LKB Ltd. DTNB, NAD^+, NADH, Oxalacetate and L-Malic acid were from Sigma, Poole, UK. All other chemicals were from BDH UK, Fisons UK or Sigma UK.

(2.2) **Equipment.**

Preparation of samples which required centrifugation, made use of either Beckman model L5-65 ultracentrifuge with a 70.1Ti rotor for purification of supercoiled DNA on caesium chloride equilibrium density gradients, DuPont Sorvall RC-5B refrigerated superspeed centrifuge for large volumes, an Eppendorf centrifuge or a refrigerated centrifuge (Ole Dich, Denmark) for small volumes. Milli-Q™ reagent grade water system was from Millipore Corp., Bedford, USA. DNA thermal cycler was from Perkin-Elmer-Cetus instrument's division, Norwalk, USA and Techne PHC-2 from Techne, Cambridge, UK. SP8-400 UV/Vis and CE272 spectrophotometers were from Pye Unicam, Cambridge, UK. and Cecil Instruments, Cambridge, UK respectively. Sonicator was supplied by Ultrasonics Ltd., Shipley, UK. Speedvac concentrator was from Stratech Scientific, London, UK. DNA sequencing apparatus was from BRL, Gothenburg USA. Falcon 0.22μm bottle top filters were from Becton Dickinson, Plymouth, UK. The transilluminator was from UVP inc., Califonia USA. Flat bed gel scanner was from LKB, UK.

(2.3) *E.coli* Strains and Culture conditions.

A freeze dried culture of *E.coli* strain W945T1-2 was a gift from Dr. K. D. Entian of the Institut für Mikrobiologie, Goethe-Universität, Frankfurt. This strain was used for expression of both wild type and mutant MDH. The culture was initially grown on (LB) agar under aerobic conditions. Further growth was under defined medium conditions. Stock medium solution consisted of:

(a) D-glucose (50%, 100 x stock) filter sterilised through a 0.22 μm (Falcon filter) into autoclaved bottles.

(b) Casamino acids (10 $mg.ml^{-1}$, 10 x stock) sterilised by autoclaving.

(c) Thiamine (500 $\mu g.ml^{-1}$, 10 x stock), L-threonine (500 $\mu g.ml^{-1}$, 10 x stock), L-leucine (500 $\mu g.ml^{-1}$, 10 x stock) and L-tryptophan (500 $\mu g.ml^{-1}$, 10 x stock) were sterilised by autoclaving.

(d) M9 salts (10 x stock) of Na_2HPO_4 (60 $g.l^{-1}$), KH_2PO_4 (30 $g.l^{-1}$), NaCl (5 $g.l^{-1}$) and NH_4Cl (10 $g.l^{-1}$) were sterilised by autoclaving. Each was added to give a 1 x final concentration, using sterile techniques, into previously autoclaved bottles. Powdered streptomycin (50 $\mu g.ml^{-1}$ final concentration) and autoclaved $MgSO_4$ (0.2% final concentration) was added to defined medium and the volume made up with sterile water.

E.coli strain TG1 was used as the host for groups of plasmids. TG1 cultures were grown in undefined, sterile modified LB (NaCl 10 $g.l^{-1}$, yeast extract 10 $g.l^{-1}$, and tryptone 10 $g.l^{-1}$) and 2 x LB media (NaCl 10 $g.l^{-1}$, yeast extract 10 $g.l^{-1}$ and tryptone 20 $g.l^{-1}$). Solid agar (agar 1.5% w/v) and top agar (agar 0.8% w/v) media was made by dissolving agar in defined and undefined media to the required final concentration, supplemented with ampicillin (100 $\mu g.ml^{-1}$) where necessary. Cell cultures were stored at -20°C and -70°C in pure glycerol.

(2.4) **General reagents.**

General reagents were prepared as indicated below, sterilised where appropriate and stored under suitable conditions.

Chloroform:	24 : 1 Chloroform : Iso-amyl alcohol.
Ethidium bromide:	10mg per ml and 1 mg per ml, stored at 4°C in dark.
Phenol:	Distilled Phenol equilibrated with (Tris. HCl 50 mM pH 8.0), stored at -20°C.
Phenol/Chloroform:	1 : 1 Equilibrated Phenol : Chloroform.
Potassium acetate:	Potassium acetate (3M) : Glacial acetic acid (2M), pH 5.4 (Autoclaved).
TBE:	Tris. base, (0.89 M), Boric acid (0.89 M), EDTA (0.2 M)
TE:	Tris. HCl (100 mM), EDTA (1 mM) (autoclaved).

(2.5) **General Methods.**

(2.5.1) Quantification of DNA.

DNA concentration and purity were assessed spectrophotometrically by recording a spectrum from 340nm to 240nm in a 1 cm path length quartz cuvette. One absorbance unit at 260nm was taken as equivalent to 50 $\mu g.ml^{-1}$ of double stranded DNA or 33 $\mu g.ml^{-1}$ of single stranded DNA. Pure DNA samples were characterised by a 260nm absorbance peak with no trace of an absorbance shoulder at 280nm.

(2.5.2) Extraction of DNA with organic solvents.

(2.5.2.1) Phenol/Chloroform extraction of DNA.

An equal volume of equilibrated phenol/chloroform (Maniatis *et al*, 1982) was added to the aqueous DNA sample. The mixture was briefly vortexed and the two phases separated by centrifugation at 5,000g for 1 minute at room temperature. The upper aqueous phase containing the DNA was transferred to a fresh tube. The lower organic phase was discarded.

(2.5.2.2) Diethyl ether extraction of DNA.

Traces of phenol were removed from aqueous DNA samples by extracting three times with equal volumes of diethyl ether, followed by centrifugation at 5,000g for 1 minute at room temperature to separate the upper organic phase from the lower aqueous phase. The upper organic phase was discarded.

(2.5.3) Precipitation of DNA using ethanol or isopropanol.

(2.5.3.1) Precipitation of DNA using ethanol.

A 0.1 volume of sodium acetate (3 M, pH 5.4) (Maniatis *et al*,1982) and 2.5 volumes of ice-cold absolute ethanol were added to aqueous DNA, briefly vortexed and incubated for 20 minutes at -20°C. The DNA was centrifuged at 15,000g for 20 minutes at -20°C. The pellet was rinsed in 70% (v/v) ice-cold ethanol and re-centrifuged. DNA was dried under vacuum and dissolved in the desired volume of water.

(2.5.3.2) Precipitation of DNA using isopropanol.

DNA was precipitated by adding 0.6 volumes of isopropanol to aqueous DNA, briefly vortexed and incubated for 20 minutes at room temperature. The DNA was centrifuged at 15,000g for 20 minutes at room temperature. The supernatant was discarded and the pellet rinsed in 70% (v/v) ice-cold ethanol and dried under vacuum.

(2.5.4) Purification of DNA on "mini" spun columns.

(2.5.4.1) Sepharose CL6-B spun columns.

The apex of a 0.5 ml eppendorf tube was pierced with a 19G needle and the cap removed. The tube was filled to a height of 4 mm with 0.4 mm diameter glass beads. 450 µl (giving a bed volume of 350 µl) of a suspension of Sepharose CL6-B resin equilibrated with TE pH 8.0, was layered on top of the glass beads. The eppendorf tube was placed in a 1.5 ml eppendorf tube and centrifuged in a bench top centrifuge with swing out rotor at 3,000g for 4 minutes at room temperature. Water (25 µl) was layered on the surface of the column which was centrifuged as above. This was

repeated twice. The DNA sample (25 µl) was layered onto the column and the column placed in a fresh 1.5 ml eppendorf tube. The column was centrifuged as above and the eluate collected.

(2.5.4.2) Sephadex G-25 and G-50 spun columns.

The bottom of a 1 ml plastic syringe barrel was plugged with a small amount of siliconised glass wool and 1 ml of Sephadex G-25 (G-50) suspension equilibrated in TE (pH 8.0) pipetted into the barrel. Buffer was allowed to elute under gravity and the column topped up with the suspension until the bed volume was 1.0 ml. The syringe barrel was placed in a 15 ml Corex tube and centrifuged using a bench top centrifuge with swing out rotor at 3,000g for 4 minutes at room temperature. The packed volume of the Sephadex G-25 (G-50) column was approximately 0.9 ml. Water (80 µl) was added to the column, which was re-centrifuged at 3000g for 4 minutes at room temperature. This was repeated twice. The DNA sample (80 µl) was layered onto the column and the column re-centrifuged. The eluate was collected in a 1.5 ml eppendorf tube.

(2.5.5) Agarose gel electrophoresis.

Normal and LMP horizontal slab gels were made by suspending agarose powder in TBE (pH 8.3) and heating in a microwave until dissolved. The solution was left to cool to 55°C and ethidium bromide (0.5 $\mu g.ml^{-1}$ final concentration) added and mixed by gentle swirling. The sample was poured into a gel mould (11 cm x 11 cm) with gel comb affixed and allowed to set. Before loading, the sample was mixed with 5 x loading dye to a final DNA concentration of 10 $ng.\mu l^{-1}$ per band of DNA. To prevent smearing of the DNA no more than 200 ng of the desired DNA band per 0.5 cm slot width of agarose gel was electrophoresed. The DNA was electrophoresed at a constant current of 80 mA in TBE.

(2.5.6) Isolation of DNA from agarose gels.

Two methods have been routinely used to isolate DNA from agarose gels: (1) Freeze-squeeze (2) Geneclean® "kit".

(2.5.6.1) Freeze-squeeze.

The DNA sample was electrophoresed in an LMP agarose gel (2.5.5), illuminated with UV light and the required band excised. The apex of a 0.5 ml eppendorf tube was pierced with a 19G needle and plugged with a small amount of siliconised glass wool. Agarose containing the DNA was layered onto the glass wool and the eppendorf tube snap frozen in liquid nitrogen. The frozen eppendorf was placed inside a 1.5 ml eppendorf tube and centrifuged at 20,000g for 20 minutes at room temperature. Eluate containing the DNA that had exuded from the agarose, was collected in the larger tube.

(2.5.6.2) Geneclean.

All solutions and glassmilk were supplied in the kit. The required DNA band was excised as described above. TBE modifier (0.5 ml) and 4.5 ml of NaI (6M) was added per gram of agarose. Agarose was dissolved by heating at 60°C for 2 minutes followed by rapid cooling on ice. Re-suspended glassmilk was added to the solution, briefly vortexed and the solution incubated on ice for 15 minutes then centrifuged at 5,000g for 30 seconds at room temperature. Supernatant was removed and the glassmilk re-suspended in 0.2 ml of Geneclean "New" wash solution, vortexed, and incubated on ice for 5 minutes. This was repeated twice. Glassmilk was dried under vacuum and re-suspended in 20 µl of water. This solution was incubated at 55°C for 3 minutes prior to centrifugation. The supernatant was removed and glassmilk re-suspended in 20 µl of water, and incubation at 55°C repeated. Combined water supernatant fractions containing eluted DNA were stored at -20°C.

(2.5.7) Restriction digestion of DNA.

DNA was incubated with restriction endonucleases in specific restriction buffers or One-Phor-All buffer. Two to five units of restriction enzyme per μg of DNA was used in each digest. When several enzymes were used on a DNA sample, One-Phor-All buffer was used according to manufacturers instructions, or specific buffers were modified for optimal reaction conditions. All digests were for 1 hour at 37°C unless otherwise indicated.

(2.5.8) Ligation of DNA.

Ligation of DNA with recessed ends was carried out with equimolar amounts of vector and insert. Flush end ligations were prepared with a vector to insert ratio of 1:3. The ligation reaction in 20 μl of buffer (Tris-HCl 50 mM pH 7.8, $MgCl_2$ 6 mM, DTT 20 mM, ATP 1 mM and BSA 100 $\mu g.ml^{-1}$) with T4 DNA Ligase (0.1 U for recessed ends, 1 U for flush ends) and approximately 50 ng of vector were incubated for 15 hours at 16°C or 4 hours at room temperature.

(2.5.9) End-fill of recessed 3' end of DNA.

Recessed 3' ends of DNA were extended by incubating in the presence of 125 μM of each dNTP with 1 U of Klenow fragment of DNA Polymerase I in 30 μl of buffer (Tris-HCl 50 mM pH 7.2, $MgSO_4$ 100 mM, DTT 0.1 mM and BSA 50 $\mu g\ ml^{-1}$) at room temperature for 30 minutes. The enzyme was inactivated by incubation at 70°C for 10 minutes. Buffer and nucleotides were removed by passing through a Sephadex G-25 column (2.5.4).

(2.6) **DNA Methods.**

(2.6.1) Manipulation of *E.coli* cultures.

Manipulation of *E.coli* cultures were carried out in accordance with "good microbiological practice". Disinfection of equipment and cell cultures was achieved by treating with 2% Hycolin solution.

(2.6.2) Preparation of *E.coli* competent cells.

Overnight cultures of TG1 and W945T1-2 were prepared by inoculating a single colony from a glucose minimal medium plate or frozen stock into 5 ml of LB (TG1) or 20 ml of defined media (W945T1-2) and shaken overnight at 37°C. Aliquots (2 ml) of the overnight cultures were transferred to 40 ml of LB (TG1) or 20 ml of defined media (W945T1-2) and incubated at 37°C in an orbital shaker (Gallenkamp) at 150 cycles per minute. When an OD_{595nm} of 0.3 was reached, 0.5 ml of the TG1 culture (2ml of W945T1-2) were transferred to 50 ml of appropriate medium (pre-warmed to 37°C) and incubation continued. When this culture reached an OD_{595nm} of 0.3, the cells were immediately chilled in ice-water for 10 minutes and centrifuged in a pre-cooled rotor at 3,000g for 10 minutes at 4°C. The pellet was re-suspended in ice-cold sterile $CaCl_2$ (50 mM), incubated on ice for 30 minutes, and re-centrifuged. Cells were re-suspended in 5 ml of $CaCl_2$ (50 mM) and kept on ice until required. Competent cells were used within 8 hours.

(2.6.3) Transformation of *E.coli* competent cells with plasmid and RF M13 DNA.

(2.6.3.1) Transformation of *E.coli* TG1 and W945T1-2 cells with Plasmid DNA.

Plasmid DNA (10 ng) was mixed with 300 µl of competent cells (2.6.2), and incubated on wet ice for 30 minutes. Cells were transferred to thin walled glass tubes (~1 mm diameter glass wall) and incubated for 2 minutes at 42°C. The transformed cells were allowed to recover in LB (1 ml) for 1 hour at 37°C without shaking. The cell culture was centrifuged at 3,000g. Supernatant was discarded, and the cells re-suspended in 150 µl of LB. Transformed cells (50 µl) were plated out on appropriate agar with appropriate antibiotics and 20 µl of IPTG (100 mM) and 50 µl of X-gal (2% w/v in dimethyl formamide) for β-galactosidase colour selection with *lac* Z plasmids.

(2.6.3.2) Transformation of *E.coli* TG1 with RF M13 DNA.

Solid agar media was prepared, poured into culture plates and allowed to solidify. Cells were transformed with RF M13 DNA (10 ng) in a similar manner to plasmid transformed cells. IPTG (20 µl ,100mM), X-gal (50 µl, 2% w/v), 200 µl of log phase cells and 50 µl of transformed cells were mixed by swirling with 3 ml of molten top agar (in lawn tubes) standing in a heating block at 45°C. The molten top agar was poured over the solid agar media, allowed to solidify and the plate incubated at 37°C.

(2.6.4) Preparation of phage stocks.

An aliquot (200 µl) of overnight TG1 culture (2.6.2) was inoculated into 5 ml of LB and incubated for 30 minutes at 37°C on an orbital shaker (2.6.2). The culture was inoculated with a single plaque, and incubation continued for 15 hours. A 1 ml aliquot

of the culture was transferred to a 1.5 ml eppendorf tube and centrifuged at 5,000g for 10 minutes at room temperature. The supernatant was transferred to a clean reaction tube and the pellet discarded. Chloroform (50 µl) was added to the supernatant and the phage stock stored in the dark at room temperature.

(2.6.5) Small scale preparation of plasmid and RF M13 DNA.

(2.6.5.1) Plasmid DNA.

A 1 ml aliquot of an overnight culture of transformed cells carrying the desired plasmid (2.6.2) was transferred to a 1.5 ml eppendorf tube and centrifuged at 5,000g for 10 minutes at room temperature. The supernatant was discarded and the pellet re-suspended by briefly vortexing in 100 µl of an ice-cold solution of (Tris HCl 25 mM pH 8.0, glucose 50 mM and EDTA 10 mM), and incubating for 10 minutes at room temperature. Cells were lysed by adding 200 µl of a freshly prepared solution of NaOH (0.2 M), SDS (1% w/v), mixed by inversion, and incubated for 10 minutes on ice. Genomic DNA protein and SDS were precipitated by adding 150 µl of an ice-cold solution of potassium acetate (3M pH 4.8), gently vortexing and incubating on ice for 10 minutes. The precipitate of chromosomal DNA and protein was pelleted by centrifugation at 20,000g for 10 minutes at 4°C. The supernatant was transferred to a fresh 1.5 ml eppendorf tube and the pellet discarded. Further purification and concentration of the DNA was achieved by phenol/chloroform extraction (2.5.2) and precipitation with ethanol (2.5.3).

(2.6.5.2) RF M13 DNA.

A 0.5 ml aliquot of overnight culture (2.6.2) was inoculated into 50 ml of 2 x LB and incubated at 37°C on an orbital shaker (2.6.2). When an OD_{595nm} of 0.3 was reached, 100 µl of phage stock (2.6.3) was inoculated into the culture and incubation

continued for a further 10 hours at 37°C. The culture was transferred to a centrifuge tube and centrifuged at 5,000g for 10 minutes at room temperature. The supernatant was discarded and the pellet suspended in a 1 ml solution (Tris. HCl 25 mM pH 8.0, glucose 50 mM, EDTA 10 mM and lysozyme 5 $\mu g.ml^{-1}$), and incubated for 10 minutes at room temperature. Cells were lysed by adding 2 ml of (NaOH 0.2 M, SDS 1% w/v) solution, mixed and incubating for 10 minutes on ice. Genomic DNA protein and SDS were precipitated by adding 1.5 ml of an ice-cold solution of potassium acetate (3 M pH 4.8), gently vortexed and incubated on ice for 10 minutes. The precipitate was pelleted by centrifugation at 10,000g for 10 minutes at 4°C. Remaining protein was removed from the DNA by phenol/chloroform extraction (2.5.2) and DNA concentrated by precipitation of DNA with ethanol (2.5.3).

(2.6.6) Large scale preparation of plasmid and RF M13 DNA.

(2.6.6.1) Plasmid DNA.

An aliquot (0.5 ml) of overnight culture (2.6.2) harbouring plasmid was inoculated into 500 ml of LB or 2 x LB containing appropriate antibiotics and incubated overnight at 37°C on an orbital shaker at 150 cycles per minute. The culture was transferred to 300 ml polyethylene centrifuge tubes and centrifuged at 5,000g for 10 minutes at room temperature. The supernatant was discarded and the cells re-suspended in a 10 ml solution of (Tris-HCl 25 mM pH 8.0, glucose 50 mM, EDTA 10 mM and lysozyme 5 $\mu g.ml^{-1}$). Cells were transferred to MSE centrifuge tubes and incubated for 10 minutes at room temperature then lysed by adding a 20 ml solution of (NaOH 0.2 M, SDS 1% w/v), briefly vortexed and incubated for 10 minutes on ice. Genomic DNA protein and SDS was removed by adding 15 ml of an ice-cold solution of potassium acetate (3 M pH 4.8). This solution was gently vortexed and incubated for 10 minutes on ice, then centrifuged at 20,000g for 10 minutes at 4°C. The supernatant was transferred to two 30 ml Corex tubes and DNA precipitated with

isopropanol (2.5.3). Plasmid DNA was purified using caesium chloride equilibrium density gradient centrifugation (2.6.10).

(2.6.6.2) RF M13 DNA.

A 3 ml aliquot of overnight culture (2.6.2) was inoculated into 500 ml of 2 x LB and incubated at 37°C on an orbital shaker at 150 cycles per minute. When an OD_{595nm} of 0.3 was reached, 1 ml of phage stock (2.6.4) was inoculated into the culture and incubation continued for a further 10 hours at 37°C. The culture was transferred to 300 ml polyethylene centrifuge tubes and processed in a similar manner as plasmid DNA (2.6.6).

(2.6.7) Preparation of single stranded M13 DNA template.

(2.6.7.1) Small scale preparation of template DNA.

A 200 µl aliquot of overnight TG1 culture (2.6.2) was inoculated into 5 ml of 2 x LB and incubated for 30 minutes at 37°C on an orbital shaker at 150 cycles per minute. The culture was inoculated with 50 µl of phage stock (2.6.3) and incubation continued for 6 hours. Phage particles were separated from cells and debris by transferring the culture to a 15 ml Corex tube and centrifuging at 5,000g for 30 minutes at room temperature. The supernatant was transferred to 1.5 ml eppendorf tubes and the pellet discarded. Phage particles were precipitated by adding 0.15 volumes of PEG/NaCl solution (PEG 6000 20% w/v, NaCl 2.5 M), briefly vortexed and incubated for 30 minutes at room temperature. The solution was centrifuged at 13,000g for 30 minutes at 10°C and the supernatant discarded. The phage pellet was re-suspended in 1 ml of LB and transferred to a 1.5 ml eppendorf tube and precipitation of phage particles repeated with 500 µl of PEG/NaCl solution. The solution was centrifuged at 20,000g for 10 minutes at room temperature and the supernatant discarded. Traces of

PEG/NaCl were removed from the pellet by re-centrifuging at 20,000g for 1 minute at room temperature and removing PEG/NaCl from the sides of the pellet with a paper tissue. This was repeated until no further PEG/NaCl could be removed. The template DNA was removed from the phage protein coat by phenol/chloroform extraction (2.5.2), and template DNA precipitated with ethanol (2.5.3).

(2.6.7.2) Large scale preparation of template DNA.

A 1 ml aliquot of overnight TG1 culture (2.6.2) was inoculated into 100 ml of 2 x LB medium and incubated at 37°C on an orbital shaker at 150 cycles per minute. When an OD_{595nm} of 0.3 was attained the culture was inoculated with 1 ml of phage stock (2.6.4) and incubation continued for 4 hours at 37°C. The culture was transferred to MSE centrifuge tubes and centrifuged at 5,000g for 30 minutes at room temperature. The supernatant was transferred to a fresh centrifuge tube, the pellet discarded, and phage particles precipitated by adding 0.2 volumes of PEG/NaCl solution (PEG 6000 20% w/v, NaCl 2.5 M), briefly vortexing and incubating on ice for 1 hour. The solution was centrifuged at 5,000g for 30 minutes at 10°C and the supernatant discarded. Traces of PEG/NaCl were removed from the pellet by re-centrifuging at 5,000g for 5 minutes at room temperature and wiping the sides of the pellet with a paper tissue. This was repeated until no further PEG/NaCl could be removed. The phage pellet was re-suspended in 500 µl of buffer (Tris-HCl 10 mM pH 8.0, EDTA 0.1 mM) and transferred to a 0.5 ml eppendorf tube. Remnants of cell debris were removed by centrifuging at 5,000g for 10 minutes at room temperature and transferring the supernatant to a fresh 1.5 ml eppendorf tube. The pellet was discarded. Phage particles were re-precipitated with 200 µl of PEG/NaCl solution and centrifuged at 20,000g for 5 minutes at room temperature in a microfuge. Traces of PEG/NaCl were removed from the phage pellet in a similar manner as above. The phage pellet was suspended in 500 µl of buffer and transferred to two 1.5 ml eppendorf tubes. The DNA template was removed from the phage protein coat by extracting: (1) twice with

100 µl of phenol (2.5.2) with the upper aqueous phase being transferred to a fresh centrifuge tube each time. (2) four times with 250 µl of diethyl ether (2.5.2) with the top layer being discarded. (3) twice with 250 µl of chloroform, with the top layer being transferred to a fresh 1.5 ml eppendorf tube. The template DNA solutions were further split into two 1.5 ml eppendorf tubes and the DNA precipitated with ethanol (2.5.3).

(2.6.8) Purification of DNA using a Nensorb column.

A Nensorb column pre-wetted with 2 ml of methanol was washed with 2 ml of buffer (Tris-HCl 0.1 M pH 7.7, Triethylamine 10 mM and EDTA 1 mM). The DNA sample was loaded onto the column and slowly passed through the sorbent with the aid of slight pressure from a 10 ml syringe. The eluate was re-loaded twice. The sorbent was washed with 2 ml of buffer followed by elution of the DNA with 0.5 ml of methanol (50%), and dried under vacuum. The DNA was dissolved in the desired amount of water.

(2.6.9) Purification of DNA using a Qiagen column.

An overnight culture (2.6.2) of TG1 (5 ml) harbouring plasmid was transferred to a 15 ml centrifuge tube (Corex) and centrifuged at 3,000g for 10 minutes at room temperature. The supernatant was discarded and the pellet re-suspended in 300 µl of buffer (Tris-HCl pH 8.0, 50 mM, EDTA 10 mM and RNAse A 400 $\mu g.ml^{-1}$) and transferred to a 1.5 ml eppendorf tube. Cells were lysed by adding 300 µl of (NaOH 200 mM, SDS 1% w/v), gently vortexing and incubating for 5 minutes at room temperature. Genomic DNA protein and SDS were precipitated by addition of 300 µl of potassium acetate (2.55 M pH 4.8). The solution was centrifuged at 15,000g for 15 minutes at room temperature and the supernatant layered onto Qiagen tip-20 resin pre-wetted with 1 ml of buffer (MOPS 50 mM pH 7.0, NaCl 0.75 M, and ethanol 15% v/v).The resin was washed with 2 ml of buffer (MOPS 50 mM pH 7.0,

NaCl 100 mM, and ethanol 15% v/v) under gravity. DNA was eluted off the resin under gravity with 0.8 ml solution (MOPS 50 mM pH 8.0, NaCl 1.5 M and ethanol 15% v/v), then precipitated with isopropanol (2.5.3). The sample was dissolved in the desired volume of water.

(2.6.10) Caesium chloride equilibrium density gradient centrifugation.

Isolation of pure supercoiled plasmid DNA was achieved by dissolving 1 gram of caesium chloride and 80 µl of ethidium bromide (10 $mg.ml^{-1}$) per ml of impure DNA solution. The final density of the solution was 1.55 $g.ml^{-1}$ with 600 $\mu g.ml^{-1}$ ethidium bromide. The solution was transferred to a polyallomer centrifuge tubes, sealed and centrifuged in a Beckman 70.1Ti rotor at 200,000g for 15 hours at 20°C. Supercoiled DNA was visualised as the lower band by illuminating the centrifuge tube with UV light. It was removed from the centrifuge tube by piercing the centrifuge tube at the top then at the side just below the band with a 19G needle, then drawing the supercoiled DNA band into a syringe attached to the needle. An equal volume of caesium chloride saturated 1-butanol was added to the DNA sample, mixed by inverting the syringe several times and the phases allowed to separate. The upper organic phase containing the ethidium bromide was discarded. This extraction process was repeated until the ethidium bromide had been removed from the aqueous phase. The sample was diluted with an equal volume of water and two volumes of absolute ethanol was added to this sample. The DNA was precipitated at room temperature for 30 minutes, then centrifuged in a Corex tube at 10,000g for 30 minutes at room temperature. The supernatant was discarded and the pellet rinsed with ice-cold ethanol (70% v/v), re-centrifuged and dried under vacuum. The DNA was re-dissolved in water and re-precipitated with ethanol three times to remove traces of caesium chloride (2.5.3).

(2.6.11) Preparation of oligonucleotides.

(2.6.11.1) Design of oligonucleotides.

Oligonucleotides were synthesised, the sequence of which were complimentary to the DNA molecule to be mutagenised, apart from one or several specific and pre-determined nucleotide changes. These changes encoded codon changes and where appropriate introduced unique restriction sites. The nucleotide changes were designed to:

- Aid directional cloning of PCR fragments DNA.
- Aid in identification of mutations by either restriction fragment analysis or colony hybridisation.

(2.6.11.2) Synthesis and purification of oligonucleotides.

Oligonucleotides were synthesised on an Applied Biosystems 381A DNA synthesiser, in 0.2 μmol quantities on solid phase support or obtained from ICI Diagnostics in a ready to use form.

The support cartridge containing the oligonucleotide was removed from the synthesiser, and the oligonucleotide cleaved from the support with 1 ml of ammonia solution (sp. gr. 0.88). One syringe containing ammonia solution was attached to the inlet of the support cartridge and 300 μl drawn into the matrix with the aid of second syringe attached to the cartridge outlet. A further 200 μl of ammonia solution was drawn into the matrix every 20 minutes. The ammonia solution containing the oligonucleotide was placed in a 2 ml screw cap eppendorf tube and incubated for a minimum of 6 hours at 55°C. The ammonia solution was removed by drying the oligonucleotide under vacuum, followed by re-dissolving the oligonucleotide in 1 ml of water. Oligonucleotides were precipitated with addition of 3 volumes of ethanol and

0.1 volumes of sodium acetate solution (3 M pH 4.8) (2.5.3), dried under vacuum and re-dissolved in water. The concentration of aqueous oligonucleotide was determined by recording a spectrum in the UV range (2.5.1). An absorbance unit of 1 at 260nm was equivalent to 37$\mu g.ml^{-1}$ of oligonucleotide.

(2.6.11.3) 5' End labelling of oligonucleotides with T4 Polynucleotide Kinase.

Oligonucleotide (25 ρmol) was incubated with 1 unit of T4 Polynucleotide Kinase, with an equimolar amount of [γ-^{32}P] ATP (3000 Ci/mmol), in 20 µl of buffer (Tris-HCl 50 mM pH 7.6, $MgCl_2$ 100 mM, dithiothreitol 5 mM, spermidine 0.1 mM and EDTA 1 mM). After incubation for 30 minutes at 37°C, 1 µl of ATP (10 nmol) was added and the solution incubated for a further 15 minutes.

(2.6.11.4) Determination of size and purity of oligonucleotide.

Oligonucleotides were checked for purity by electrophoresis in a 20% (w/v) polyacrylamide gel of dimensions (15cm x15cm x 0.35mm). Ammonium persulphate (8 µl per ml of 10%w/v) and 0.4 µl per ml of TEMED were added to Sequagel™ acrylamide solution and quickly mixed by swirling. Gels were cast by silanizing one side of the front glass plate with dimethyldichlorosilane solution and pouring acrylamide solution between the two plates whose edges were sealed (the silanized surface being in contact with the acrylamide solution). A rectangular toothed comb was inserted before polymerisation. The end-labelled oligonucleotide (3.75 ρmol) was mixed with 5 x formamide loading dye (formamide 95%, EDTA 20 mM, bromophenol blue 0.05% and xylene cyanol FF 0.05%) prior to loading and incubated for 2 minutes at 70°C. Oligonucleotides were electrophoresed in TBE at 16 W for 1 hour. The glass plates were separated, and the gel which adhered to the back plate was covered in Saran-wrap™, and exposed to pre-flashed X-ray film at -70°C with an intensifying

screen. The quality of the oligonucleotide was assessed by observing the range of bands and their intensities in relation to known standards.

(2.6.12) Sequencing of DNA.

The sequencing protocol used was that of the USB corporation Sequenase™ kit as outlined below. This Kit is based on the dideoxynucleotide chain termination method of Sanger *et al*, (1977).

(a) Preparation of template DNA from Plasmid DNA.

Denaturing solution (5 µl of NaOH 1 M, EDTA 1 mM) was added to 20 µl of plasmid preparation (0.5 $\mu g.\mu l^{-1}$) and incubated for 5 minutes at room temperature. The denatured DNA solution was desalted by passing the solution through a Sepharose CL6-B column (2.5.4). A volume of 7 µl of the denatured DNA was used for one sequencing reaction.

(b) Annealing.

DNA solution (1 µg of single stranded DNA or 3 µg of denatured plasmid DNA) in a total volume of 7µl was mixed with 2 µl of 5 x sequencing buffer (Tris-HCl 200 mM pH 7.5, $MgCl_2$ 100 mM and NaCl 250 mM) and 1 µl of oligonucleotide primer (1 ρmol) in a 1.5 ml eppendorf tube and incubated for 2 minutes at 65°C, followed by slow cooling (30 minutes) to 30°C in water.

(c) Labelling reaction.

Sequenase sequencing enzyme was diluted 1:8 just before use with ice-cold buffer (Tris-HCl 10 mM, DTT 5 mM and BSA 0.5 $mg.ml^{-1}$) and kept on ice. To the

"annealing" reaction mixture was added 1 µl of DTT 0.1 M, 0.5 µl of 5 µCi [α-^{35}S] ATP, and 2 µl of labelling mix (dGTP 1.5 µM, dCTP 1.5 µM and dTTP 1.5 µM), mixed and equilibrated at 23°C in a water bath. Diluted Sequenase™ enzyme (2 µl) was added to the labelling mixture, briefly mixed and incubated at 23°C for 3 minutes. Reaction tubes containing 2.5 µl of termination mixture (Nucleotides dATP 80 µM, dCTP 80 µM, dGTP 80 µM, dTTP 80 µM and NaCl 50 mM with 8 µM of one of the following dideoxynucleotides ddATP, ddCTP, ddGTP, ddTTP) were pre-warmed to 37°C in a water bath. To each of the termination mixes, 3.5 µl of the labelling reaction was added, gently mixed then incubated at 37°C for 5 minutes. Stop solution, (4 µl of formamide 95%, EDTA 20 mM, bromophenol blue 0.05% and xylene cyanol FF 0.05%) was added to the termination reaction, mixed by vortexing and stored at -20°C until required.

(2.6.13) Polyacrylamide gel electrophoresis (sequencing gel).

Sequencing reactions were analysed by electrophoresis in an 8% (w/v) polyacrylamide gel (33.3cm x 39.5cm x 0.4-1mm wedge spacers). Ammonium persulphate (8µl per ml of 10 % w/v) and 0.4 µl per ml of TEMED were added to Sequagel™ acrylamide solution and quickly mixed by swirling. One side of the front glass plate was treated with 2 % dimethyldichlorosilane solution, the gels cast by pouring acrylamide between the two glass plates whose edges were sealed (the treated surface being in contact with the acrylamide solution). The back of a shark tooths comb was inserted into the acrylamide before polymerisation.

Samples in stop solution (2.6.12) were heated to 70°C for 2 minutes. The sharks tooth comb was reversed and 3 µl of sample electrophoresed at 45W in TBE buffer for 3 hours. The plates were separated, and the gel, attatched to the back plate, cross linked in (methanol 5%, acetic acid 5%) solution for 40 minutes, then washed in running water for 40 minutes and transferred to Whatman 3 MM paper. The gel was

dried under vacuum at 70°C, then exposed to X-ray film at room temperature for 24 hours to 1 week and developed.

(2.6.14) Site directed mutagenesis of the *E.coli* MDH gene.

Two methods were employed for site directed mutagenesis of the cloned *E.coli* MDH gene: (1) Oligonucleotide-directed *in vitro* mutagenesis (Amersham mutagenesis system version 2), and (2) Site directed mutagenesis using the polymerase chain reaction (Reidhaar-Olson and Sauer 1988).

(2.6.14.1) Mutagenesis of the *E.coli* MDH gene using the Amersham Oligonucleotide-directed *in vitro* mutagenesis system.

All solutions were provided in the Amersham Oligonucleotide-directed *in vitro* mutagenesis kit. Single stranded M13 template (5μg), 5' end labelled mismatched oligonucleotide (4.0 ρmol) and buffer#1 were mixed and made up to volume with water. The mismatched oligonucleotide was annealed to the positive strand template by incubating for 3 minutes at 37°C, then extended and ligated in a single reaction by addition of nucleotide "mix 1" (substituting dCTPαS), Klenow fragment of DNA Polymerase I (6 U) and T4 DNA Ligase (2 U) and incubating for 15 hours at 16°C. Closed circle heteroduplex DNA was separated from template DNA and partially synthesised heteroduplex DNA, by the addition of NaCl (0.62 M final concentration), and centrifuged at 500g for 10 minutes through a nitrocellulose membrane of a centrifuge cartridge. The heteroduplex DNA was precipitated with ethanol (2.5.3), dried under vacuum and dissolved in buffer#2.

The non-mutated positive strand of the heteroduplex DNA was partially digested by first mixing heteroduplex DNA solution with buffer#3 and restriction enzyme *Nci* I (5 U) and incubating for 90 minutes at 37°C. The nicked heteroduplex DNA was

then mixed with buffer#4, NaCl (67 mM final concentration) and Exonuclease III (50 U) and incubated for 30 minutes at 37°C. Homoduplex DNA was prepared by mixing the digested heteroduplex DNA with nucleotide "mix 2", $MgCl_2$ solution, DNA Polymerase I (3 U) and T4 DNA Ligase (2 U), then incubating for 4 hours at 16°C. The homoduplex DNA was precipitated using ethanol (2.5.3) and dissolved in 100 µl of water.

(2.6.14.2) Mutagenesis of the *E.coli* MDH gene using the PCR.

A sense and anti-sense oligonucleotide (1.0 µM final) were mixed with 10 µl of reaction buffer (Tris-HCl 100 mM, pH 8.3, KCl 500 mM and gelatine 0.1% w/v) and dNTPs (200 µM) in a dimethyldichlorosilane treated eppendorf tube. Target DNA (approx. 2 x 10^8 copies) and $MgCl_2$ (final concentration of 1 to 5 mM), were mixed and the volume made up to 100 µl with water. This solution was chilled on ice for 10 minutes prior to addition of Ampitaq™ Taq DNA Polymerase (0.025 $U.\mu l^{-1}$). DNA amplification was allowed to proceed for 25 cycles. Amplification on the Techne PHC-2 DNA thermal cycler required 50 µl of light mineral oil (Sigma) to be layered onto the surface of the DNA solution. The time allowed for synthesis of template DNA depended on the size of the target DNA being amplified (Table 2.1).

(2.6.15) Colony hybridisation.

Recombinant clones of MDH mutants in either phage or plasmid were identified by hybridisation at high stringency with the oligonucleotide used to create them. Either colonies or plaques were picked and grown in 0.1 ml LB in titre plates overnight at 37°C (2.6.3). Hybond™-N nitrocellulose membrane was placed on the surface of an agar plate and samples from each titre well streaked onto the membrane and incubated overnight at 37°C. The membrane was removed from the agar and placed colony side up on Whatman 3 MM paper soaked in denaturing solution (NaCl 1.5 M,

Step	Time (minutes)	Fragment size (base pairs)	Temperature (°C)
Template melting	1.5		94
Oligonucleotide annealing	1.25		50
Template DNA Synthesis	1.0	<400	72
	1.25	>400 <700	72
	2.0	>700	72

Table 2.1: Conditions used for PCR amplification with 25 cycles of amplification.

NaOH 0.5 M) for 7 minutes at room temperature, then transferred to 3 MM paper soaked in neutralising solution (NaCl 1.5 M, Tris-HCl 0.5M, EDTA 10 mM) for 3 minutes at room temperature. The membrane was washed in 2 x SSC and allowed to air dry. The membrane was covered in Saran-wrap and DNA fixed to the membrane by placing colony side down on a transilluminator and exposing to UV light for 4 minutes.

The membrane was pre-hybridised for 15 hours at 37°C in 25 ml of (5 x SSC, 5 x Denhartd's solution, and SDS 0.5 % w/v) on an orbital shaker set at 25 cycles per minute, then 25 ρmol of [^{32}P] end-labelled oligonucleotide was added and incubation continued for a further 15 hours at 37°C. The membrane was washed with wash solution (2 x SSC, SDS 0.1% w/v) for 10 minutes at 37°C, then covered in Saran-wrap and exposed to pre-flashed X-ray film at -70°C between two intensifying screens. The membrane was washed at increasing stringent conditions increasing temperatute and exposed to X-ray film. Generally strongly hybridising clones could be identified after washing the membrane at temperatures above the T_m of the oligonucleotide.

(2.7) **Expression and purification of MDH.**

(2.7.1) Expression and purification of plasmid encoded MDH.

(2.7.1.1) Preparation of Procion red H3-B/CL6-B matrix.

Procion red H3-B/CL6-B matrix was prepared using a modification of the method of Atkinson *et al,* (1982).

Moist Sepharose CL6-B slurry, water (5.5 ml per gram of slurry) and powdered Procion red (41 mg per gram of slurry) were mixed, and incubated for 10 minutes at 37°C on an orbital shaker set at 75 cycles per minute. Sodium chloride (0.4 ml per gram of CL6-B of 5M) was then added to the suspension and incubation continued for

30 minutes. NaOH (0.12 $ml.ml^{-1}$ of suspension of 5M) was added to the suspension and incubation continued for 48 hours at 37°C on an orbital shaker at 25 cycles per minute. Unbound Procion red was removed by washing sequentially with copious volumes of water, NaCl (1M) in 25% ethanol, a further washing in water and finally NaCl (1M). The derivatized Procion red/Sepharose matrix was stored in phosphate buffer (0.1M pH7.2) at 4°C.

This matrix was re-suspended in phosphate buffer (0.1 M pH 7.2) and packed into a 1.5 cm diameter chromatography column. Phosphate buffer (0.1M pH 7.2) was allowed to elute under gravity and the column topped up with suspension until a bed volume of 35ml was obtained. Prior to loading the dialysate of the ammonium sulphate purification step, the column was pre-equilibrated for 15 hours with phosphate buffer (0.1 M pH 7.2), containing β-mercaptoethanol (1 mM) at a flow rate of 2 ml per minute at 4°C.

(2.7.1.2) Preparation of modified Sepharose CL6-B matrix containing thiol groups.

Modified Sepharose matrix containing thiol groups was prepared using a modification of the method of Axen *et al*, (1975).

Moist Sepharose CL6-B was added slowly to a solution of sodium hydroxide (0.8 ml 1 M) containing 1-chloro-2,3-epoxypropane (700 μmol) per gram of Sepharose and incubated for 1 hour at room temperature on an orbital shaker set at 75 cycles per minute. The temperature was increased to 60°C and incubation maintained for 2 hours. The activated Sepharose was washed with copious amounts of water until the pH of the suspension was ~7.0. Activated Sepharose was washed in phosphate buffer (0.5 M pH 6.3), interstitial fluid removed from the Sepharose by filtration and re-suspended on 2 ml of phosphate buffer (0.5 M pH 6.3) per gram of Sepharose. A

solution of sodium thiosulphate (1 ml of 2M per gram of Sepharose) was added and incubation continued for 6 hours at room temperature. The Sepharose was washed with copious amounts of water, interstitial fluid removed and the Sepharose re-suspended in a solution of sodium bicarbonate (2ml of 0.1 M per gram of Sepharose). To the suspension was added excess DTT and the suspension stored at 4°C. The matrix was packed into a 0.5 cm diameter chromatography column. The buffer was allowed to elute under gravity and the column topped up with suspension until a bed volume of 1 m was obtained. Prior to loading the cell-extract the column was equilibrated with phosphate buffer (0.1 M pH 7.2).

(2.7.2) Preparation of cell-free extracts of plasmid encoded MDH.

(2.7.2.1) Small scale preparation of cell-free extract.

An aliquot from an overnight culture (2.6.2) harbouring the plasmid was transferred to a 1.5 ml eppendorf tube and centrifuged at 5,000g for 10 minutes at room temperature. The supernatant was discarded and the pellet re-suspended by briefly vortexing in 1 ml of phosphate buffer (0.1M pH 7.2). The cell suspension was centrifuged at 5,000g for 10 minutes at room temperature and the supernatant discarded. Cells were re-suspended in 200 µl of phosphate buffer (0.1 M pH 7.2) and the eppendorf tube packed in ice. Cells were sonicated at 50 W with a 3 mm probe for 15 seconds followed by a pause of 30 seconds. This was repeated 4 times. The gelatinous lysate was centrifuged at 5,000g for 10 minutes at room temperature and the supernatant transferred to a fresh eppendorf tube and stored at 4°C. The pellet was discarded.

MDH activity was ascertained under standard conditions at 30°C by optimising the method of Smith *et al,* (1982). A cell-free extract (10µl) was added to 980 µl of phosphate buffer (0.1 M pH 7.2) containing NADH (0.14 mM final concentration) in a

1 cm path length polystyrene cuvette, incubated at 30°C. Oxaloacetate (10 µl, 0.3 mM final concentration) was added and the solution mixed. The rate of decrease in absorbance at 340nm due to the oxidation of NADH to NAD^+ was measured on a recording spectrophotometer. One unit of MDH activity was defined as catalysing the oxidation of 1 µmol NADH per minute at 30°C.

(2.7.2.2) Large scale preparation of cell-free extract.

An aliquot from an overnight culture (2.6.2) harbouring plasmid was inoculated into 50 ml of defined medium containing appropriate antibiotics and incubated overnight at 37°C on an orbital shaker at 150 cycles per minute. A 25 ml aliquot of this culture was inoculated into 2.5 l of pre-warmed defined medium containing antibiotics and incubation continued for 16 hours at 37°C on an orbital shaker at 75 cycles per minute. The culture was transferred to 300 ml Sorvall polyethylene centrifuge tubes and centrifuged at 5,000g for 10 minutes at room temperature. The supernatant was discarded and the cells re-suspended in a 100 ml of phosphate buffer (0.1 M pH 7.2). Cell suspensions were pooled and centrifuged as above. MDH cell-free extracts were prepared by a modified method of Smith *et al*, (1982). The supernatant was discarded and the cells re-suspended in 20 ml of lysis buffer, (Tris-HCl 40 mM pH 8.0, EDTA 5 mM and lysozyme 250 $\mu g.ml^{-1}$) transferred to MSE centrifuge tubes, and incubated for 30 minutes at room temperature. A solution of Brij 58 and $MgSO_4$ (0.5% and 20 mM final concentrations) was added to the cell suspension, vortexed and incubation continued for 30 minutes at room temperature. The centrifuge tube was embedded in ice and the cell suspension sonicated at 50 W for 1 minute with a 3 mm probe, followed by a pause of 1 minute. This was repeated 6 times. The gelatinous lysate was centrifuged at 15,000g for 30 minutes at 4°C and the pellet discarded. The supernatant was transferred to a fresh MSE centrifuge tube, sealed with Nesco film and kept at 4°C until required.

(2.7.3) Purification of MDH.

(2.7.3.1) Method I.

Initially the method used for purification of MDH from cell-free extract was a modified method of Smith *et al,* (1982). The cell-free extract (2.7.2) was layered onto the surface of the Procion red/Sepharose chromatography column and allowed to bind overnight at a flow rate of 2 ml per minute at 4°C. The column was washed with 3 litres of phosphate buffer (10 mM pH 7.2) containing KCl (20 mM), 200 ml of phosphate buffer containing L-malate (10 mM), 100 ml of phosphate buffer containing KCl (20 mM), 350 ml of phosphate buffer containing KCl (20 mM) and NAD^+ (0.35 mM). The MDH was eluted from the column using phosphate buffer containing NAD^+ (0.35 mM) and L-malate (10 mM). The active fractions were pooled and dialysed against phosphate buffer containing, β-mercaptoethanol (1 mM).

This method was found to be unsatisfactory because (1) The time required for large volumes of buffer to filter through the chromatography column was inconvenient, and (2) The cost of L-malate and NAD^+ present in the large volumes of buffer was prohibitive. A less expensive and quicker method for purification of MDH from the crude extract was therefore developed.

(2.7.3.2) Purification of *E.coli* MDH by precipitation of proteins with ammonium sulphate.

The proteins in a cell-free extract (5 ml) were subjected to precipitation by saturation with ammonium sulphate on 20% increments at 4°C. The solution was centrifuged in a 15 ml Corex tube at 10,000g for 20 minutes at 4°C, then the supernatant transferred to a fresh Corex tube and the pellet re-suspended on 0.5 ml of phosphate buffer (0.1 M pH 7.2). The pellet (50μg) was electrophoresed in an SDS-polyacrylamide gel.

(2.7.3.3) Purification of *E.coli* MDH by Procion red/CL6-B affinity chromatography.

Cell-free extract (10 ml) was added to a suspension of Procion red/CL6-B (bed volume 10 ml) in phosphate buffer (0.1 M pH 7.2) and allowed to bind for 30 minutes at 4°C on an orbital shaker set at 25 cycles per minute. The suspension was centrifuged at 5,000g for 5 minutes at 4°C and the supernatant discarded. The Procion red/CL6-B was washed in 3.5 volumes of phosphate buffer (0.1 M pH 7.2) at 4°C and re-centrifuged. The supernatant was discarded, then the protein eluted off the matrix in 3.5 volumes of phosphate buffer (0.1 M pH 7.2) containing NaCl (0 - 2 M). Protein was precipitated with 5 volumes of acetone and 50µg of protein electrophoresed in an SDS-polyacrylamide gel.

(2.7.3.4) Purification of *E.coli* MDH using modified Sepharose CL6-B matrix containing thiol groups.

Cell-free extract was dialysed in a solution phosphate buffer (0.1 M pH 7.2) at 4°C and the dialysate containing MDH separated from the precipitate. This solution was loaded onto the modified Sepharose CL6-B matrix and allowed to elute under gravity at 4°C. This solution was eluted twice through the matrix. The matrix was eluted with 5 ml of phosphate buffer containing β-mercaptoethanol and the eluate stored at 4°C.

(2.7.4) Estimation of protein concentration.

Sample protein concentration was estimated according to the method of Bradford, (1976).

Control samples containing of 0-25µg of BSA in 100 µl phosphate buffer (0.1 M pH 7.2) were added to 900 µl of Bradford reagent in a 1 cm path length

cuvette. The solution was mixed, and the absorbance at 595nm recorded. A calibration curve was constructed of A_{595nm} vs BSA concentration. Test protein samples were made up to 100 µl with phosphate buffer (0.1 M pH 7.2) and added to 900 µl of Bradford reagent, mixed and the A_{595nm} recorded. Test protein sample concentration was estimated by calculating equivalent concentration of BSA at a given A_{595nm} from the BSA standard curve.

(2.7.5) SDS-polyacrylamide gel electrophoresis.

Protein samples were analysed by electrophoresis in an SDS-polyacrylamide gel (16 cm x 20 cm x 0.5 mm). To prepare the resolving gel, ammonium sulphate and TEMED were added to 6.5 ml of 30% acrylamide solution, 6.0 ml of resolving buffer and 16.5 ml of water added, then mixed by swirling (Table 2.2). Gels were cast by pouring acrylamide between the two glass plates whose edges were sealed. Butan-1-ol was layered onto the acrylamide solution and the gel left to polymerise at room temperature. For the stacking gel, ammonium persulphate and TEMED were added to 0.9 ml of 30% acrylamide solution, 2.4 ml of stacking buffer and 3.6 ml of water added, then mixed by swirling (Table 2.2). Butan-1-ol was removed from the surface of the resolving gel and the stacking gel poured onto the resolving gel. A rectangular toothed comb was inserted before polymerisation. The protein sample was precipitated with five volumes of 10% TCA and centrifuged at 15,000g for 5 minutes at room temperature. The supernatant was discarded and the protein re-suspended in 100 µl of water. Prior to electrophoresis 2 x loading dye (Tris-HCl 100mM pH 6.8, DTT 200 mM, SDS 4%, bromophenol blue 0.2% and glycerol 20%) was added and the protein solution and the protein solution incubated for 5 minutes at 80°C. The protein sample was electrophoresed at 25 mA in a solution of (Tris-HCl 50 mM, SDS 1% w/v, glycine 0.4%) until the protein had run into the resolving gel then electrophoresed at 40 mA for 6 hours.. Glass plates were separated and the gel cross linked and stained overnight in Coomassie blue R250 (1%) in (methanol 15%, glacial

acetic acid 5%) at 37°C. Excess stain was removed by soaking the gel in destain solution (methanol 15%, glacial acetic acid 5%) at 37°C.

(2.7.6) Determination of the properties of wild type and mutant MDH.

MDH activity was assessed at 30°C by a modified method of Smith *et al*, (1982). MDH (100 µl) was added to 800 µl phosphate buffer (0.1 M pH 7.2) containing NADH (0 - 0.3 mM final concentration) in a 1 cm path length polystyrene cuvette, incubated at 30°C. To this solution was added 100 µl of oxaloacetate (0 - 15 mM final concentration) and the solution mixed. The rate of decrease in absorbance at 340nm due to the oxidation of NADH to NAD^+ was measured on a recording spectrophotometer.

(2.7.7) Derivatization of MDH with DTNB and N-ethylmaleimide.

(2.7.7.1) Derivatization of MDH with DTNB.

The MDH solution was desalted by passing through a Sephadex G-50 column (2.5.4). MDH (approximately 2 nmol) was added to de-gassed phosphate buffer (0.1 M pH 7.2) containing DTNB (150 nmol) in a 1 cm path length polystyrene cuvette. The solution was made up to volume (1 ml), mixed and the increase in absorbance at 412nm due to the formation of NTB measured on a recording spectrophotometer.

(2.7.7.2) Derivatization of MDH with N-ethylmaleimide.

Derivatization of MDH with N-ethylmaleimide was performed in a similar manner as derivatization of MDH with DTNB. MDH was added to phosphate buffer containingN-ethylmaleimide (0 to 5000 nmol). This solution was made up to volume

(980 µl), mixed, then incubated for 20 minutes at room temperature. The rate of decrease in absorbance at 340nm due to the oxidation of NADH to NAD^+ was measured at 30°C on a recording spectrophotometer according to method (2.7.2).

(2.7.8) Iso-electric focussing of MDH.

The MDH solution was desalted by passing through a Sephadex G-50 column (2.5.4). A protein sample (1 µg) in phosphate buffer (0.1 M pH 7.2) was loaded onto a pre-focused iso-electric focussing Phast gel™ and the protein electrophoresed under the conditions outlined. (Table 2.3). The gel was immersed in a solution of (L-malate 0.9 M, NAD^+ 7.5 mM, Citrate synthase, Acetyl CoA 10 mM, NBT 3.7 mM, PMS 0.6 mM, Tris-HCl 50 mM pH 8.0) and activity stained for MDH at 37°C in the dark using a modified method of Smith (1976). The gel was rinsed in water, then cross-linked and stained overnight in Coomassie blue R250 (1%) in (methanol 15%, glacial acetic acid 5%) at 37°C. Excess stain was removed by soaking the gel in destain solution (methanol 15%, glacial acetic acid 5%) at 37°C.

(2.8) **Homology modelling of *E.coli* MDH.**

The primary structure of the *E.coli* MDH was used to model its tertiary structure based on the 3D co-ordinates of the porcine cytoplasmic MDH. These co-ordinates were used as a framework structure to build a model of *E.coli* MDH. This relied on the ability to superimpose the amino acids of *E.coli* MDH on the known crystal structure. Primarily, the amino acid sequence for a single polypeptide for *E.coli* MDH (Vogel *et al,* 1987) was manually aligned with the amino acid sequence of NAD-dependent eukaryotic and eubacteria MDHs. Conserved residues were given a greater weighting than conserved substitutions, which were in turn given a greater weighting than non-conserved substitutions. The alignment highlighted regions of

Stacking Gel	Composition	Volume
Ammonium persulphate	10% (w/v)	76 µl
TEMED		5 µl
Acrylamide	30% (acrylamide 19:1 bis-acrylamide)	0.9 ml
Stacking buffer	Tris-HCl 1.0 M pH 6.8 and SDS 10%	2.4 ml
Water		3.6 ml
Resolving Gel		
Ammonium persulphate	10% (w/v)	100µl
TEMED		26 µl
Acrylamide	30% (acrylamide 19:1 bis-acrylamide)	6.5 ml
Resolving buffer	Tris-HCl 0.375 M pH 8.8, SDS 0.1%	6.0 ml
Water		16.5 ml

Table 2.2: Composition of SDS-PAGE stacking and resolving gels.

Step	Voltage (V)	Current (mA)	Power (W)	Volt/hour (V/h)	Temperature (°C)
Pre-focussing	2000	2.0	3.5	75	15
Sample application	200	2.0	3.5	15	15
Sample focussing	2000	5.0	3.5	410	15

Table 2.3: Conditions for iso-electric focussing.

similarity and dissimilarity between the MDHs. An *E.coli* model was built by substituting residue side chains of the *E.coli* sequence for their counterpart residues of the porcine holoenzyme cytoplasmic co-ordinates in a single subunit using "INSIGHT (Biosym Technologies Inc., San Diego, CA, USA) modelling program. Regions where the *E.coli* sequence deviated from the porcine sequence were built using co-ordinates obtained from the Brookhaven protein data bank. The co-ordinates of polypeptides with an optimum number of residues and conformation were superimposed onto the co-ordinates of the porcine MDH at the initiation and termination points where sequence divergence occurred. Polypeptide conformations were chosen which did not clash with the protein structure were used to span the "gap" of the protein "backbone". Optimisation of the atomic co-ordinates to prevent steric clashing of residues was achieved using a potential energy minimisation program DISCOVER (Biosym Technologies Inc., San Diego, CA, USA). Solvent accessibility of each residue was determined by generating a "Connolly" surface. Atoms were designated solvent accessible if contact was made with a probe of radius 1.4Å (calculated radius of a water molecule) rolled over the surface of the molecule (Connolly, 1983) (Fig 2.1).

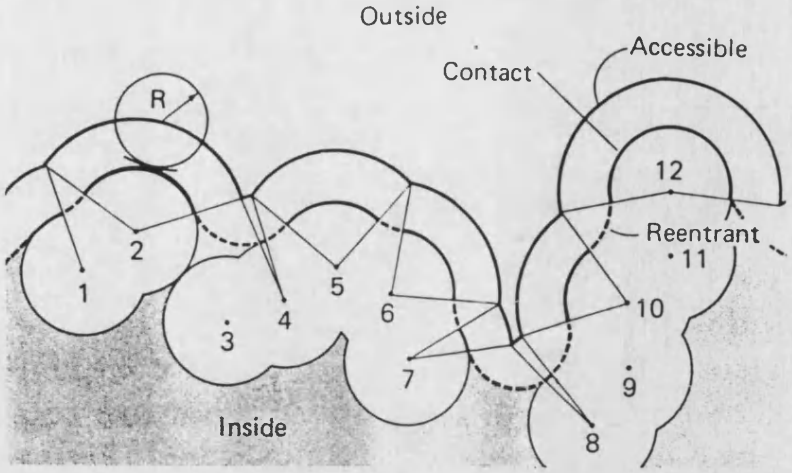

Fig 2.1: Two dimensional representation of a hypothetical protein composed of atoms 1 to 10.

Connolly surface is generated by rolling hypothetical probe (R) of radius 1.4 Å over the surface of the protein indicated by their van der Waals surface. Those parts of the protein surface that make contact with the probe are designated the solvent accessible surface. When the probe is simultaneously in contact with more than one atom, the probe interior surface defines the reentrant surface. The contact surface and the reentrant surface define the molecular surface.

CHAPTER THREE:

PURIFICATION OF *E.COLI* WILD TYPE MDH.

(3.1) **Introduction.**

E.coli wild type MDH was used as a model MDH for ascertaining the conditions used to purify subsequent *E.coli* MDH mutants. This chapter describes the work involved in the optimisation of conditions for purifying wild type MDH.

(3.2.1) Purification of *E.coli* MDH using ammonium sulphate.

The optimum concentration of ammonium sulphate for purification of wild type *E.coli* MDH was determined. Samples of cell-free extract were treated with ammonium sulphate in 20% increments and the amount of protein precipitated in each step determined using the Bradford assay. Samples of 50 μg of protein were then analysed by SDS-PAGE. In all cases MDH migrated as a 33kD subunit and is shown in (Fig 3.1). It was found that at concentrations below 60% ammonium sulphate, *E.coli* MDH accounts for less that 10% of the precipitated protein, but at concentrations in excess of 60% the *E.coli* MDH accounts for more than 50% of the precipitated protein.

The conditions chosen for purifying wild type and mutant *E.coli* MDH by precipitation with ammonium sulphate were by dialysis of the cell-free extract in a solution of 60% saturation ammonium sulphate, phosphate buffer (0.1 M pH 7.2) containing β-mercaptoethanol (1 mM) at 4°C and separating the dialysate containing MDH from the precipitate.

(3.2.2) Purification of *E.coli* MDH by Procion red H3-B affinity chromatography.

The MDH from *E.coli* cell-free extract was purified by chromatography using a Procion red matrix. Samples were loaded onto the column in phosphate buffer (0.1 M pH 7.2) containing β-mercaptoethanol (1 mM) and the protein eluted by using an increasing gradient of sodium chloride from 0.01 to 2 M. A comparison of protein content and MDH activity for each of the collected fractions indicated that the majority of the contaminants eluted at low (0.01M) NaCl concentrations whereas MDH eluted at 0.5 M NaCl (Fig 3.2). The optimum method for purifying wild type and mutant MDH depended therefore on washing the column with a large volume of phosphate buffer (0.1 M pH 7.2), β-mercaptoethanol (1 mM) containing 0.01M NaCl buffer to elute contaminants and then to elute the MDH using 1M NaCl in buffer.

(3.2.3) Purification of pUCWT MDH.

The MDH of *E.coli* W945T1-2 expressing pUCWT was purified from cell-free extracts in two steps, using ammonium sulphate (section 3.2.1) and affinity chromatography (section 3.2.2). At each purification step both the protein concentration and MDH activity were determined. This method was used throughout for the purification of MDH mutants.

A typical purification result is presented in table 3.1. There was an apparent increase in the total activity during purification, possibly because of the removal of an inhibitor from the crude preparation. The final specific activity of the wild type MDH protein preparation was 1000 $\mu mol.min^{-1}.mg$ of $protein^{-1}$, corresponding to a yield of 53% of the total activity. Analysis of the protein on SDS-PAGE (Fig 3.3) indicated that the MDH was approximately 70% pure, which would raise the specific activity of homogeneous wild type MDH to 1430 $\mu mol.min^{-1}.mg$ of $protein^{-1}$.

Fig 3.1: SDS-PAGE analysis of fractions from the purification of *E.coli* MDH using ammonium sulphate.

Lanes 1 is Cell-free extract. Lanes 2 to 6 are protein after precipitation with ammonium sulphate in 20% increments, 20% (lane 2), 40% (lane 3), 60% (lane 4), 80% (lane 5) and 100% (lane 6). 33kD MDH subunit is indicated on the right hand side.

Fig 3.2: SDS-PAGE analysis of fractions from the purification of *E.coli* MDH by Procion red H3-B affinity chromatography.

Lanes: (1) Cell-free extract: 2 to 6 elution with phosphate buffer (0.1 M) containing, β-mercaptoethanol (1 mM) and 0.01, 0.1, 0.5, 1 and 2 M NaCl. 33kD MDH subunit is indicated on right hand side.

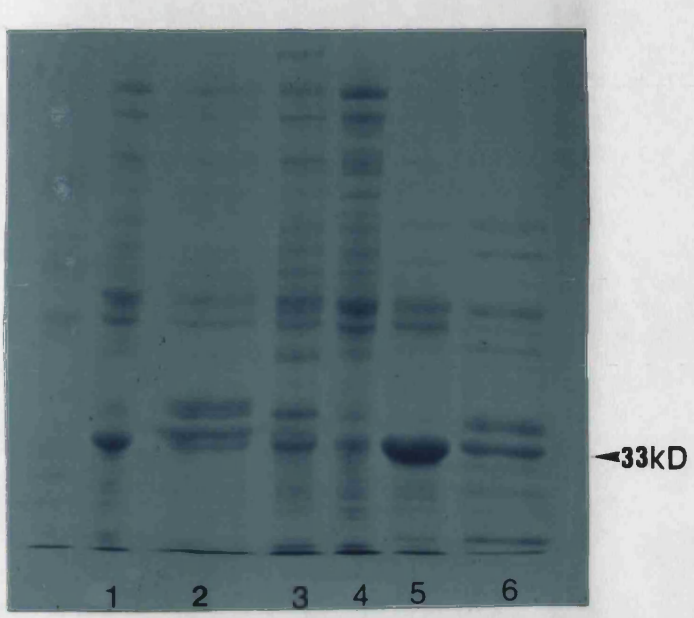
33kD
1
2
3
4
5
6

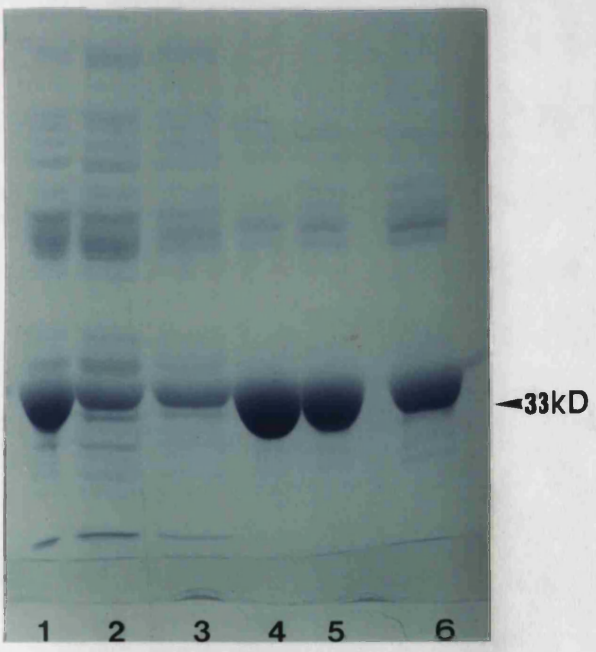
33kD
1
2
3
4
5
6

Fraction	Protein Concentration ($mg.ml^{-1}$)	MDH Activity (μ $mol.min^{-1}.ml^{-1}$)	Volume (ml)	Total Protein (mg)	Total Activity (μ $mol.min^{-1}$)	Specific Activity (μ $mol.min^{-1}.mg$ of $protein^{-1}$)
(1)	2	700	25	50	17500	350
(2)	8	860	2	16	1720	108
(3)	3	1240	25	75	31000	413
(4)		460	20		9200	
(5)	6	6000				1000
(6)						1430

Table 3.1: Purification of *E.coli* wild type MDH.

Lanes: (1) Cell-free extract; (2) Precipitate of 60% saturation ammonium sulphate dialysis; (3) 60% saturation ammonium sulphate dialysate; (4) Eluate of Procion red matrix; (5) Precipitate of 100% saturation ammonium sulphate dialysis; (6) Homogeneous MDH.

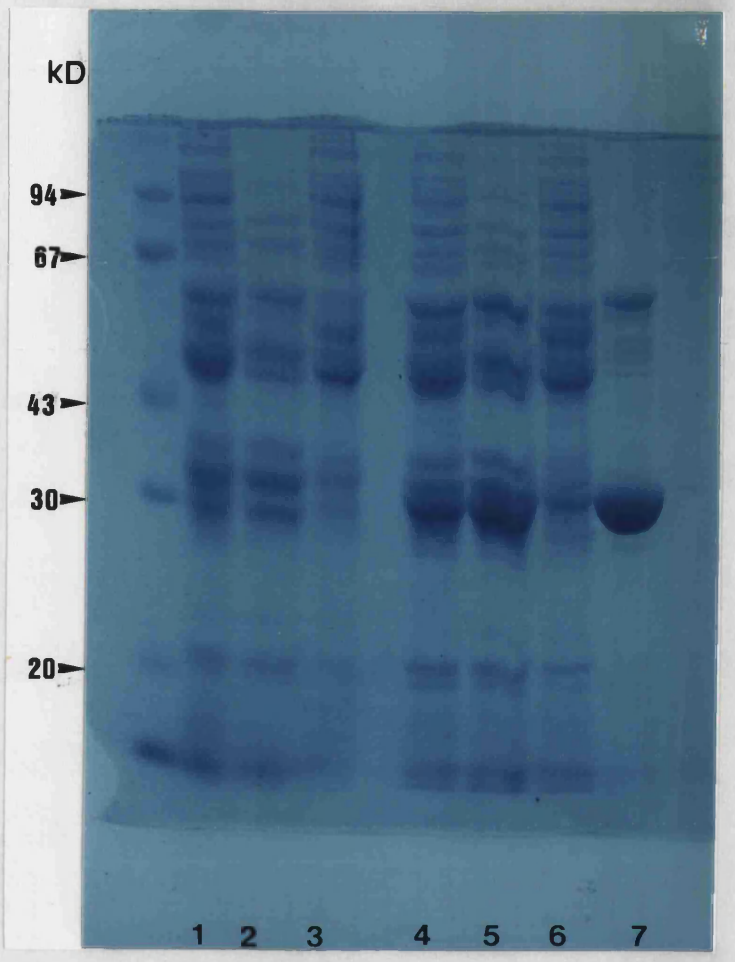

Fig 3.3: SDS-PAGE analysis of fractions from the purification of wild type *E.coli* MDH by precipitation of protein with ammonium sulphate and Procion red H3-B affinity chromatography.

Lanes from left to right: (1 to 3 are of *E.coli* W945T1-2), (1) Cell-free extract; (2) 60% saturation ammonium sulphate dialysate; (3) Precipitate of 60% saturation ammonium sulphate dialysis; (4 to 7 are *E.coli* W945T1-2 expressing plasmid MDH) (4) Cell-free extract: (5) 60% saturation ammonium sulphate dialysate; (6); Precipitate of 60% saturation ammonium sulphate dialysis; (7) Elution off Procion red matrix. Left hand lane are standard molecular weight markers.

(3.3) **Discussion.**

Precipitation of protein with ammonium sulphate indicated that below 60% saturation, *E.coli* MDH accounted for a small percentage of the precipitated protein, but at concentrations of 60% or greater the MDH was a major component of the precipitated protein. Similar qualtiative results have been observed by Ferneley *et al*, (1981) and Murphey *et al*, (1967)

Purification of the MDH by elution off a Procion red affinity chromatography matrix, indicated that at sodium chloride concentrations above 0.5 M the MDH was a major component of the eluted protein. At concentrations below 0.5 M sodium chloride it was less pure.

The calculated specific activity for the wild type MDH was 1430 $\mu mol.min^{-1}$ .mg of $protein^{-1}$ and a yield of 53%. These value compares favourably with that obtained by Smith *et al*, (1982) (1820 $\mu mol.min^{-1}$.mg of $protein^{-1}$) and Nicholls *et al*, (1989) (1730 $\mu mol.min^{-1}$.mg of $protein^{-1}$) with similar yields. However, this value is three and five times the specific activities observed by Ferneley *at al*, (1981) of 350 $\mu mol.min^{-1}$.mg of $protein^{-1}$ and Murphey *et al*, (1967) of 542 $\mu mol.min^{-1}$.mg of $protein^{-1}$ (at 22°C).

CHAPTER FOUR:

SUBSTITUTION OF ENDOGENOUS CYSTEINES IN *E.COLI* WILD TYPE MDH.

(4.1) **Introduction.**

The initial strategy was to create a mutant MDH with all three endogenous cysteines removed. Studies on the folding intermediates of proteins suggest that in some instances transient disulphide bonds "steer" the folding of a protein through intermediate structures into the final native conformation (Creighton, 1980; Konishi *et al*, 1981; Wetzel *et al*, 1988; Zale and Klibanov 1986). Introduction of solvent accessible cysteines into the wild type MDH could adversely influence the folding of MDH resulting in inactivation (Browning *et al*, 1986). Removal of endogenous cysteines could prevent incorrect folding upon introduction of solvent accessible cysteines into the MDH.

(4.2.1) Substitution of the cysteine 113 codon (113S).

The gene encoding wild type *E.coli* MDH was ligated into *Hind* III restricted RF M13 mp19 and 5μg of DNA template prepared. This template was used to generate mutant 113S using sense oligonucleotide-1 via the oligonucleotide-directed *in vitro* mutagenesis system (Amersham) (Fig 4.1). Oligonucleotide -1 was designed to convert the codon for cysteine 113 to a serine and introduce a unique *Nhe* I restriction site. Clones were screened for the presence of the mutation by colony hybridisation, restriction fragment analysis and sequencing of the DNA (Fig 4.1).

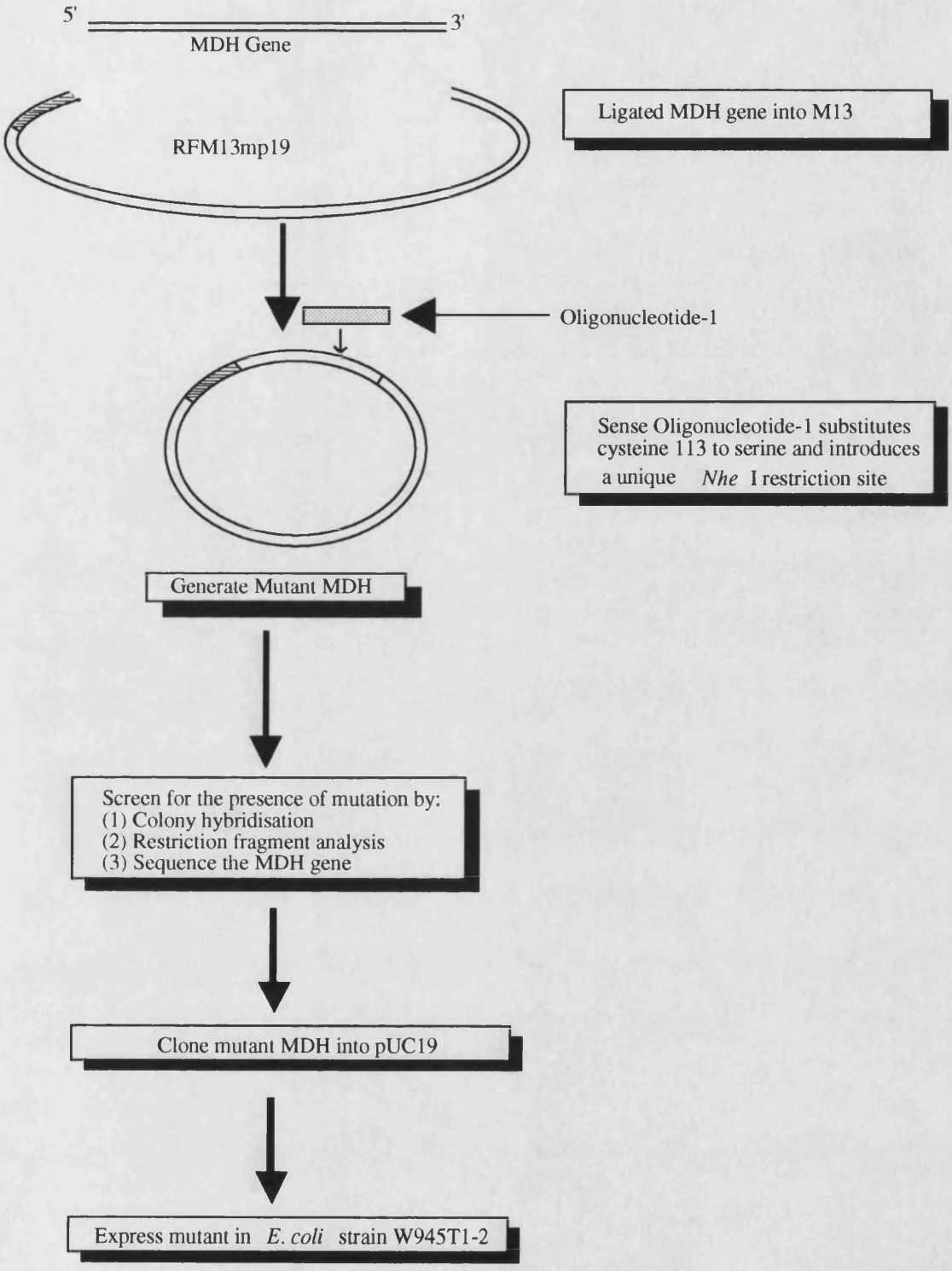

Fig 4.1: Flow diagram of steps used to generate mutant pUC113S.

(4.2.2) Screening for the mutation in the codon for cysteine 113 (113S).

Plaques harbouring M13 virus were screened for the presence of the mutation by colony hybridisation (Fig 4.2). RF M13 was prepared from one of the strongly hybridising plaques and the mutated gene, excised and ligated into *Hind* III restricted pUC19. Plasmid pUC113S was then transformed into *E.coli* TG1. Restriction of pUCWT and pUC113S with *Hind* III indicates that both plasmids contain a DNA fragment of similar size of approximately 1300 bp (Fig 4.3). *Kpn* I has two restriction sites in the pUC19/MDH gene: one in the polylinker and one in the gene at nucleotide position 848. *Kpn* I restriction will therefore produce two distinct DNA fragments which, depending on the orientation of the gene in pUC19, will be 1166 or 223 bp long. Restriction of wild type and 113S mutant with *Kpn* I excised a DNA fragment of 1166 bp indicating a similar orientation of both genes. Restriction of 113S mutant and wild type plasmids with *Nhe* I produced a linearised plasmid with the 113S mutant, but did not cut the wild type MDH gene. This confirmed the presence of a unique *Nhe* I recognition site and therefore the presence of the 113S mutation.

Oligonucleotide-2 which hybridised at positions 251 to 267 of the gene was used as a sequencing primer to confirm the nucleotide substitutions introduced into pUC113S (Fig 4.4).

(4.2.3) Purification of pUC113S MDH.

Purification of mutant 113S produced a decrease in specific activity from 1810 μmol.min^{-1}.mg of protein^{-1} in cell-free extract to 1185 μmol.min^{-1}.mg of protein^{-1} in the precipitated protein fraction, a decrease of 34% (Table 4.1). This indicated that the mutant was being inactivated upon purification. The final specific activity of the MDH preparation was 1185 μmol.min^{-1}.mg of protein^{-1}, corresponding to a yield of 65%. Analysis of the protein preparation on SDS-PAGE (Fig 4.5) indicated that the

Fig 4.2: Hybridisation of 113S MDH gene with 5' [^{32}P] labelled oligonucleotide-1 probe.

(1) Wash of Hybond-N membrane at 37°C for 10 minutes in 2 x SSC, SDS (0.1% w/v).

(2) Wash of Hybond-N membrane at 63°C for 10 minutes in 2 x SSC, SDS (0.1% w/v).

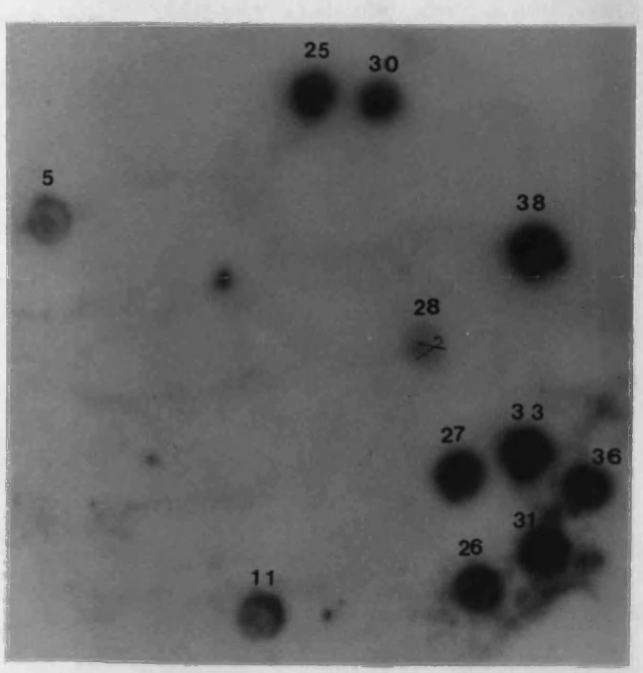
25
30
5
38
28
33
27
36
31
26
11

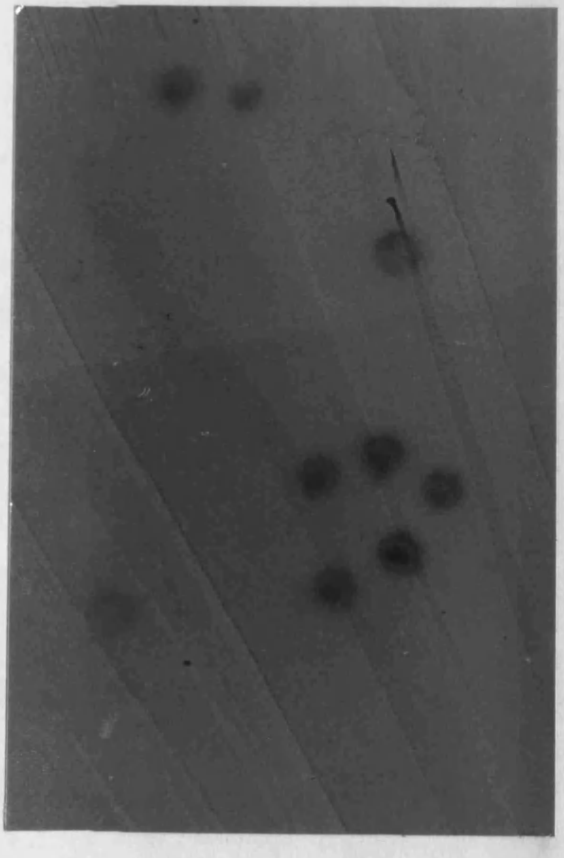

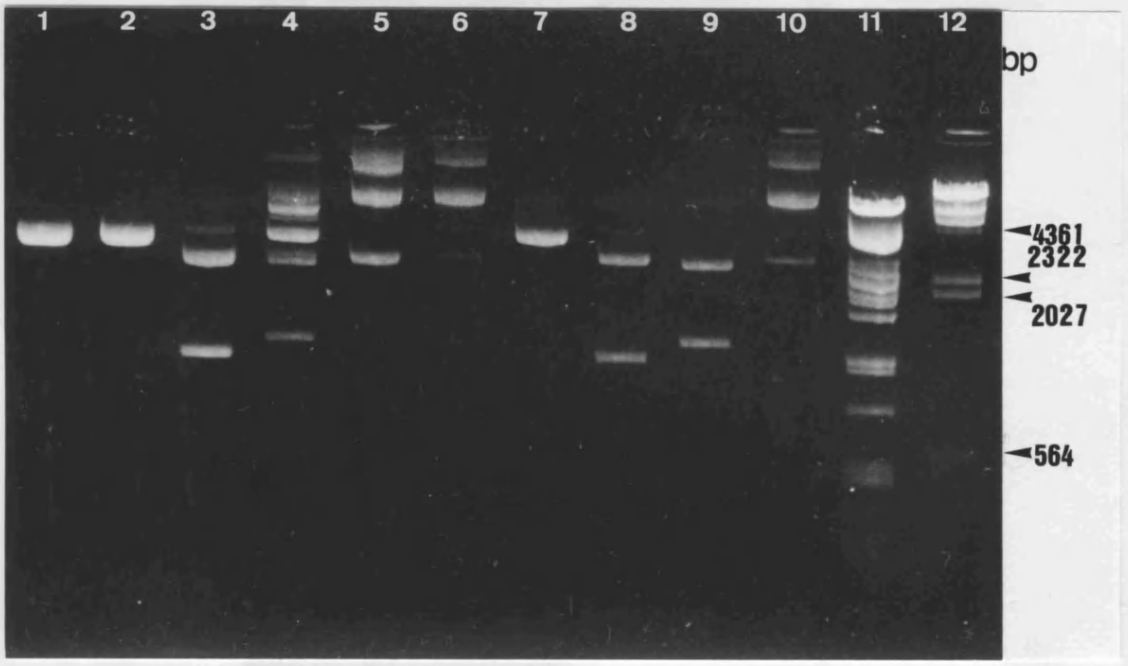

Fig 4.3: Restriction fragment analysis of wild type and 113S MDH gene in pUC19 on a 0.8% agarose gel.

Lane from left to right: (1 to 4 113S MDH gene in pUC19 restricted with), (1) *Nhe* I; (2) *Sal* I; (3) *Kpn* I; (4) *Hind* III; (5) 113S MDH gene in pUC19. (6 to 9 wild type MDH gene in pUC19 restricted with), (6) *Nhe* I; (7) *Sal* I; (8) *Kpn* I; (9) *Hind* III; (10) wild type MDH gene in pUC19; (11) Lambda DNA restricted with *Pst* I; (12) Lambda DNA restricted with *Hind* III. The size of *Hind* III restricted Lambda is indicated on the right.

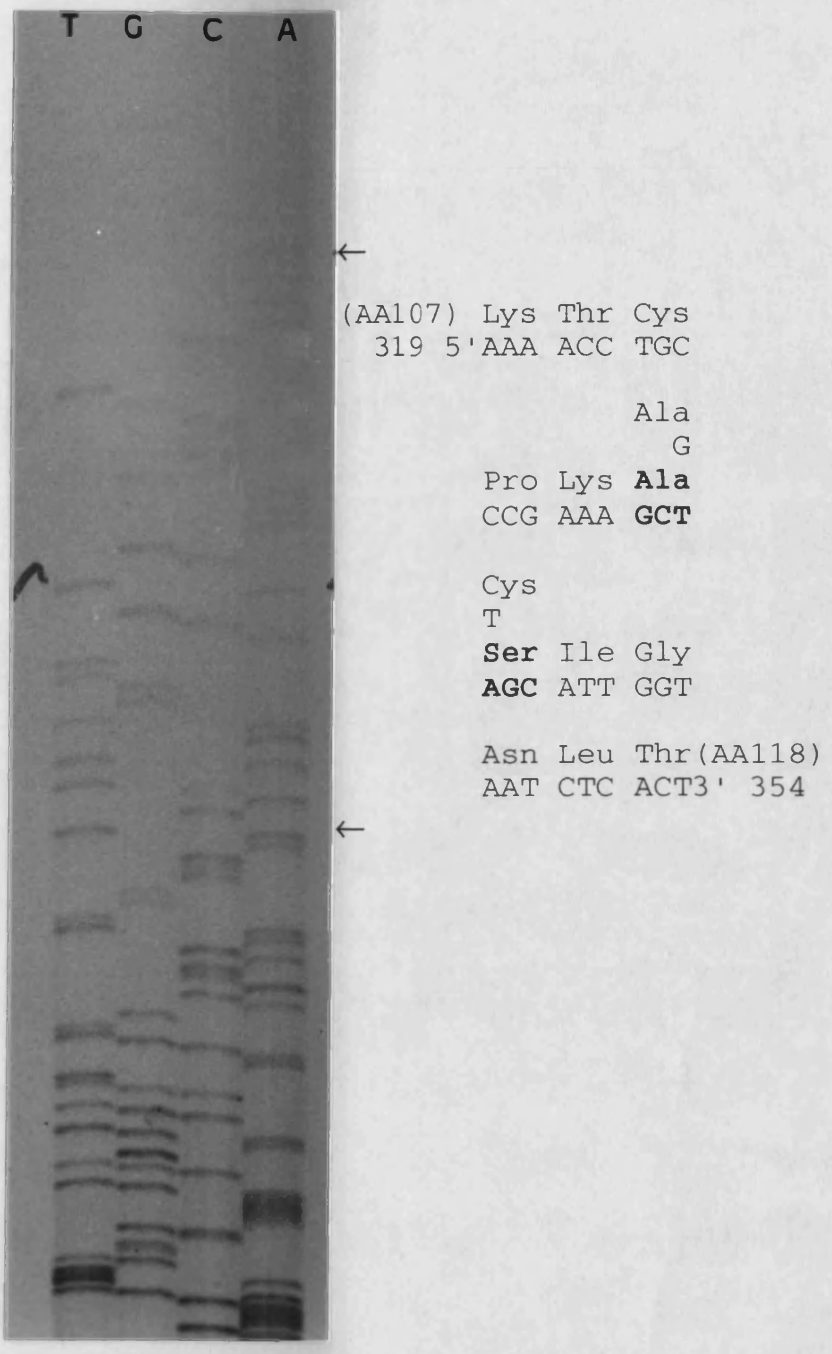

Fig 4.4: Dideoxy sequence analysis of mutant 113S gene using oligonucleotide-2 as primer.

Lanes from left to right: Thymine (T); Guanine (G); Cytosine (C); Adenine (A) with corresponding codon usage. Bold uppercase indicates introduced *Nhe* I restriction site. Corresponding triple letter amino acid code is indicated above codon.

Fraction	Protein Concentration ($mg.ml^{-1}$)	MDH Activity (μ $mol.min^{-1}.ml^{-1}$)	Volume (ml)	Total Protein (mg)	Total Activity. (μ $mol.min^{-1}$)	Specific Activity (μ $mol.min^{-1}$.mg of $protein^{-1}$)
(1)	2	3620	25	50	90500	1810
(2)	11	1280	2	22	2560	116
(3)	3	3330	25	75	83250	1110
(4)		2570	20		51400	
(5)	2	2370				1185
(6)						1261

Table 4.1: Purification of *E.coli* 113S MDH.

Lanes: (1) Cell-free extract; (2) Precipitate of 60% saturation ammonium sulphate dialysis; (3) 60% saturation ammonium sulphate dialysate; (4) Eluate of Procion red matrix; (5) Precipitate of 100% saturation ammonium sulphate dialysis; (6) Homogeneous MDH.

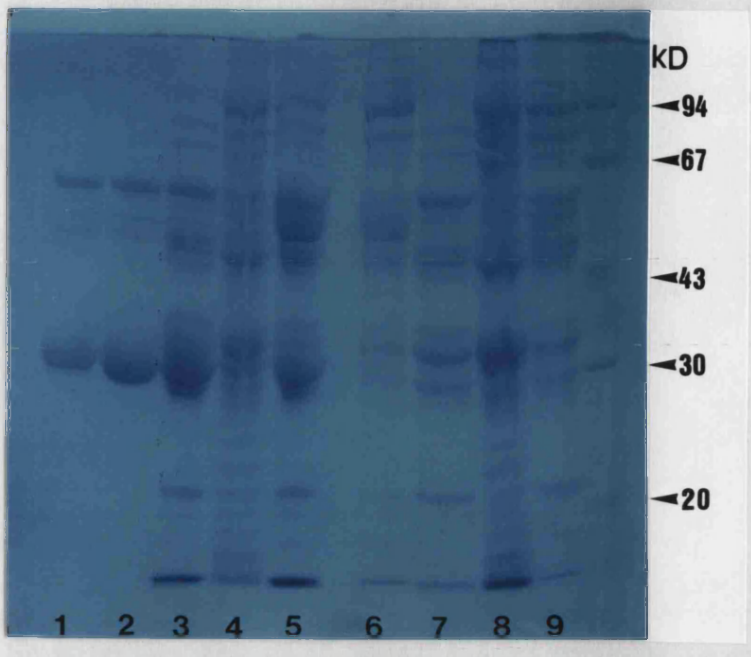

Fig 4.5: SDS-PAGE analysis of fractions from the purification of mutant 113S *E.coli* MDH by precipitation of protein with ammonium sulphate and Procion red H3-B affinity chromatography.

Lanes from left to right: (1) Wild type MDH (2 to 5 are of *E.coli* W945T1-2 expressing plasmid 113S MDH); (2) Elution of Procion red matrix; (3) 60% saturation ammonium sulphate dialysate; (4) Precipitate of 60% saturation ammonium sulphate dialysis; (5) Cell-free extract; (6 to 9 are of E.coli W945T1-2); (6) 60% saturation ammonium sulphate dialysate; (7) Precipitate of 60% saturation ammonium sulphate dialysis; (8) Precipitated protein of cell-free extract; (9) Cell-free extract. Right hand lane are standard molecular weight markers.

113S MDH was approximately 94% pure which would raise the specific activity of homogeneous 113S to 1261 $\mu mol.min^{-1}.mg$ of $protein^{-1}$. This compares favourably with the specific activity obtained for wild type MDH, a decrease of only 12%.

(4.3.1) Substitution of the codons for cysteines 109 and 113 (109S/113S).

The first mutation (113S) had required that the gene in M13 was shuttled into pUC19 after mutagenesis for expression, and that the 1.3 kbp fragment was sequenced throughout to check for spurious mutations. To avoid these extra manipulations a different strategy was followed with subsequent substitutions being introduced into gene segments using cassette PCR mutagenesis (Reidhaar-Olson and Sauer 1988) (Fig 4.6).

Substitution of the codons for cysteines 109 and 113 to serine was achieved using the scheme outlined in figure 4.6. The PCR was restricted with *Sal* I and *Nhe* I and ligated into appropriately restricted pUC113S vector, then transformed into *E.coli* TG1 and selected for the presence of plasmid on agar plates. Clones were screened for the presence of the mutation by restriction fragment analysis and sequencing of the DNA (Fig 4.6).

(4.3.2) Screening for the substitutions in the codons for cysteine 109 and 113 (109S/113S).

Restriction of wild type MDH gene in pUC19 and pUC109S/113S plasmid with *Hind* III, indicated that the wild type excised a 1.3 kbp fragment, but pUC109S/113S was linearised (Fig 4.7). Restriction of the mutant with *Sal* I and *Hind* III excised a DNA fragment of similar size to *Hind* III restricted wild type, indicating successful removal of the *Hind* III restriction site in the polylinker. Restriction with *Nhe* I produced a linearised plasmid with the pUC109S/113S mutant, but did not cut the wild

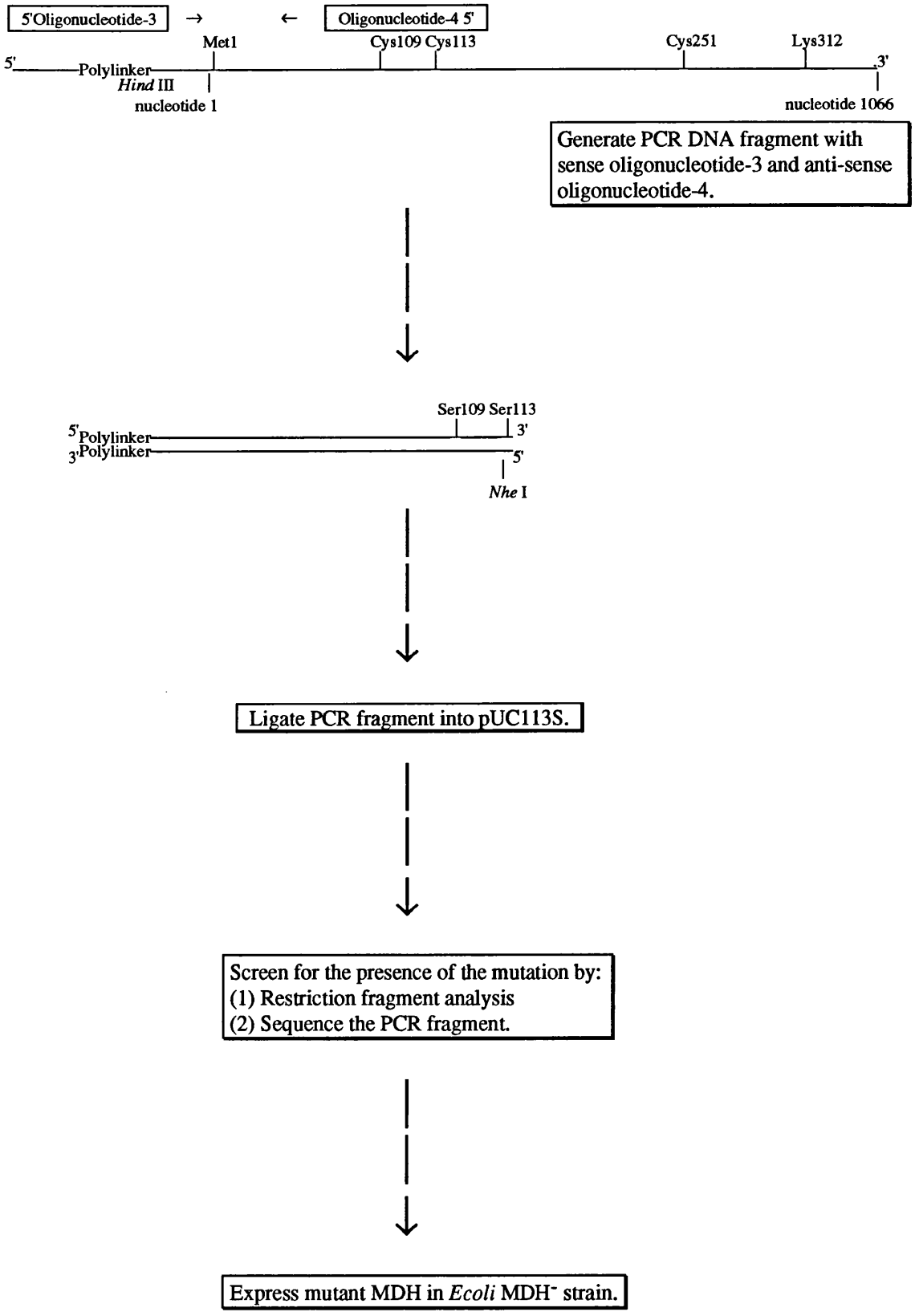

Fig 4.6: Flow diagram of steps used to generate mutant pUC109S/113S.

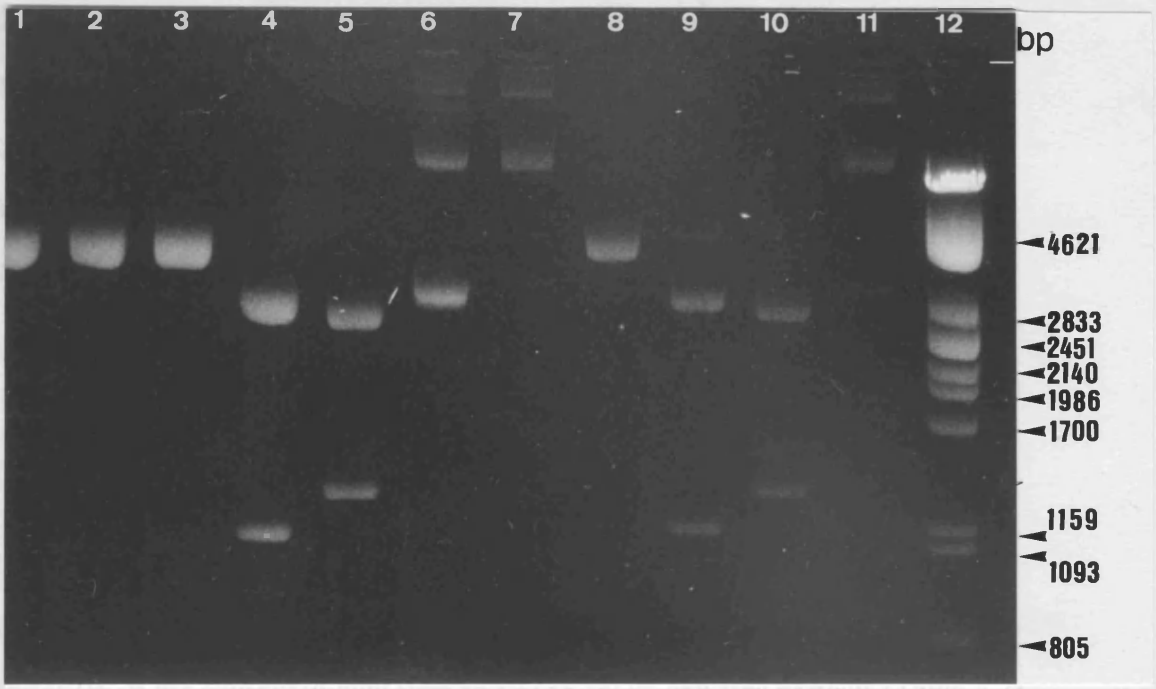

Fig 4.7: Restriction fragment analysis of wild type and 109S/113S MDH gene in pUC19 on a 0.8% agarose gel.

Lane: 1 to 5 are 109S/113S MDH gene restricted with; (1) *Nhe* I; (2) *Sal* I; (3) *Hind* III; (4) *Kpn* I; (5) *Hind* III and *Sal* I; (6) 109S/113S MDH gene; 7 to 10 are wild type MDH gene restricted with; (7) *Nhe* I; (8) *Sal* I; (9) *Kpn* I; (10) *Hind* III; (11) wild type MDH gene; (12) Lambda DNA restricted with *Pst* I. The size of *Pst* I restricted Lambda is indicated on the right.

type gene. The presence of the unique *Nhe* I and *Hind* III restriction site, confirmed the presence of the 109S/113S mutation. Oligonucleotide-5 which hybridised to nucleotide positions -372 to -356 of the gene was used as a sequencing primer to confirm the nucleotide substitutions introduced into the polylinker. Oligonucleotide-2, annealing to nucleotide positions 251 to 267 was used to confirm the nucleotide substitutions introduced into the codons of residues 109 and 113 by sequencing (Fig 4.8).

(4.3.3) Purification of pUC109S/113S.

In contrast to the purification of wild type and mutant 113S MDH the total activity of the cell-free extract of mutant 109S/113S only 125 $\mu mol.min^{-1}$. This was only 0.8% and 0.1% of the activity in wild type and 113S MDH cell-free extracts (Table 4.2). Analysis of the protein on SDS-PAGE indicated that the 33kD band was not a major component of the cell-free extract (Fig 4.9). The precipitated protein from the dialysate (fraction 2) contained 14% of the protein from the cell-free extract and 10% of the activity. This indicated that 109S/113S was not being purified successfully using this procedure. The final specific activity of the 109S/113S MDH protein preparation was 18 $\mu mol.min^{-1}$.mg of $protein^{-1}$, corresponding to a yield of 16%. This yield compares poorly with that observed for wild type (53%) and mutant 113S (65%). Gel scans of SDS-PAGE gels of this material showed 23% of the protein migrated at 33kD, this would raise the specific activity of homogeneous 109S/113S MDH to 78 $\mu mol.min^{-1}$.mg of $protein^{-1}$. This value is only 5% and 6% of that calculated for wild type and 113S MDHs.

(4.4.1) Substitution of the cysteine codons 109, 113 and 251 (109S/113S/251S).

Substitution of the codons for cysteines 109, 113 and 251 to serine codons in the *E.coli* MDH gene was carried out according to figure 4.10. The PCR products were

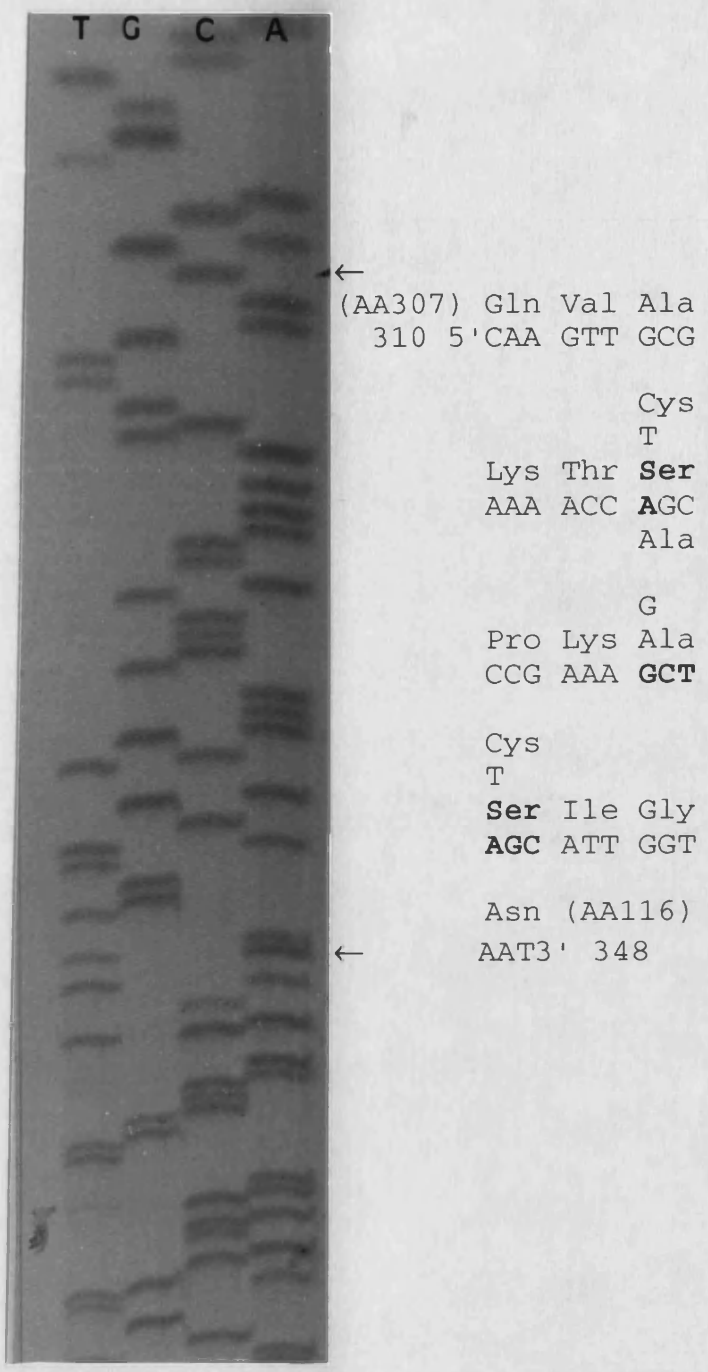

Fig 4.8: Dideoxy sequence analysis of mutant 109S/113S gene using oligonucleotide-2 as primer.

Lanes from left to right: Thymine (T); Guanine (G); Cytosine (C); Adenine (A) with corresponding codon usage. Bold uppercase indicates introduced *Nhe* I restriction site and mutations. Corresponding triple letter amino acid code is indicated above codon.

Fraction	Protein Concentration ($mg.ml^{-1}$)	MDH Activity (μ $mol.min^{-1}.ml^{-1}$)	Volume (ml)	Total Protein (mg)	Total Activity (μ $mol.min^{-1}$)	Specific Activity (μ $mol.min^{-1}$.mg of $protein^{-1}$)
(1)	2	5	25	50	125	3
(2)	7	10	1	7	10	1
(3)	2	10	6	12	60	5
(4)		1	20		20	
(5)	4	70				18
(6)						78

Table 4.2: Purification of *E.coli* 109S/113S MDH.

Lanes: (1) Cell-free extract; (2) Precipitate of 60% saturation ammonium sulphate dialysis; (3) 60% saturation ammonium sulphate dialysate; (4) Eluate of Procion red matrix; (5) Precipitate of 100% saturation ammonium sulphate dialysis; (6) Homogeneous MDH.

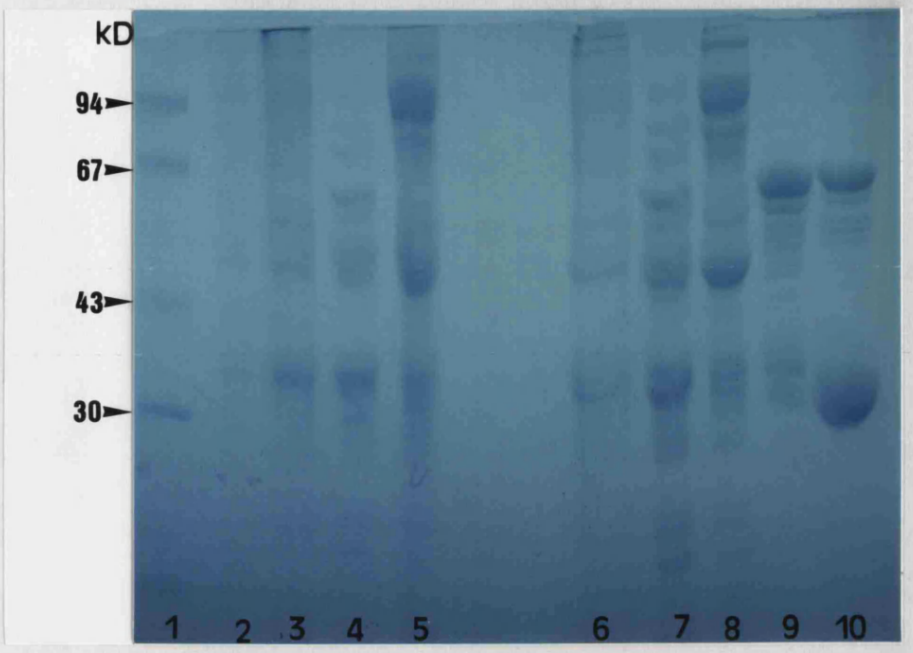

Fig 4.9: SDS-PAGE analysis of fractions from the purification of mutant 109S/113S *E.coli* MDH by precipitation of protein with ammonium sulphate and Procion red H3-B affinity chromatography.

Lanes from left to right: (1) Standard molecular weight markers; (2) (2 to 5 are of *E.coli* W945T1-2); (2) Cell-free extract; (3) Precipitated protein of cell-free extract; (4) 60% saturation ammonium sulphate dialysate; (5) Precipitate of 60% saturation ammonium sulphate dialysis; (6 to 9 are *E.coli* W945T1-2 expressing plasmid 109S/113S MDH); (6) Cell-free extract; (7) 60% saturation ammonium sulphate dialysate; (8) Precipitate of 60% saturation ammonium sulphate dialysate; (9) Elution of Procion red matrix; (10)Wild type MDH.

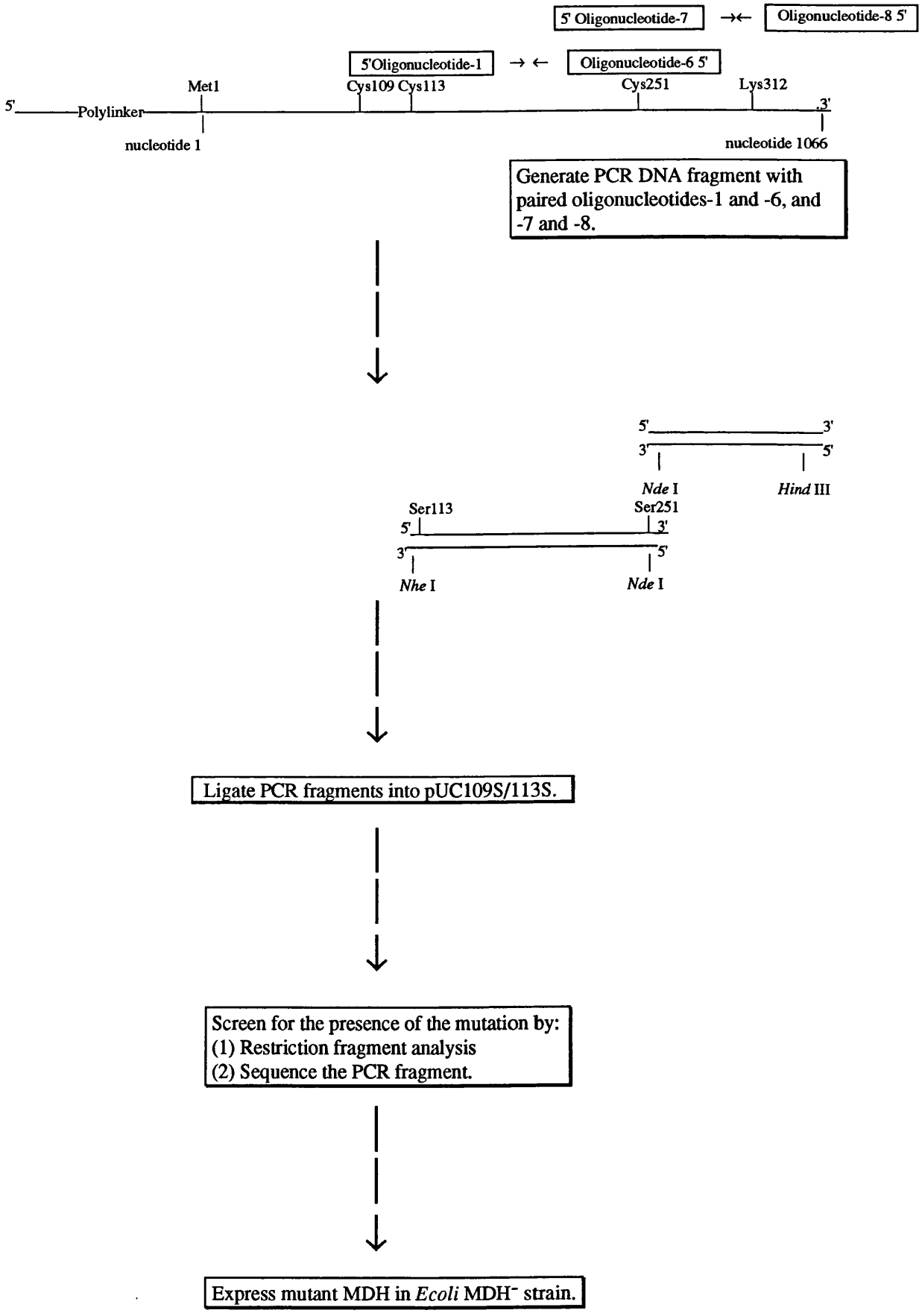

Fig 4.10: Flow diagram of steps used to generate mutant pUC109S/113S/251S.

restricted with *Nhe* I, ligated then restricted with *Hind* III and *Nde* I. PCR products was ligated into appropriately restricted pUC109S/113S vector and transformed into *E.coli* TG1. Colonies harbouring plasmid were grown on agar plates.

(4.4.2) Screening for the substitutions for the codons of cysteines 109, 113 and 251 (109S/113S/251S).

Restriction of pUC109S/113S/251S with *Hind* III, *Sal* I or *Nhe* I linearised the plasmid, whereas restriction with *Hind* III and *Sal* I excised a DNA fragment of similar size to the *Hind* III restricted wild type MDH gene in pUC19 (Fig 4.11). This confirmed the codon change to cysteines 109 and 113. *Nde* I has a restriction site in pUC19 at the nucleotide position 183. Introduction of a second *Nde* I site at nucleotide position 756 will produce a DNA fragment of 1304 bp, when restricted with *Nde* I. Restriction with *Nde* I produced a DNA fragment of 1300 bp, confirming the presence of the second *Nde* I site and therefore the substitution at cysteine 251.

Prior to confirmation of the sequence the gene was expressed in MDH^- *E.coli.* No activity or protein band corresponding to the 33kD subunit was found. Subsequently, oligonucleotide-15 which hybridised at the nucleotide position 658 to 676 was used to sequence through the introduced *Nde I* restriction site (Fig 4.12). An insertion at nucleotide position 768 of 5'TAT GTT GAA GGC had occurred 3' to the sense oligonucleotide which is identical to the nucleotide sequence between nucleotides 757 to 767. This resulted in a silent mutation to codon glycine 256 from 5'GGC to 5'GGT and a shift in the reading frame 3' with respect to this codon (Fig 4.13). Further attempts to locate the correct gene were unsuccessful.

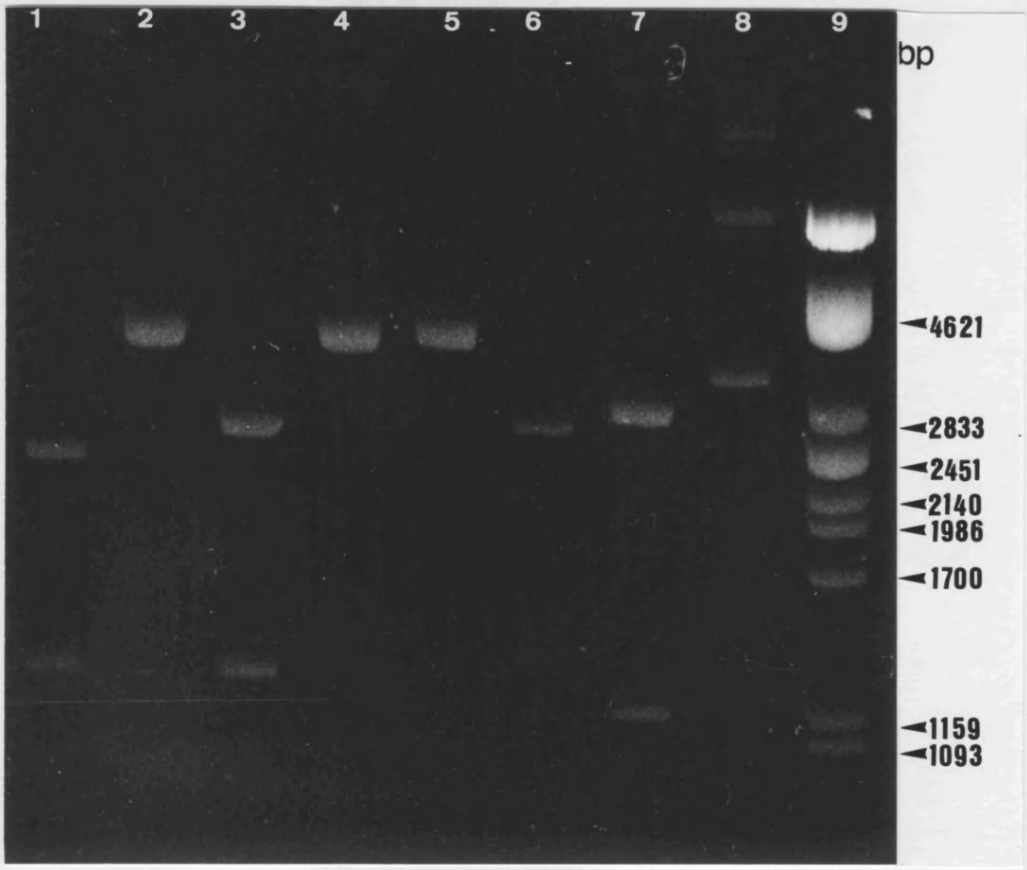

Fig 4.11: Restriction fragment analysis of 109S/113S/251S MDH gene in pUC19 on a 0.8% agarose gel.

Lane: (1) 1 to 7 are pUC109S/113S/251S MDH gene restricted with, (1); *Nde* I and *Hind* III; (2) *Nhe* I; (3) *Nde* I; (4) *Sal* I; (5) *Hind* III; (6) *Hind* III and *Sal* I; (7) *Kpn* I; (8) pUC109S/113S/251S MDH gene; (9) Lambda DNA restricted with *Pst* I. The size of *Pst* I restricted Lambda is indicated on the right.

Fig 4.12: Dideoxy sequence analysis of mutant 109S/113S/251S gene using oligonucleotide-15 as primer.

Lanes from left to right: Thymine (T); Guanine (G); Cytosine (C); Adenine (A) with corresponding codon usage. Bold uppercase indicates introduced *Nde* I restriction site and mutations. Italic uppercase indicate deviation in sequence. Corresponding triple letter amino acid code is indicated above codon.

```
                      C GAA TCT GCA TAT GTT
(+739)  5'GGC GTT GTC GAA TCT GCA TAT GTT 3'    (+762)
(AA 247)  Gly Val Val Glu Cys Ala Tyr Val     (AA 254)

          GAA GG
(+763)  5'GAA GGT ATG TTG AAG GCG ACG GTC 3'    (+786)
(AA 255)  Glu Gly Met Leu Lys Ala Thr Val     (AA 262)

(+787)  5'AGT ACG TCC GTT TCT TCT CTC AAC       (+810)
(AA 263)  Ser Thr Ser Val Ser Ser Leu Asn      (AA270)

(+811)  5'CGC 3' (+813)
(AA 271)  Arg  (AA 271)
```

Fig 4.13: Deduced amino acid sequence from dideoxy sequence of mutant 109S/113S/251S.

Amino acids are indicated in three letter code with sequence deviation in italics; nucleotide insertion are indicated in uppercase, sequence deviation in italics; oligonucleotide is indicated in uppercase bold.

(4.5.1) Substitution of the cysteine codon 251 (251S).

MDH mutant 251S was constructed according to the scheme illustrated in Fig 4.14. No MDH activity or protein band corresponding to the 33kD subunit was found. This mutant was constructed using pUC109S/113S/251S as a vector (which was subsequently shown to contain an error). It is likely that the lack of observed mutant MDH is a result of the incorporated error.

(4.6) **Discussion.**

Conserved substitutions of cysteine to serine were made to the codons encoding cysteine 113 and 109, singularly and in tandem to produce two mutant MDHs. The gene encoding mutant 113S when expressed in the *E.coli* MDH$^-$ strain W945T1-2 produced a high level of the 33kD MDH subunit in the cell-free extract, comparable with that observed for the expressed wild type MDH. This mutant had an apparent specific activity of 1261 μmol.min^{-1}.mg of protein^{-1} which is only marginally less (12.0%) than that calculated for the wild type MDH (1430 μmol.min^{-1}.mg of protein^{-1}). However the gene encoding the double mutation (109S/113S) when expressed, resulted in a lower level of the 33kD subunit observed in the cell-free extract and a lower specific activity of only 78 μmol.min^{-1}.mg of protein^{-1}. These results suggest that the single substitution did not greatly affect the expression or activity of the MDH, whereas the double mutation did. The codon substitutions introduced for these and the other MDH mutants were designed not to increase "rare" codon usage in the gene (Vogel *et al*, 1987), introduce or delete potential stem loop structures which might influence protein synthesis (Winnacker, 1987). Decreased levels of expression and activity have been observed for many mutant proteins (Green *et al*, 1992; Mitchinson and Wells, 1989; Pakula *et al*, 1986). The decrease in the levels of expression have been attributed to an increased susceptibility of the mutant to degradation both proteolytic and autolytic (Pakula *et al*, 1986), while decreases in the

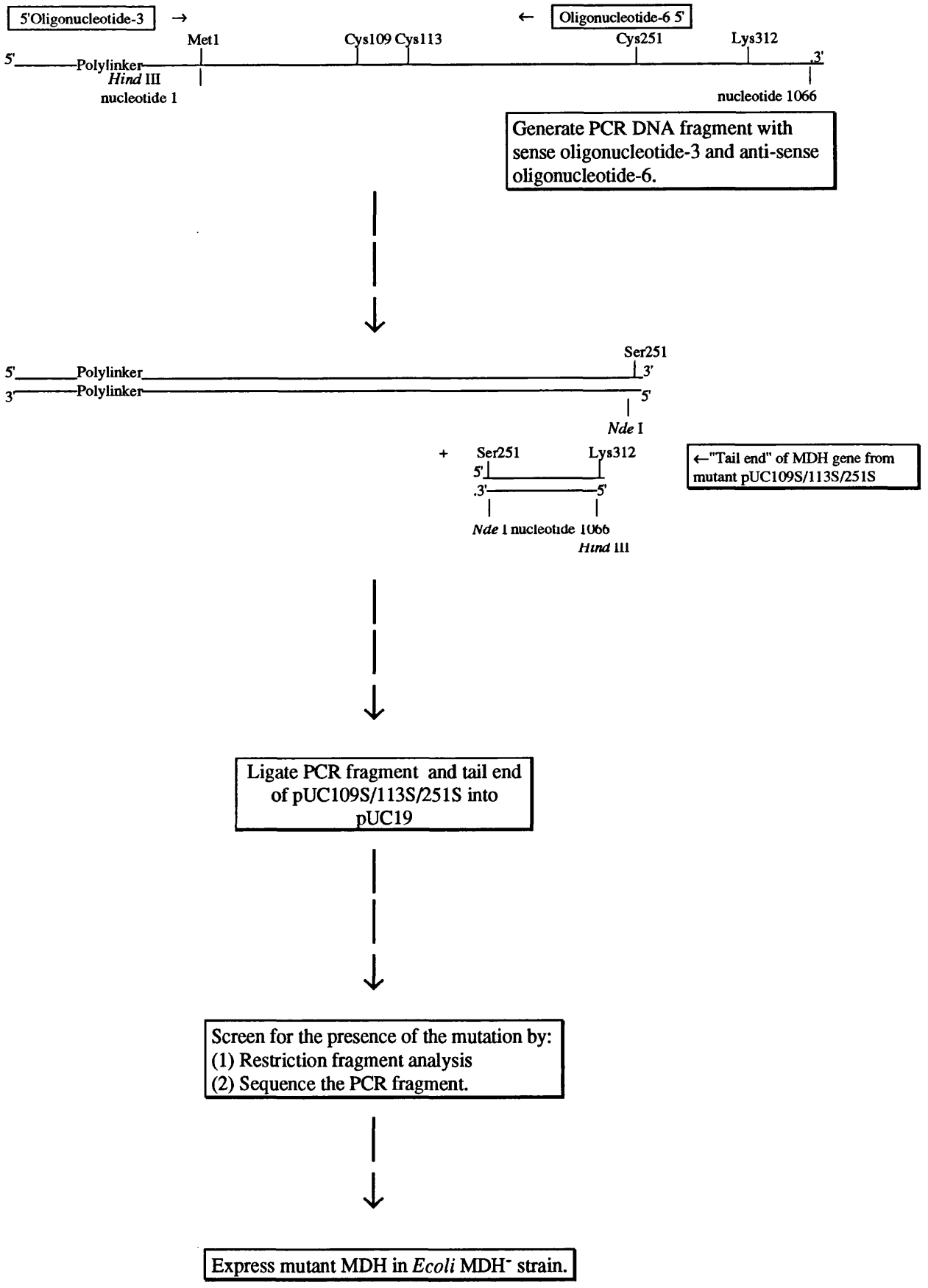

Fig 4.14: Flow diagram of steps used to generate mutant pUC251S.

activity of these proteins has been attributed to conformational changes in the protein and increased flexibility as a result of mutation (Mitchinson and Wells, 1989). The increased susceptibility to degradation could be due to:

- Change in conformation of secondary structure caused by change the side chain area.
- Change in conformation of secondary structure caused by alteration of the residue charge.
- Change in conformation of secondary structure caused by change in the residue hydrophobicity.
- Change in conformation of secondary structure caused by loss of hydrogen bonding interaction
- Incorrectly folded protein.

Serine (115Å^2) has a similar side chain (R) area to cysteine (135Å^2) and represents the most conserved substitution, from R = -SH to R = -OH a change of one atom and a decrease in side chain area of only 15% (Creighton, 1983). This small decrease in side chain area upon substitution is not likely to cause a large perturbation in the local conformation and are likely to be accommodated by small changes in the local conformation (Daopin *et al*, 1991; Matthews *et al*, 1987). However small changes in local conformation have been attributed in some instances to changes in protein activity and stability (Daopin *et al*, 1991). The rational for using serines as the substitution residues is further substantiated by the fact that amino acid sequence alignment of MDHs (Fig 6.1) indicate that serine is substituted for cysteine in the MDHs and that serine has been used by other workers as substituting residue for cysteine. For example Browning *et al*, (1986) has substituted a reduced cysteine which was thought to participate in disulphide scrambling of interleukin-2 for serine and found that protein stability was enhanced.

Both sulphur and oxygen are group six elements and are able to participate in similar side chain hydrogen bonding interactions. However analysis of the *E.coli* MDH crystal structure (Hall *et al*, 1992) indicates that the side chains of cysteines 109 and 113 do not participate in hydrogen bonding interactions, but only the backbone atoms of these residues participate in hydrogen bonding The oxygen and nitrogen of cysteine 109 with the nitrogens of residues 111, 112 and oxygen of residue 105, while the oxygen and nitrogen of residue113 hydrogen bond with the nitrogen of residue 74 and oxygen of residue 71 (Fig 4.15). Substitution with serines will not initiate new hydrogen bonding interactions between the side chains of the serines and the surrounding residues, or terminate any existing hydrogen bonds.

α-Helices possess a dipole moment due to the alignment of the backbone amide group along the axis, resulting in a positive charge developing at the N-terminus and a negative charge at the C-terminus (Hol, 1985). This dipole in some instances is counteracted by charged residues. Richardson and Richardson (1988) have shown that some residues have a positional preference on α-helices. Serine has a greater preference for the N-terminus position than the C-terminal position. Cysteine does not have a marked preference for either the N- or C-terminus of α-helices. Cysteine 109 is located at the C-terminus of α-helix αDE (Hall *et al*,1992). It is possible that substitution of cysteine 109 at the C-terminus of αDE destabilises the α-helix by influencing the dipole resulting in the destabilising the MDH (Ihara *et al*, 1982; Shoemaker *et al*, 1985; Shoemaker *et al*, 1987). If this is the case substitution into the wild type MDH of lysine which is positively charged at physiological pH should stabilise the α-helix, whereas substitution of aspartate which is negatively charged should destabilise the α-helix.

Analysis of MDH amino acid sequence alignments (Fig 6.1) indicates that cysteine 113 is non conserved, with only two of the twelve aligned sequences having an equivalent cysteine, but cysteines 109 and 251 are conserved. Cysteine 109 had an equivalent

(1)

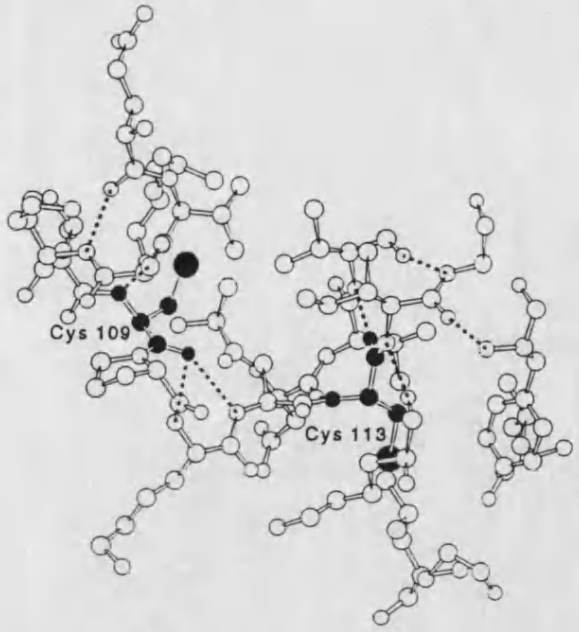

(2)

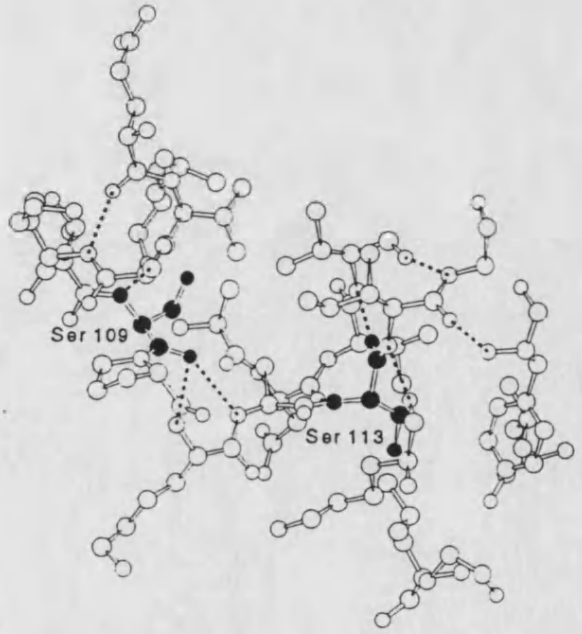

Fig 4.15. Conformation of α-helix αDE, β-strand βE and turn αDE/βE in *E.coli* MDH crystal structure.

(1) Cysteines 109 and 113 are indicated by triple letter code and highlighted in black. Stippled lines indicate proposed hydrogen bonding interactions.

(2) Substituted serines 109 and 113 are indicated by triple letter code and highlighted in black. Stippled lines indicate proposed hydrogen bonding interactions.

Figure 4.15 indicates that the side chains of residues 109 and 113 do not participate in hydrogen bonding.

cysteine in eight out of twelve of the sequences and cysteine 251 had an equivalent in seven out of twelve of the sequences. Three out of four of the sequences which did not possess an equivalent cysteine to cysteine 109 did not have an equivalent cysteine for cysteine 251. This observation together with the fact that the largest decrease in protein expression is associated with the double mutation suggests that cysteine 109 and 251 are involved in disulphide bond formation in a folded intermediate of the *E.coli* MDH (Creighton, 1980; Konishi *et al*, 1981; Wetzel *et al*, 1988; Zale and Klibanov, 1986). Removal of either cysteine 109 or 251 would prevent correct transient disulphide bond formation and alter the folding pathway of the protein. This would result in an increased susceptibility to degradation. Conformation that cysteine 109 and 251 take part in a disulphide intermediate in *E.coli* MDH protein folding could be obtained by substituting cysteine 251 for serine. If no decrease in stability is observed then these residues do not take part in a disulphide bond formation.

CHAPTER FIVE:

SUBSTITUTION OF CYSTEINES INTO THE *E.COLI* MDH βD/αD SURFACE LOOP.

(5.1) **Introduction.**

Prior to building a model of the *E.coli* dimeric MDH, residues chosen as candidates for substitution to cysteine were determined by analysis of the porcine cytoplasmic MDH crystal structure and sequence alignment of MDHs. Comparison of the MDH crystal structures indicate that regions of high sequence identity have the most similar conformations (Birktoft *et al*, 1989). To gain confidence that solvent accessible residues in the porcine crystal structure would also be solvent accessible in the *E.coli* MDH only regions of high sequence identity in the sequence alignment were analysed. Sequence alignments (Fig 6.1) indicated that the βD/αD loop was highly conserved. This loop is also solvent accessible and constitutes part of the active site when in the "collapsed" state (Hall *et al*, 1992). Analysis of the crystal structure indicated that the side chains of arginine 91, glycine 94 and leucine 100 of this conserved βD/αD surface loop were solvent accessible and in a suitable orientation for substitution to cysteines. Amino acid sequence alignment indicated that the corresponding *E.coli* MDH residues were arginine 81, glycine 84 and leucine 90. These residues were chosen for substitution to cysteine.

(5.2.1) Substitution of the codons for arginine 81, glycine 84 and leucine 90.

Substitution of the codons for residues 81, 84 and 94 was achieved using the scheme outlined in figure 5.1. Oligonucleotides (-9 and -10) were designed to utilise a unique *Nae* I restriction site. Oligonucleotide-9 allowed substitution of the codons for residues 81 and/or 84, while oligonucleotide-10 substituted the codon for residue 90. The intention of this strategy was to cut down on the cost of oligonucleotide synthesis.

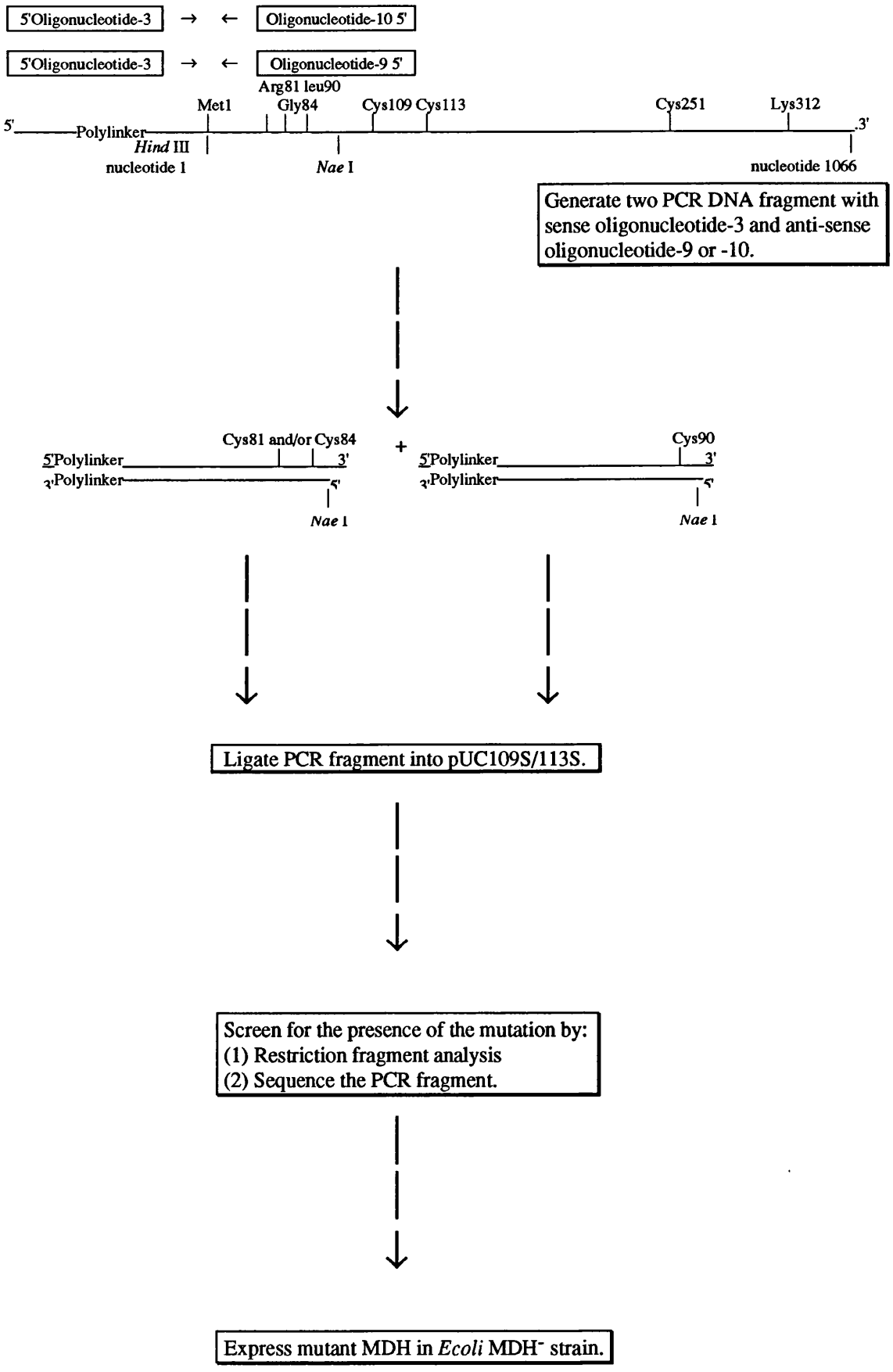

Fig 5.1: Flow diagram of steps used to generate mutant pC109S/113S(81C,84C,90C).

Clones were screened for the presence of the mutations in a similar manner to MDH mutant 109S/113S.

(5.2.2) Screening for the substitutions in the codons for arginine 81, glycine 84 and leucine 90.

Transformation of *E.coli* TG1 with pUCWT and pUC109S/113S containing the βD/αD substitutions resulted in a low number of transformed colonies. Plasmids from colonies were screened for the presence of the mutations by restriction fragment analysis with *Sal* I and *Kpn* I. If the PCR product was successfully ligated into the vector, restriction with *Kpn* I would excise a DNA fragment of 1166 bp. However, if it was unsuccessful, *Kpn* I restriction would excise a DNA fragment of 580 bp. Linearisation of the plasmid with *Sal* I would confirm the presence of the PCR product. Oligonucleotide-4 which annealed between nucleotides 319 to 347 was used to confirm the presence of nucleotide substitutions (Fig 5.2 to 5.4). Sequence analysis indicated that the introduced mutations were present in the pUC109S/113S, but absent in pUCWT. Further attempts to insert PCR product into pUCWT were unsuccessful.

(5.2.3) Purification of pUC109S/113S/81C, pUC109S/113S/84C and pUC109S/113S/90C MDHs.

E.coli W945T1-2 harbouring the mutants, grew poorly under the growth conditions used, MDH activity was not detected in the cell-free extract. Analysis of the cell-free extract, precipitated dialysate and dialysate by SDS-PAGE showed that the 33kD subunit of MDH was absent.

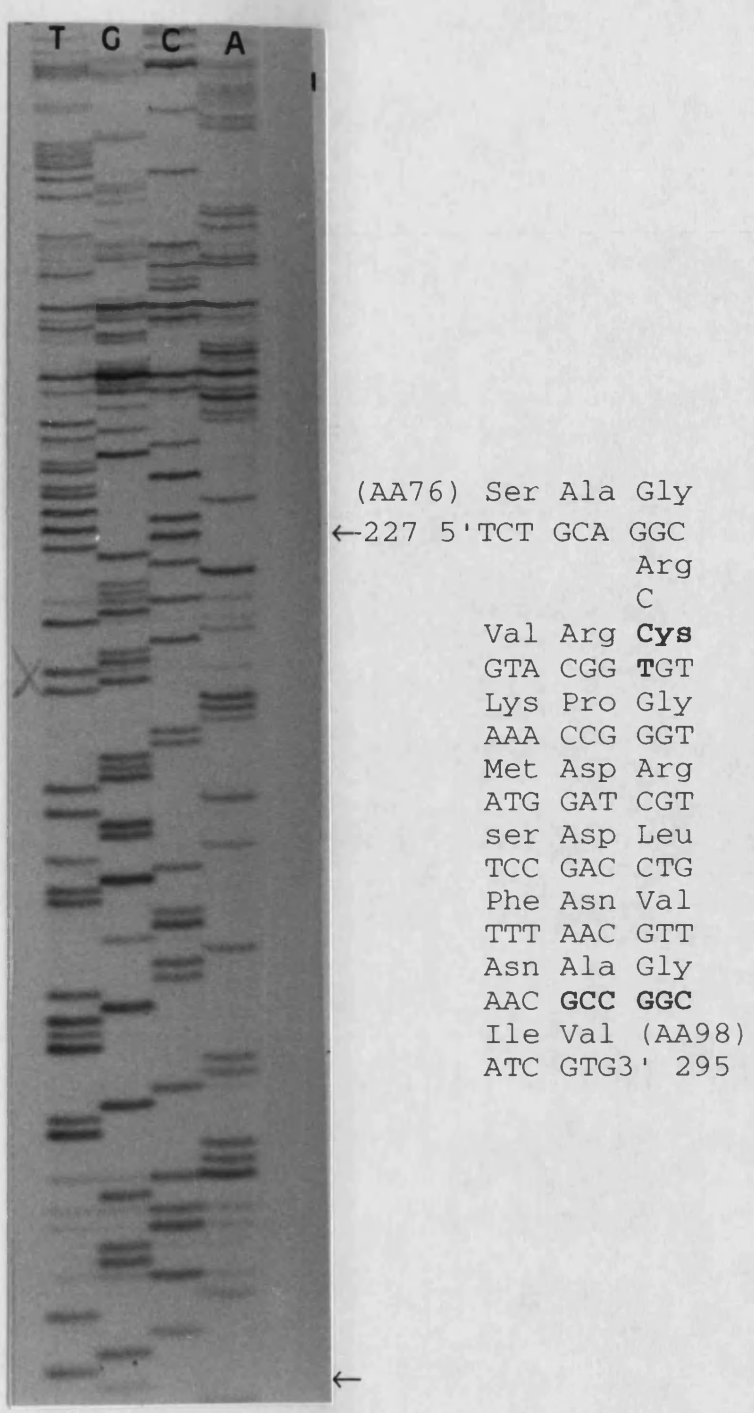

Fig 5.2: Dideoxy sequence analysis of mutant 109S/113S/81C gene using oligonucleotide-4 as primer.

Lanes from left to right: Thymine (T); Guanine (G); Cytosine (C); Adenine (A) with corresponding codon usage. Bold uppercase indicates *Nae* I restriction site and mutations. Corresponding triple letter amino acid code is indicated above codon.

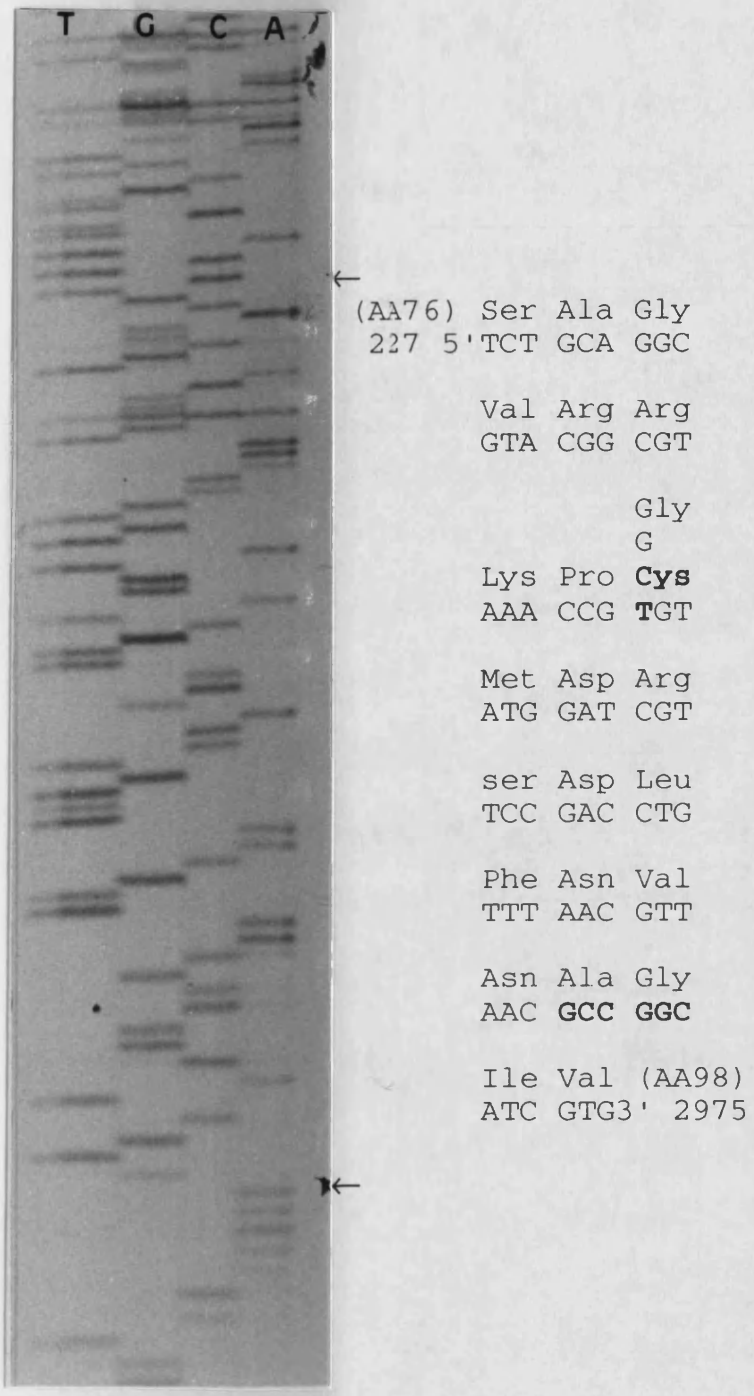

Fig 5.3: Dideoxy sequence analysis of mutant 109S/113S/84C gene using oligonucleotide-4 as primer.

Lanes from left to right: Thymine (T); Guanine (G); Cytosine (C); Adenine (A) with corresponding codon usage. Bold uppercase indicates *Nae* I restriction site and mutations. Corresponding triple letter amino acid code is indicated above codon.

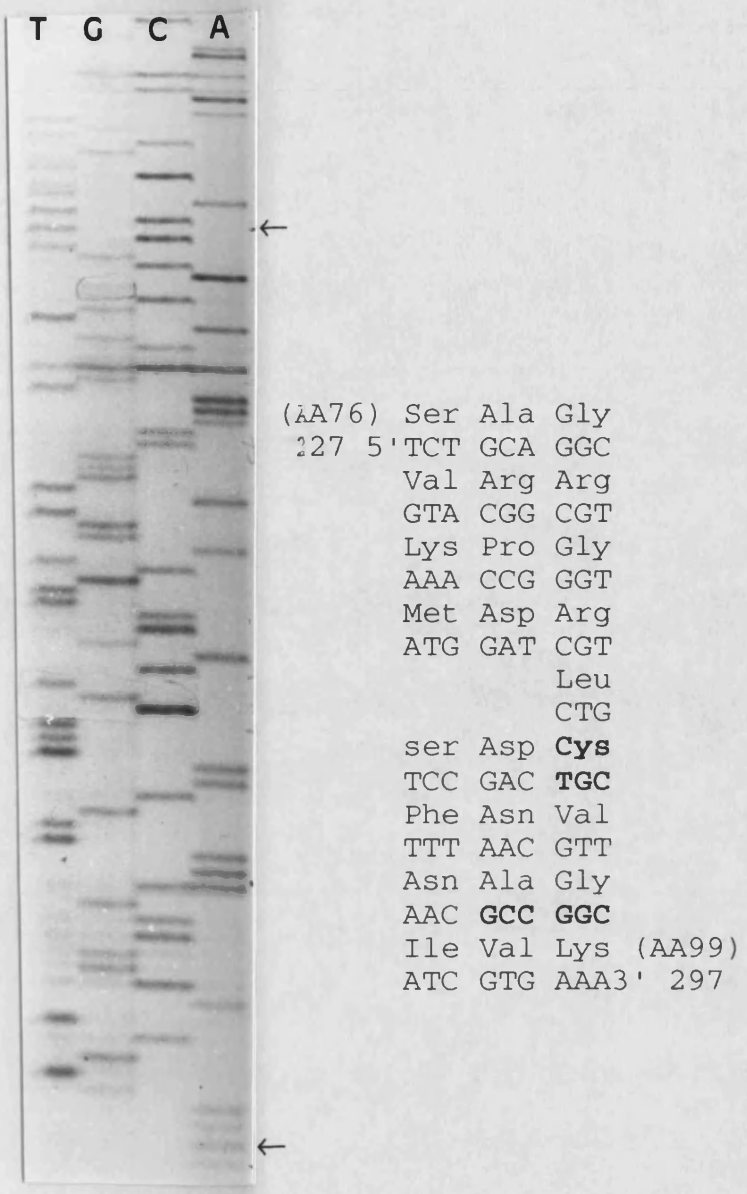

Fig 5.4: Dideoxy sequence analysis of mutant 109S/113S/90C gene using oligonucleotide-4 as primer.

Lanes from left to right: Thymine (T); Guanine (G); Cytosine (C); Adenine (A) with corresponding codon usage. Bold uppercase indicates *Nae* I restriction site and mutations. Corresponding triple letter amino acid code is indicated above codon.

(5.3) **Discussion.**

Three cysteines were individually substituted into the conserved βD/αD loop of *E.coli* MDH mutant 109S/113S at residues arginine 81, glycine 84 and leucine 90. Attempts to introduce similar mutations into the wild type MDH failed to produce recombinant colonies. The genes encoding these mutations in 109S/113S MDH when expressed in *E.coli* MDH^- strain W945T1-2, failed to exhibit MDH "like" activity in cell-extracts. No 33kD band corresponding to an MDH subunit was observed in the cell-extracts when analysed by SDS-PAGE. This suggests that the introduction of cysteines into the βD/αD loop of mutant 109S/113S made this mutant more susceptible to degradation. The increased susceptibility to degradation could be due to:

- An unforeseen error incorporated into the MDH gene.
- Change in conformation of secondary structure caused by change the side chain area.
- Change in conformation of secondary structure caused by alteration of the residue charge.
- Change in conformation of secondary structure caused by change in the residue hydrophobicity.
- Change in conformation of secondary structure caused by loss of hydrogen bonding interaction.
- Incorrectly folded protein.

Although the gene was sequenced in the region of the introduced mutation and was found to be correct, regions of DNA sequence were "compressed" and difficult to read. These compressed regions of DNA sequence might contain errors which alter the genes reading frame or introduce a stop codon. This would manifest in the above observation.

Pakula *et al*, (1986) has reported that in general mutants bearing solvent exposed substitutions do not show a high degree of instability when compared to wild type. Substitution of arginine 81, glycine 84 and leucine 90 for cysteine resulted in a 66% decrease, 44% increase and a 25% decrease in side chain area respectively (Creighton, 1983). Residues with similar changes in side chain area have been introduced by other workers. Arginine 81 has been substituted by glutamine in *E.coli* MDH (Nicholls *et al*, 1992) and glycine has been substituted by tryptophan in the homologous loop in lactate dehydrogenase (Waldman *et al*, 1988). These substitutions represent a 20% decrease and 340% increase in the side chain area respectively. Likewise these substitutions represent a similar array of charge and hydrophobicity. Wilks *et al*, (1992) has substituted this loop for longer and shorter loops in lactate dehydrogenase and maintained integrity. If it is assumed that the βD/αD loop in the native protein is initially in the "up" conformation upon completion of protein folding then instability in the MDH could be caused by loss of hydrogen bonding interactions in this conformation. The porcine cytoplasmic crystal structure indicates that the side chain of arginine 91 (*E.coli* arginine 81) hydrogen bonds with the side chain oxygen of aspartate 99 (*E.coli* aspartate 89) and the backbone oxygen of methionine 95 (*E.coli* methionine 85). Glycine 94 (*E.coli* glycine 84) did not hydrogen bond, while the backbone oxygen of leucine 100 (*E.coli* leucine 90) hydrogen bonded with the backbone nitrogen of lysine 109 (*E.coli* lysine 99) (Fig 5.5). If the conformation of the loop does not change upon substitution it would be expected that only the arginine substitution would affect hydrogen bonding. However, protein was not observed with all three substitutions, loss of hydrogen bonding in the loop is not likely to be the major cause of instability in the mutant. The introduced βD/αD loop cysteines could be influencing the folding of the protein (Browning *et al*, 1986), resulting in an incorrect folded protein which is susceptible to degradation (Pakula *et al*, 1986).

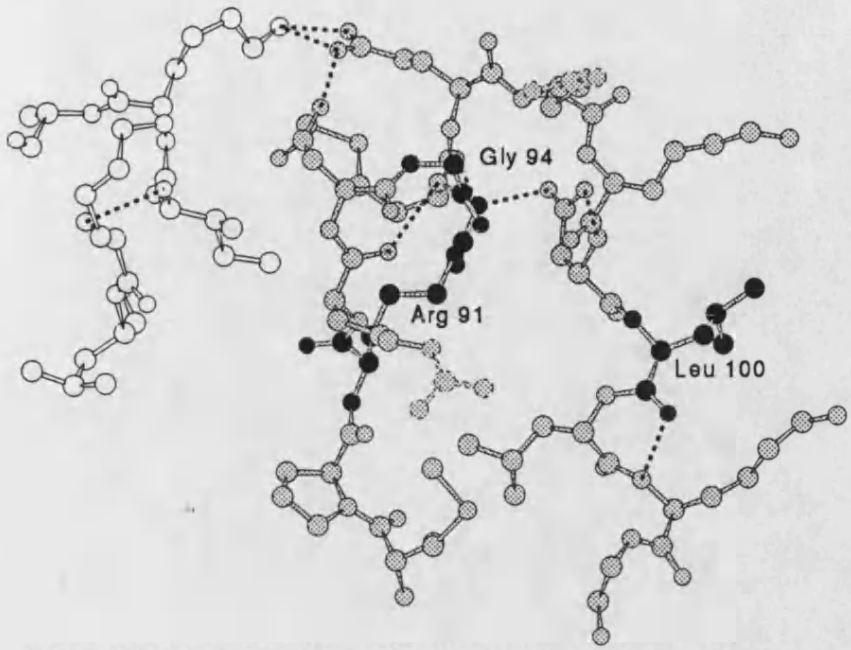

Fig 5.5: Conformation of the βDαD loop in porcine cytoplasmic MDH.

Residues are indicated by triple letter code in black shade. Stippled lines indicate proposed hydrogen bonding interactions.

CHAPTER SIX:

HOMOLOGY MODELLING OF *E.COLI* MDH.

(6.1) Amino acid sequence alignment.

Amino acid sequence alignment of a single subunit of *E.coli* MDH with eukaryotic and eubacterial MDHs indicated a diversity of sequence identities (Fig 6.1). The cytoplasmic MDHs of porcine (18%), mouse (20%) and *Thermus aquaticus* (18%) have a low sequence identity when compared to *E.coli* MDH, but mitochondrial enzymes (porcine (55%), rat (56%), *Saccharomyces cerevisiae*, (49%), mouse (57%) and *Citrullus vulgaris* (53%)), *Citrullus vulgaris* (glyoxysomal) (51%) and *Salmonella typhimurium* MDH (87%) show high sequence identity. *Saccharomyces cerevisiae* (glyoxysomal) MDH exhibits an intermediate sequence identity of 35%. With the exception of the βD/αD loop (conserved region three, residues 146 to 153), regions of high sequence identity are located in the interior of the MDH subunit or at the subunit interface. Conserved region one, corresponds to residues in β-strand βA and α-helix αB of the coenzyme binding domain. This β-strand and α-helix are located at the subunit interface (Birktoft *et al*, 1989; Hall *et al*, 1992). Conserved regions two and five correspond to α-helices αC (coenzyme binding domain) and α3G (catalytic domain) and are located at the subunit interface. Conserved region four corresponds to α-helix α2F and is found in the active site of the MDHs and contains arginine 153 which interacts with the C^1 carboxy moiety of the substrate and aspartate 150 of the histidine-aspartate pair (Birktoft and Banaszak, 1983; Hall *et al*, 1992).

Two anomalies in the sequence alignment are apparent. *E.coli* MDH histidine 177 associated with the histidine-aspartate pair (sequence alignment residue 257), is located on the βG/βH interior facing turn (Hall *et al*, 1992). The position of this histidine varies by one residue in the sequence alignment. In cytoplasmic MDHs and *T. aquaticus* the histidine is at position 258 with conserved residues glycine 256,

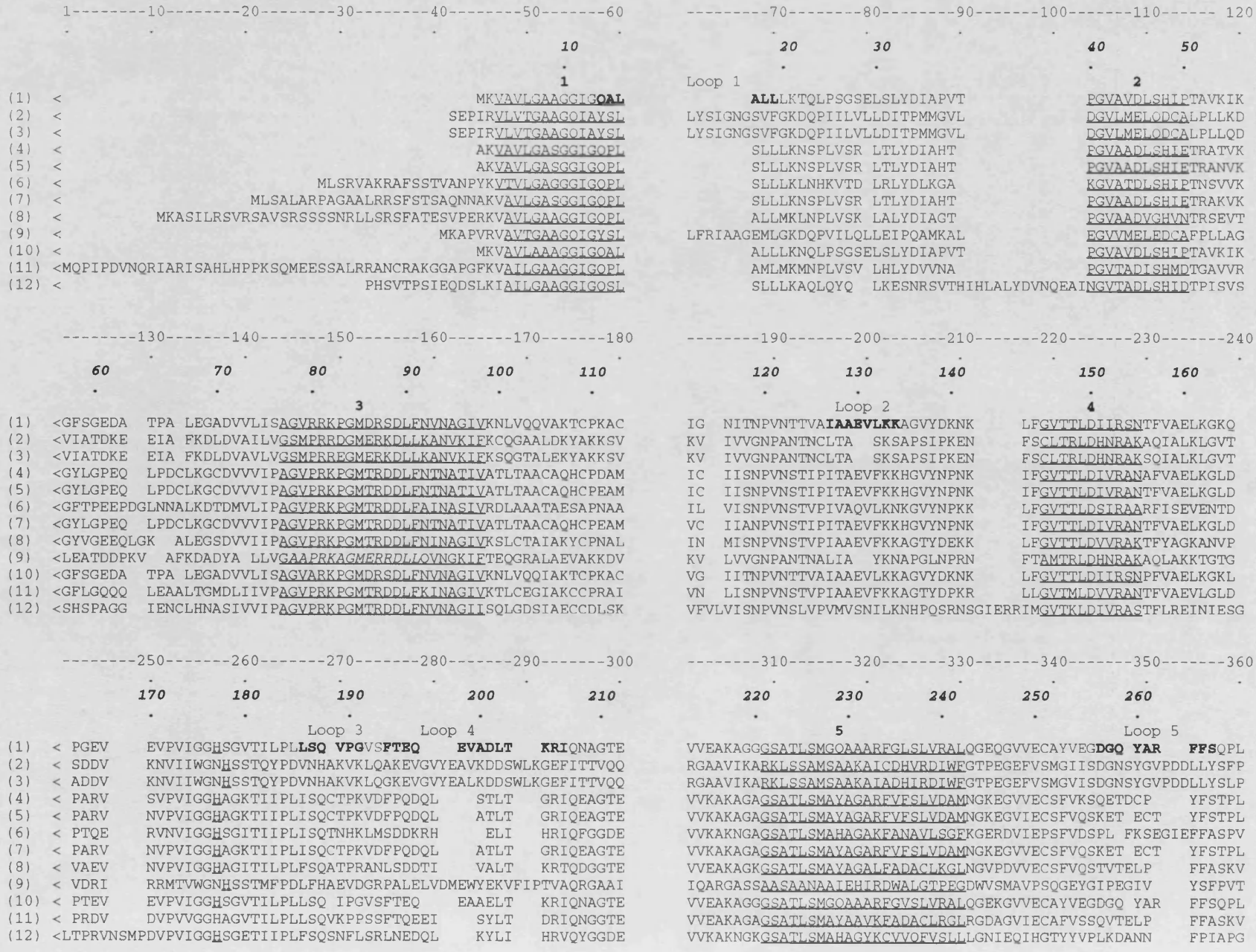
Loop 1
Loop 2
Loop 3
Loop 4
Loop 5

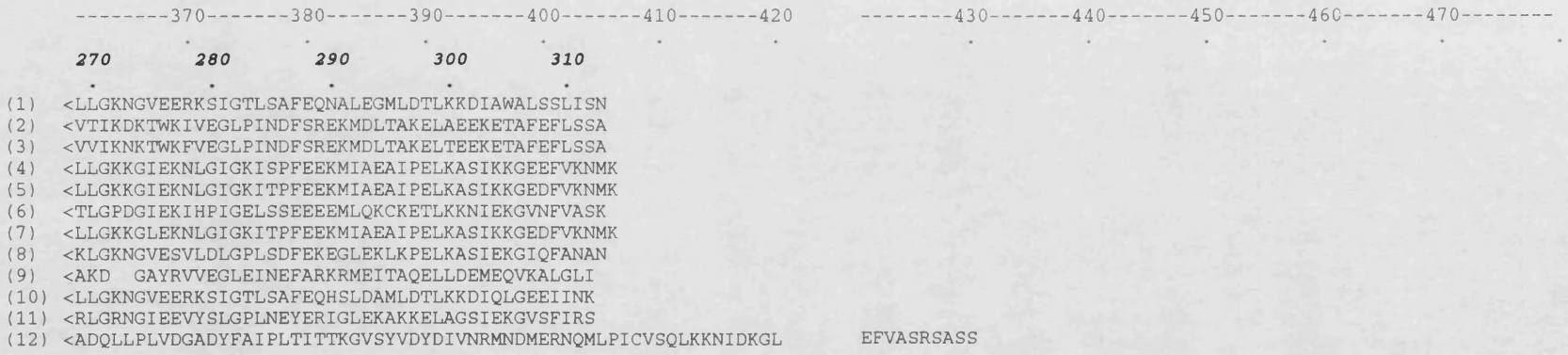

Fig 6.1: Primary amino acid sequence alignment of eukaryotic and eubacterial MDHs.

Lanes: (1) MDH from *E.coli*; (2) cytoplasmic MDH from porcine; (3) cytoplasmic MDH from mouse; (4) mitochondrial MDH from porcine; (5) mitochondrial MDH from rat; (6) mitochondrial MDH from *Saccharomyces cerevisiae* (yeast); (7) precursor mitochondrial MDH from mouse; (8) precursor mitochondrial MDH from *Citrullus vulgaris* (watermelon); (9) MDH from *Thermus Aquaticus* (SUBSP. *Flavus*); (10) MDH from *Salmonella typhimurium*; (11) precursor glyoxysomal MDH from *Citrullus vulgaris* and (12) mitochondrial MDH from *Saccharomyces cerevisiae* (yeast). Conserved regions 1 to 5 are underscored. Constructed loop regions are indicated as Loops 1 to 5 in bold. Regions of non sequence similarity are indicated by gaps in sequence. *E.coli* MDH amino acid sequence numbering is indicated in bold italics with sequence alignment numbering indicated above.

threonine 261 and proline 264 located on either sides in the sequence alignment. Complimentary alignment of the histidines could only be achieved by insertion of a space between residues 254 and 255 in the *E.coli* and mitochondrial sequence alignments, consequently removing conservation of the threonine and proline residues. The second anomaly is apparent with residues asparagines 188, 191 and proline 189 in the *E.coli* sequence. Alignment of the asparagines and proline could only be achieved with the insertion of one "gap" between residues 192 and 193 thus moving residues 185 to 192 to the left in the cytoplasmic and *T aquaticus* MDHs and out of sequence alignment.

(6.2) *E.coli* MDH model

Sequence alignment highlighted seven regions of deviation between *E.coli* and porcine cytoplasmic MDH (Fig 6.1). These regions of sequence deviation were constructed with five loops.

Loop-1 was built to bridge *E.coli* MDH leucine 16 and alanine 17 using glutamine 14 and leucine 19 as the initiation and termination points of the loop. To span the gap (16Å) with four residues, it was necessary to use a polypeptide with an extended conformation (translation of an α-helix and β-strand are 1.5Å and 3.4Å respectively between Cα atoms, Creighton, 1983). This resulted in a deviation to the local environment from α-helix to an extended sheet (Fig 6.2).

Loop-2 was built between *E.coli* residues, alanine 129 and leucine 132 using isoleucine 127 and lysine 134 as the initiation and termination points on the loop. A polypeptide of six residues was used to span the gap of 6Å. This polypeptide maintained the α-helix conformation (Fig 6.3).

Fig 6.2: Superposition of constructed *E.coli* model Loop-1 with template Porcine structure.

E.coli polypeptide backbone is in blue between residues12 and 30 and template porcine structure in green between residues 134 and 153, indicating a change in conformation from α-helix to β-strand.

Fig 6.3: Superposition of constructed *E.coli* model Loop-2 with template Porcine structure.

E.coli polypeptide backbone is in blue between residues124 and 145 and template porcine structure in green between residues 134 and 153, indicating a conservancy of α-helix conformation.

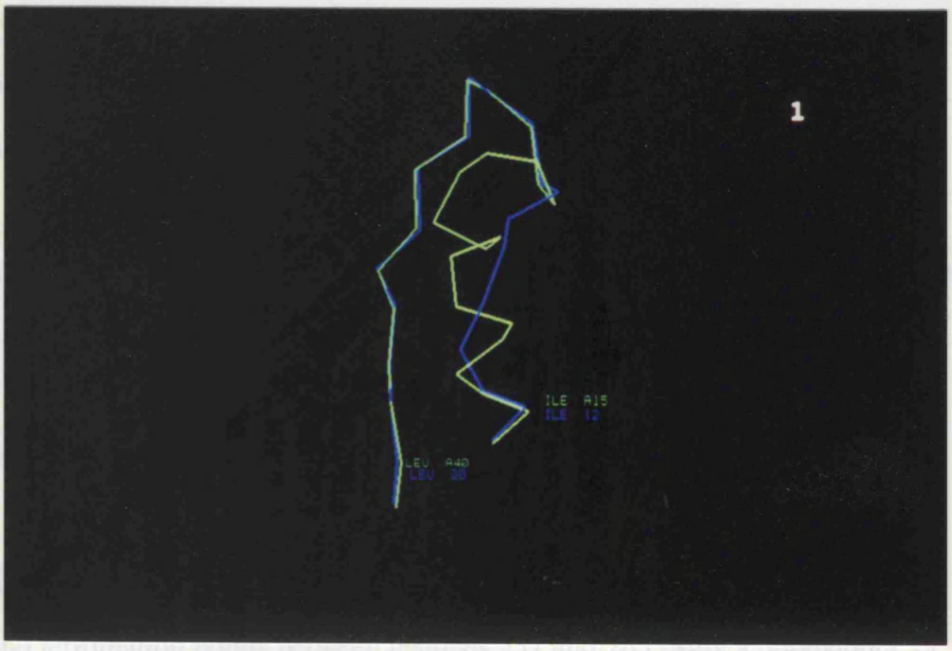
1
ILE A15
ILE 12
LEU A40
LEU 38

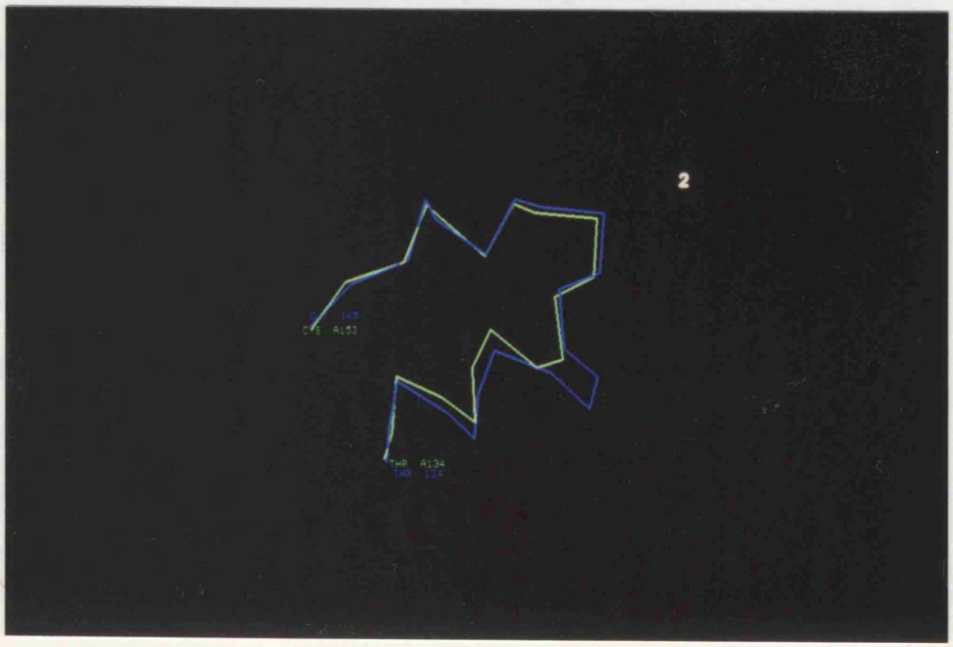
2
CYS A151
THR A134
THR 124

Loop-3 was built between *E.coli* residues, glutamine 188 and valine 189 using leucine 186 and glycine 191 as the initiation and termination points of the loop. The gap was bridged using a polypeptide of four residues which maintained the β-strand conformation (Fig 6.4).

Loop-4 was constructed between residues glutamine 197 and lysine 204 with initiation and termination points at residues phenylalanine 194 and isoleucine 206. This gap could only be bridged with a polypeptide of eleven residues, changing the conformation from β-strand to an extended conformation (Fig 6.4).

Loop-5 was built between residues, glutamine 259 and phenylalanine 263 with initiation and termination points between residues 257 and 265 using a polypeptide of 7 residues. This maintained the β-turn conformation (Fig 6.5).

The side chains of residues of the *E.coli* MDH sequence were substituted for their counterparts in the modified porcine MDH template to produce a modelled non-energy minimised *E.coli* MDH subunit. Prior to optimisation of the atomic co-ordinates by potential energy minimisation (Karplus, 1987), the modelled subunit was duplicated and superimposed onto the original porcine MDH template to produce a non-energy minimised dimeric *E.coli* MDH model. The potential energy minimised dimeric model had a mean deviation of the polypeptide backbone from the porcine MDH template of only 0.3Å (Fig 6.6) and a potential energy in the expected range. Visual examination of the polypeptide "backbone" of the *E.coli* model superimposed onto the porcine MDH template indicated that regions of greatest deviation occurred around the introduced loops (loops 1 to 5) (Fig 6.6).

Fig 6.4: Superposition of constructed *E.coli* model Loop-3 and Loop-4 with template porcine structure.

E.coli polypeptide backbone is in blue between residues186 and 206 and template porcine structure in green between residues 194 and 222, indicating a conservancy of β-strand of Loop-3, but change in conformation for Loop-4.

Fig 6.5: Superposition of constructed *E.coli* model Loop-5 with template porcine structure.

E.coli polypeptide backbone is in blue between residues 252 and 267 and template porcine structure in green between residues 268 and 287, indicating a conservancy of β-turn motif.

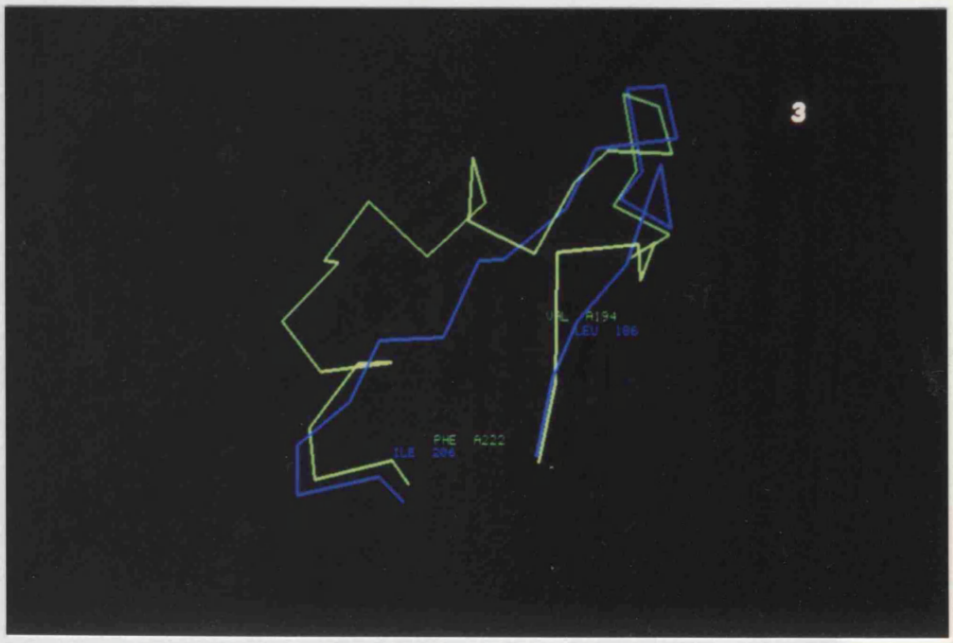
3
PHE A222
ILE 206

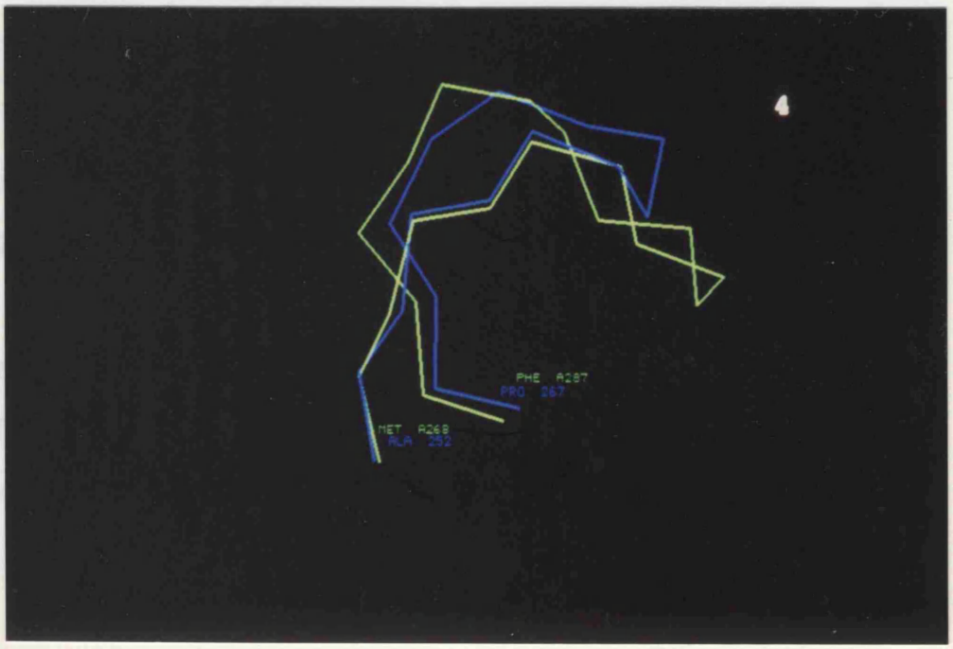
4
PHE A287
PRO 267
MET A268
ALA 282

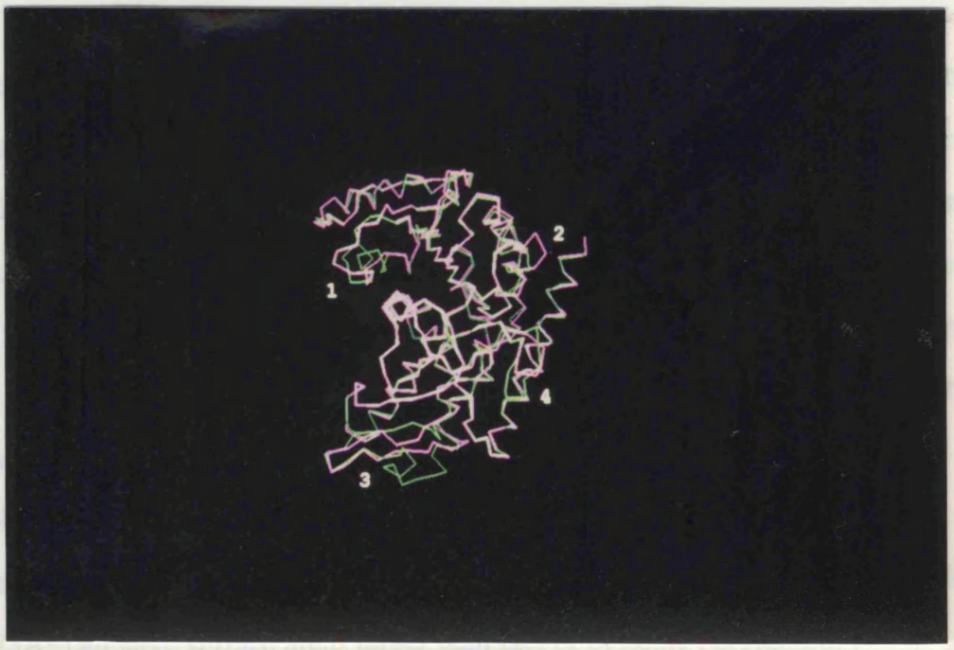

Fig 6.6: Superimposition of constructed *E.coli* model (subunit) with template porcine structure (subunit).

The superposition of *E.coli* model (magenta) with Porcine template (green) with mean deviation of 0.3 Å is indicated. The positions of generated loop 1 is indicated by number 1, loop 2 by number 2, loops 3 and 4 by number 3 and loop 5 by number 4.

(6.3) **Identification of suitable residues for substitution to cysteine.**

The residue chosen as the ligand coupling residue was cysteine. To minimise the possibility of perturbation of the *E.coli* MDH structure upon substitution of surface residues it was necessary to target residues which have the most similar characteristics to cysteine. Serine is the most similar residue to cysteine (Chapter four), however to maximise the number of potential substituting residues, other residues were appraised for their suitability for substitution. Bordo and Argos (1991) have suggested that cysteines are most often substituted with threonine, proline, valine, leucine and isoleucine. Cysteine has a predicted surface area of 135Å^2 (Creighton, 1983). Threonine (140Å^2), proline (145Å^2), valine (155Å^2), leucine (170Å^2) and isoleucine (175Å^2) all have surface areas larger than that of cysteine (Creighton, 1983). Threonine and proline have the most similar surface area to cysteine. However proline is less similar than threonine when the residues hydropathy is considered (Kyte and Doolittle, 1982; Roseman, 1988). Proline is associated with disruption of secondary structure (Hall *et al*, 1992; Richardson and Richardson, 1988). This makes proline unsuitable for use as a target residue for substitution. Conversely threonine is not associated with disruption of secondary structure. The rational for using threonine as a target residue for substitution to cysteine is further substantiated by the fact that threonine has successfully been substituted for cysteine by other workers. For example Wells and Powers (1986) have substituted threonine for cysteine in *Bacillus amyloliquefaciens* subtilisin. This residue took part in disulfide bond formation. Serine and threonine residues were chosen as target residues for substitution to cysteine.

The radius of an antibody combining site is approximately 15Å (Davies and Padlan, 1990). Attachment of an antibody to a ligand which is within 15Å of the βD/αD loop residue 85 (determined to be the apex of this catalytically important loop) could inhibit this loop and/or prevent movement of the substrate into the active site (Rowley *et al*, 1975). Attachment of an antibody to a ligand greater than 15Å from residue 85 could

hinder catalysis by preventing conformation change of the enzyme which occurs during catalysis. Two residues were chosen, one within a radius of 15Å and one outside the 15Å radius. A Connolly surface prediction indicated that eleven serine and threonine residues had a solvent accessibility greater than 60Å^2 (approximate surface area of two methyl groups) in the *E.coli* model, as did their counterparts in the porcine cytoplasmic crystal structure (Table 6.1). Analysis of the model indicated that serines 88 and 222 were within 15Å of residue 85. However, serine 88 was in a conserved region of the model making this residue unsuitable for substitution. Serine 222 is in a non-conserved loop of the model making it suitable for substitution. The remaining residues were outside the 15Å radius. Threonine 203 was in a conserved region making this residue unsuitable for substitution. Serine 193 was in a constructed loop region (loops 3 and 4), resulting in low confidence in the prediction of solvent accessibility. Residues 308 and 312 were determined to be part of a secondary structure motif making these unsuitable for substitution. Of the remaining residues threonine 64 was determined to be in an optimum conformation on a non-conserved loop suitable for substitution. Residues 64 and 222 were chosen as candidates for substitution to cysteine (Fig 6.7).

(6.4) **Appraisal of the model.**

The energy minimised model had a similar shape and volume to that of the porcine crystal structure. Confidence was further gained in the model as it had an average deviation from the porcine crystal structure of only 0.3Å (Fig 6.6). Comparison with the recently published *E.coli* MDH ternary model (crystal structure) indicated regions of similarity and dissimilarity. The ternary model was based upon an energy minimised crystal structure of *E.coli* MDH (Hall *et al*, 1992). The directory of secondary structure in proteins (DSSP) (Kabsch and Sander, 1983) output of secondary structure of the *E.coli* model, crystal structure and porcine crystal structure alignment against the *E.coli* MDH primary structure indicated that the majority of the α-helices were predicted (α-Helix αB was not predicted) (Fig 6.8). However the initiation and

Residue Number (*E.coli*)	Residue Type	Distance from residue 85 (Å)	solvent accessibilities ($Å^2$)	Residue Number porcine	Residue Type	solvent accessibilities ($Å^2$)	Conserved Yes/No	Secondary structure α, β, t or *
22	Thr	42.46	131	32	Asp	121	N	t
64	Thr	34.43	97	74	Glu	99	N	t
88	Ser	6.19	100	98	Lys	167	Y	*
193	Ser	41.60	128	202	Gln	199	N	t
203	Thr	22.97	66	216	Ser	96	Y	t
222	Ser	11.488	107	238	Lys	139	N	t
280	Ser	35.45	100	300	Glu	103	N	*
283	Thr	34.82	133	303	Pro	97	N	*
285	Ser	32.14	65	305	Asn	70	N	*
308	Ser	21.99	79	328	Glu	147	N	α
312	Ser	24.58	71	332	Ser	76	N	α

Table 6.1: Comparison of solvent accessibility of residues in *E.coli* model and porcine template structure.

Residue solvent accessibilities for the *E.coli* model and porcine template were determined via a Connolly surface prediction. The distance of residues from βD/αD loop residue 85 with a solvent accessibility of greater than 80% is given in table 5.5. Secondary structure was determined by DSSP, α signifies α-helix, β signifies β-strand, t signifies turn and * signifies not determined.

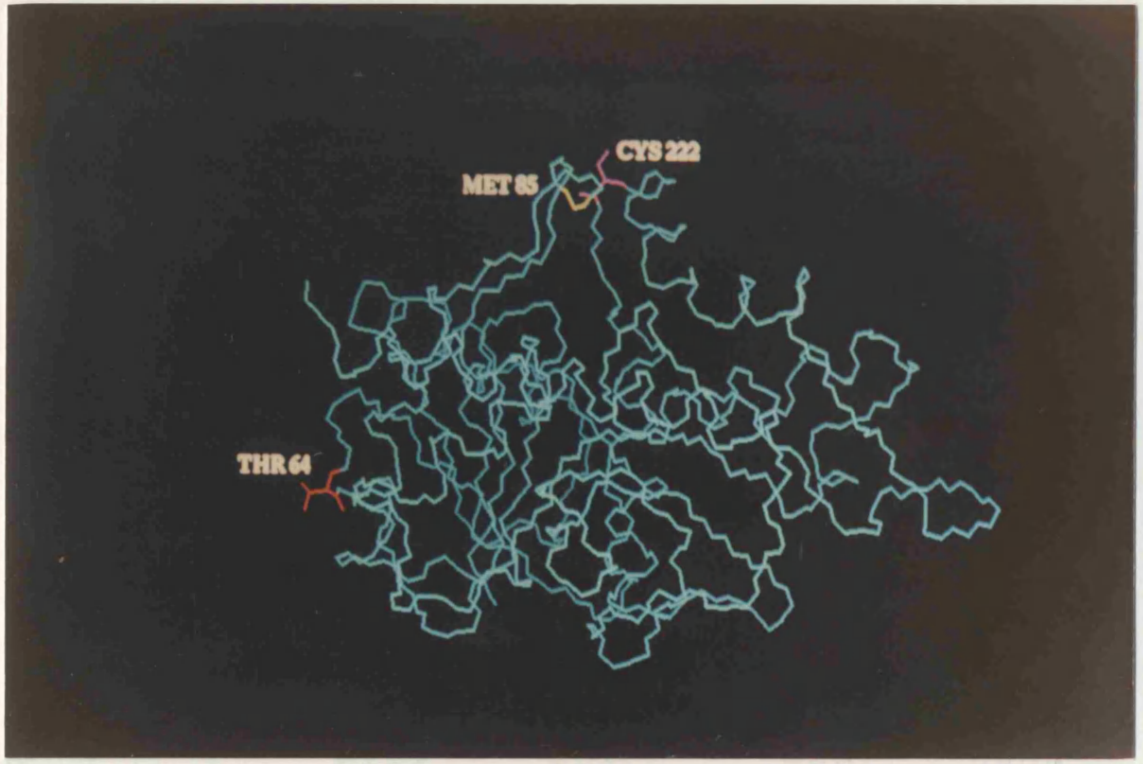

Fig 6.7: Alpha carbon representation of a single subunit of the *E.coli* MDH model.

The relative positions and side chain orientation of residues 64 and 222 (cyan) relative to residue 85(yellow) are indicated. The model predicts that the side chains of residues 64 are outwardly pointing from the interior and solvent accessible.

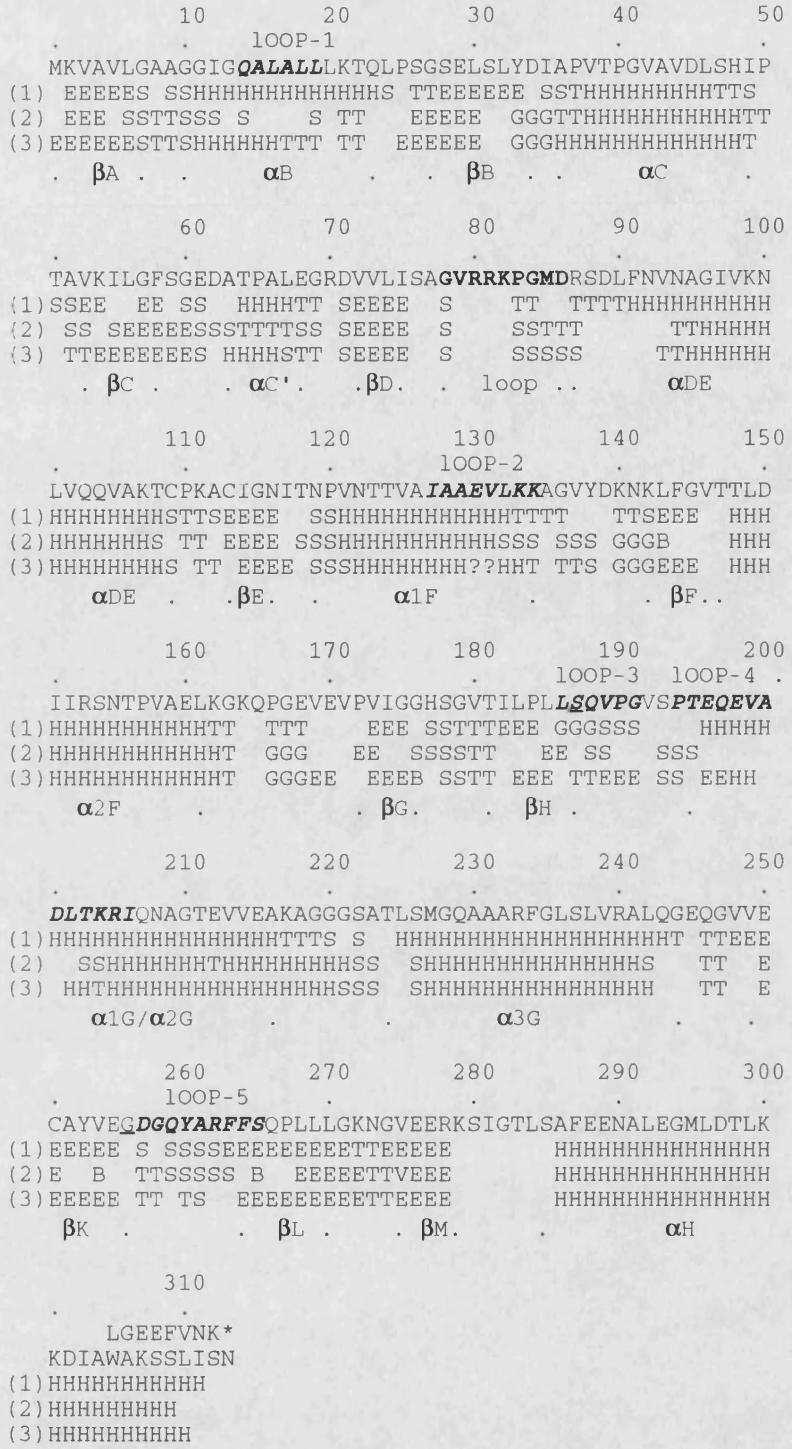

Fig 6.8: Comparison of DSSP predictions of *E.coli* model MDHs and *E.coli* and porcine cytoplasmic MDH crystal structures aligned against *E.coli* MDH primary structure.

(1), (2) and (3) signify secondary structure prediction of *E.coli* crystal structure, *E.coli* model and Porcine cytoplasmic crystal structure; E = β-strand; H = α-Helix; G = 3/10 Helix; T = Turn and S = Bend/Kink. Initiation and termination of secondary structure is indicated below with α signifying α-Helix and β signifying β-strand.

termination points of the α-helices were less well predicted. Five out of nine of the α-helices initiation points were correctly modelled, but only one out of nine termination points were correctly modelled. This trend is mirrored with the modelling of the β-strands. The majority of the cores of the β-strands were correctly modelled, but the points of initiation and termination are less well predicted. Connolly solvent accessibilities predictions (Connolly, 1983) of the *E.coli* model and crystal structure indicate that threonine 64 and cysteine 222 have different solvent accessibilities. In the model the predicted solvent accessibilities were 97Å^2 for threonine and 107Å^2 for serine, whereas in the crystal structure these residues had solvent accessibilities of 42Å^2 and 28Å^2. The *E.coli* MDH model and crystal structure DSSP indicated that model residue 64 was in the middle of turn βC/αC', whereas in the crystal structure it was positioned at the C-terminus of the turn. However comparison of the model and crystal structure suggests that the decrease in solvent accessibility is due to the surrounding secondary structure (Fig 6.7 and 6.9). The secondary structures project further into the solvent than in the model, decreasing solvent accessibility of residue 64. Serine 222 is found on a turn motif (α2G/α3G) in both the model and the crystal structure. However, in the the model it is positioned at the N-terminus and in the crystal structure it is positioned in the middle of the turn. This results in serine 222 repositioning from the surface to a position at the mouth of the active site cleft

Structural alignment of the *E.coli* model and crystal structure and comparison with the sequence identity of the porcine cytoplasmic MDH (Fig 6.1) (based on the Dayhoff *et al*,1983 mutation matrix) indicated the closeness of fit to the crystal structure in relation to sequence identity (Fig 6.10‡). The majority of the regions in *E.coli* MDH which had high sequence identity with the porcine sequence had a corresponding low deviation between the *E.coli* model and crystal structure (<2.0Å). Regions of low sequence identity have larger deviations between the model and crystal structure. However, in several instances regions of high sequence identity have large deviations

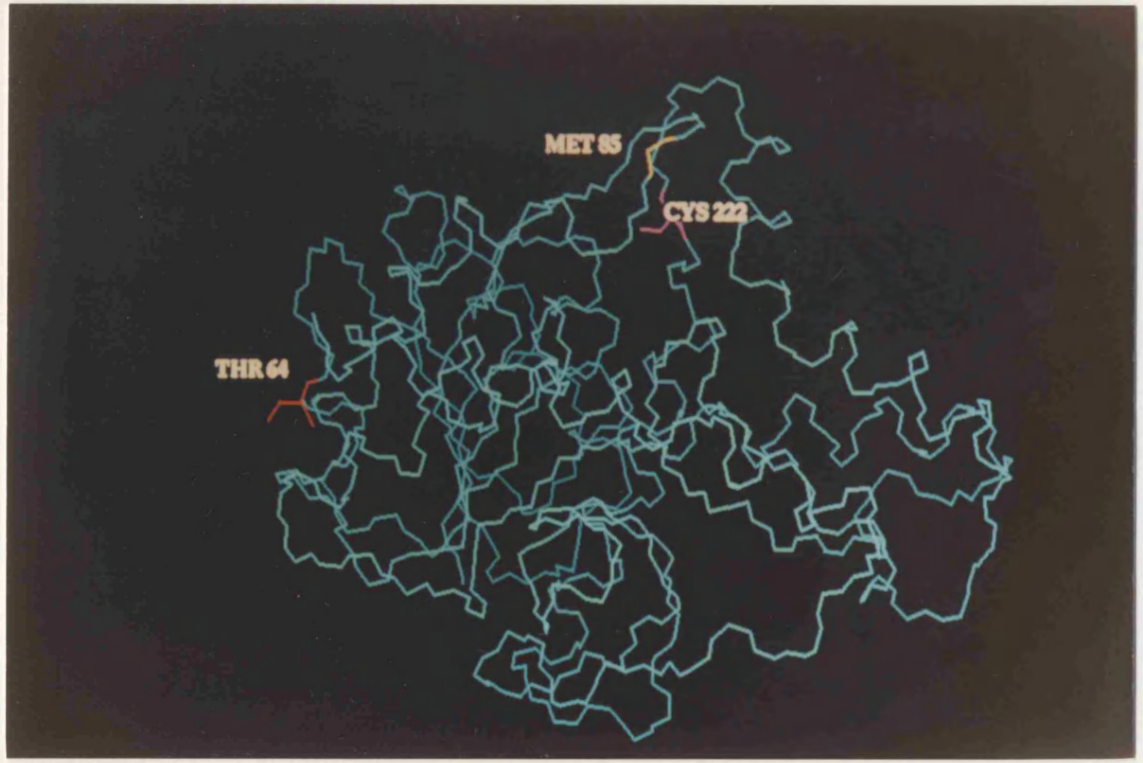

Fig 6.9: Alpha carbon representation of a single subunit of the *E.coli* MDH crystal structure.

The relative positions and side chain orientation of residues 64 and 222 (cyan) relative to residue 85(yellow) are indicated. The model predicts that the side chains of residues 64 are outwardly pointing from the interior and solvent accessible.

Fig 6.10: Comparison of sequence homology between *E.coli* and porcine cytoplasmic MDHs and deviation in conformation of the *E.coli* model and crystal structure.

"Seq homology" is a comparison of the sequence identity between the porcine cytoplasmic and *E.coli* MDHs based on the Dayhoff mutation matrix (1983) according to the sequence alignment indicated below. "Mod vs. X-ray" is the deviation in conformation between the superimposed *E.coli* model and crystal structure based on this sequence alignment. The X axis represents the residue number in the sequence alignment while residues indicated as text refer to the *E.coli* MDH polypeptide sequence. Score window length was five residues.

```
                  10        20        30        40        50          60        70        80        90       100
1 pig      :SEPIRVLVTGAAGQIAYSLLYSIGNGSVFGKDQPIILVLLDITPMMGVLD      GVLMELQDCALPLLKDVIATDKEEIAFKDLDVAILVGSMPRRDGMERKDL
2 ecolimod :---MKVAVLGAAGGIGQALSLLLKTQLPSGSELSLYDIAPVTP          GVAVDLSHIPTAVKIKGFSGEDATPALEGRDVVLISAGVRRKPGMDRSDL
3 ecolistr :---MKVAVLGAAGGIGQALSLLLKTQLPSGSELSLYDIAPVTP          GVAVDLSHIPTAVKIKGFSGEDATPALEGADVVLISAGVRRKPGMDRSDL

                 110       120       130       140       150         160       170       180       190       200
1 pig      :LKANVKIFKCQGAALDKYAKKSVKVIVVGNPANTNCLTA--SKSAPSIPK      ENFSCLTRLDHNRAKAQIALKLGVTSDDVKNVIIWGNHSSTQYPDVNHAK
2 ecolimod :PNVNAGIVKNLVQQVAKTCPKACIGNITNPVNTTVAIATEVIKKAGVYDK      NKLPGVTTLDIIRSNTFVAELKGKQPGEVEVPVIGGHSGVTILPLLSQ-V
3 ecolistr :PNVNAGIVKNLVQQVAKTCPKACIGIITNPVNTTVAIAAEVLKKAGVYDK      NKLPGVTTLDIIRSNTFVAELKGKQPGEVEVPVIGGHSGVTILPLLSQ-V

                 210       220       230       240       250         260       270       280       290       300
1 pig      :VKLQAKEVGVYEAVKDDSWLKGEFITTVQQRGAAVIKARKLSSAMSAAKA      ICDHVRDIWFGTPEGEFVSMGIISDGNSYGVPDDLLYSFPVTIKDKTWKI
2 ecolimod :PGVSFTEQ----EVAPLT---KRIQNAGTEVVEAKAGGGSATLSMGQAAA      RPGLSLVRALQGEQGVVECAYVEGDGQ-PAR---PFSQPLLLGKNGVEER
3 ecolistr :PGVSFTEQ----EVADLT---KRIQNAGTEVVEAKAGGGSATLSMGQAAA      RPGLSLVRALQGEQGVVECAYVEGDGQ-YAR---PFSQPLLLGKNGVEER

                 310       320       330       340       350
1 pig      :VEGLPINDFSREKMDLTAKEEEKETAPEFLSSALA*
2 ecolimod :KSIGTLSAFEQNALEGMLDTLQKDIAWAKSSLISN*
3 ecolistr :KSIGTLSAFEQNALEGMLDTLKKDIALGQEPVNK-*
```

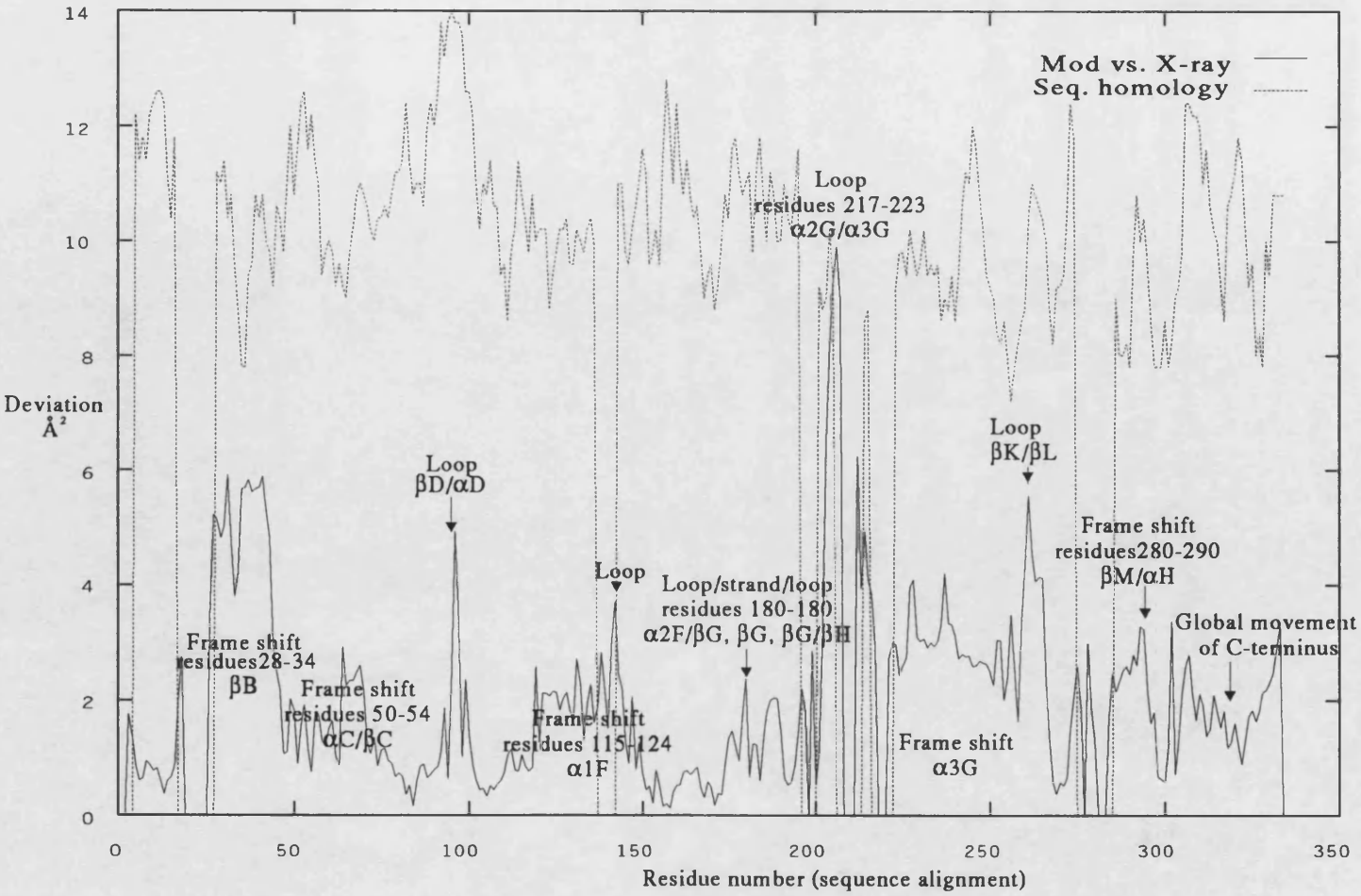

Fig 6.10: Comparison of sequence homology between the *E.coli* and porcine cytoplasmic MDHs and deviation in conformation of the *E.coli* model and crystal structure.

between the crystal structure and model. This can be attributed to surface turn motifs which show a high degree of variation and frame shift in the sequence alignment.

(6.5) **Discussion.**

It is generally regarded that ~20% sequence identity is the limit that homology modelling can be used to construct a 3D model. The sequence identity between the porcine and cytoplasmic and *E.coli* MDH was 18%. Comparison of the *E.coli* model and crystal structure show several anomalies which can be attributed to the low sequence identity:

Regions of deviation in sequence necessitate the introduction of gap(s) in the sequence alignment. These gaps are bridged with polypeptides obtained from the Brookhaven protein data bank. Due to the limited number of structures available these polypeptides represent the best available fit to bridge the gap as opposed to the optimum fit. At the present moment the Brookhaven protein data bank contains about 600 unique crystal structures. The number of deposited crystal structures is however increasing. This will result in a greater polypeptide repertoire to choose from and therefore better polypeptides to bridge gaps.

Low sequence identity increases the difficulty in correctly aligning polypeptide sequences. This will result in frame shifts in the sequence alignment which will alter the initiation and termination of the gap(s) and secondary structure.

The low sequence identity means that the secondary and tertiary structures of *E.coli* and porcine cytoplasmic MDH although similar will not be identical. Modelling of the *E.coli* MDH on the porcine crystal structure will therefore bias the modelled structure to the template conformation.

CHAPTER SEVEN:

SUBSTITUTION OF THREONINE 64 AND SERINE 222 FOR CYSTEINES IN *E.COLI* WILD TYPE MDH.

(7.1) **Introduction.**

Threonine 64 and serine 222 were uniquely substituted for cysteines in the wild type MDH gene according to the scheme illustrated (Fig 7.1 and 7.2). Colonies harbouring plasmid were screened for the presence of the substitutions by colony hybridisation, restriction fragment analysis and DNA sequencing. Plasmids possessing these substitutions were expressed in MDH^- strain W945T1-2.

(7.2.1) Screening for the substitution in the codon for threonine 64 (64C).

Plasmid from colonies were screened for the presence of the mutation by colony hybridisation using 5' [^{32}P] labelled oligonucleotides-11 and -13 as probes (Fig 7.3). The plasmid from the colony which showed strong hybridisation to the probes at 74°C was subjected to restriction fragment analysis. Restriction with *Hind* III and *Sph* I, linearised the plasmid, indicating successful removal of the polylinker *Hind* III and *Sph* I restriction sites (as the polylinker *Sph* I restriction site was removed by oligonucleotide-11) (Fig 7.4). Restriction with *Hind* III/*Sal* I excised a DNA fragment of similar size to *Hind* III restricted pUCWT. The presence of the unique *Sph* I and *Hind* III restriction sites and the excision of the correct size DNA fragment with *Hind* III/*Sal* I restriction, confirmed the substitution of the codon for threonine 64 to cysteine. An oligonucleotide-4 hybridised to nucleotide positions 319 to 347 of the gene and was used as a sequencing primer to confirm the nucleotide substitutions introduced into the codon of residue 64.

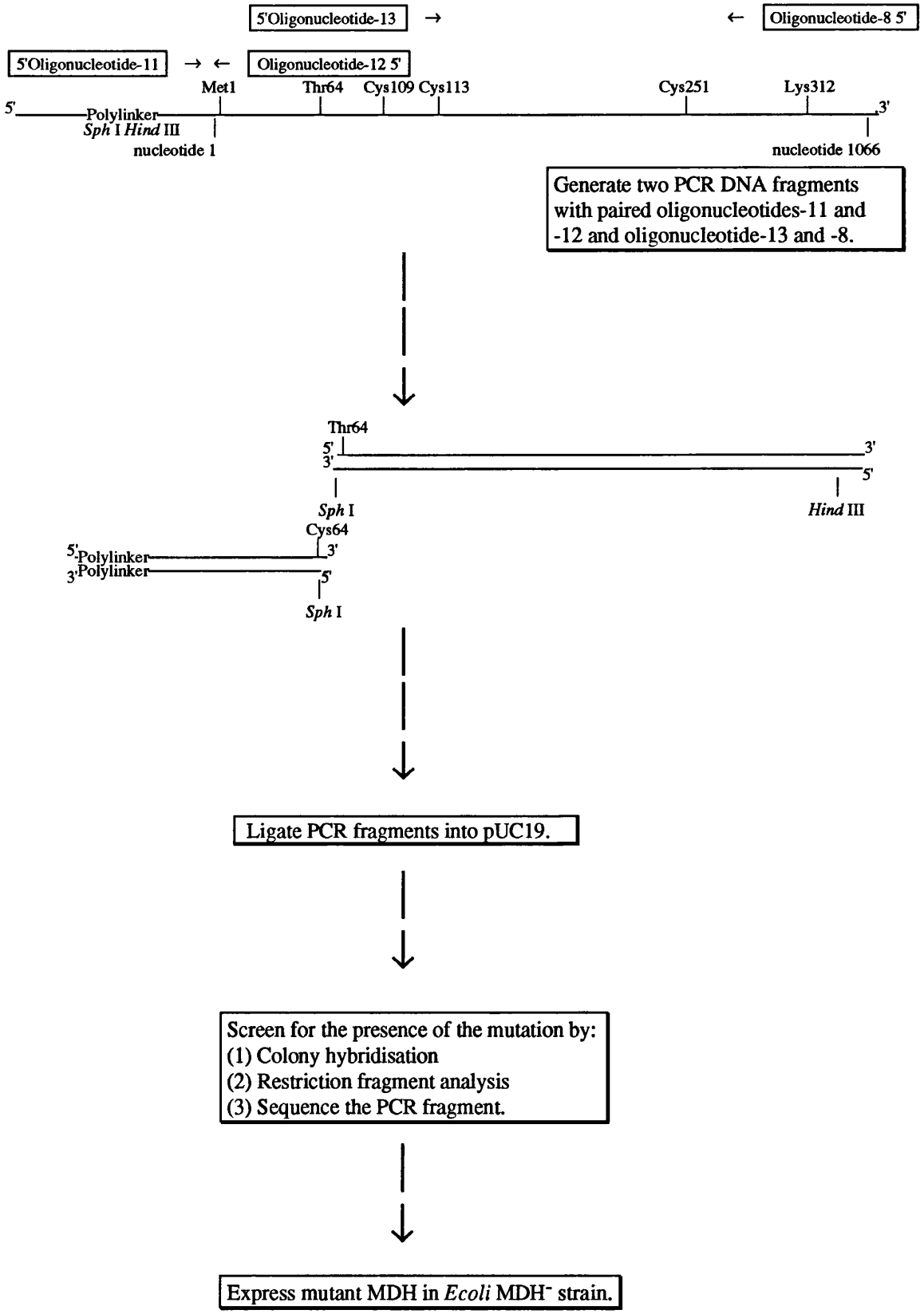

Fig 7.1: Flow diagram of steps used to generate mutant pUC64C.

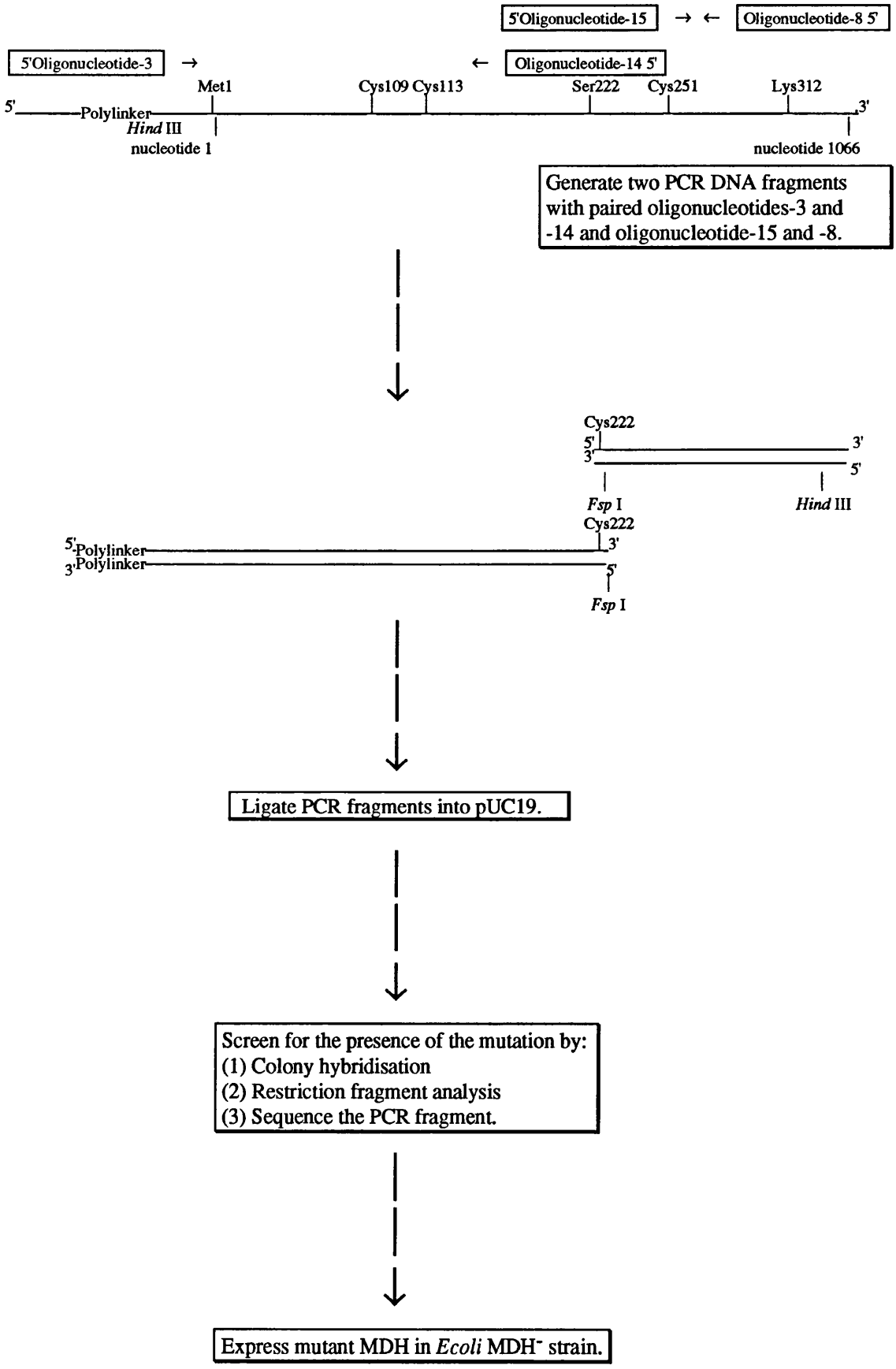

Fig 7.2: Flow diagram of steps used to generate mutant pUC222C.

Fig 7.3: Hybridisation of 64C MDH gene with 5' [^{32}P] labelled oligonucleotides-11 and -13 probes.

(1) Hybridisation with probe -11; Wash Hybond-N membrane at 37°C for 10 minutes in 2 x SSC, SDS (0.1% w/v), (2) Wash of Hybond-N membrane at 74°C for 2 minutes in 2 x SSC, SDS (0.1% w/v). (3) Hybridisation with probe -13; Wash of Hybond-N membrane at 37°C for 10 minutes in 2 x SSC, SDS (0.1% w/v); (4) Wash of Hybond-N membrane at 74°C for 2 minutes in 2 x SSC, SDS (0.1% w/v).

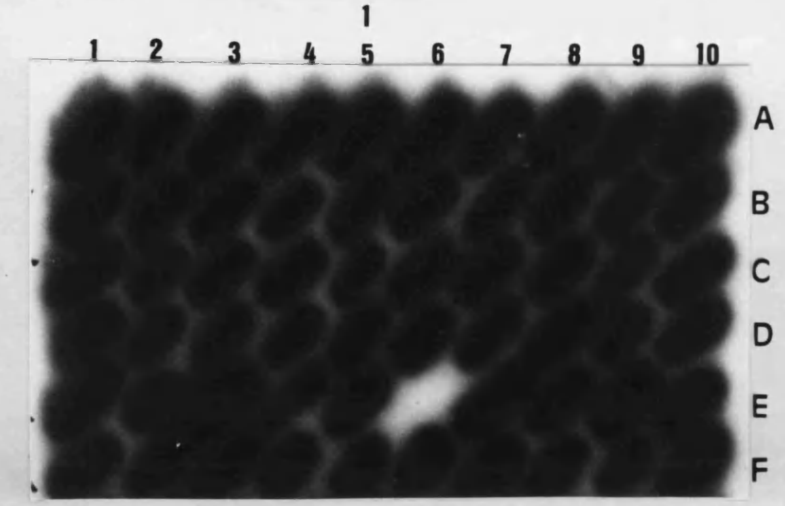
1
1 2 3 4 5 6 7 8 9 10
A
B
C
D
E
F

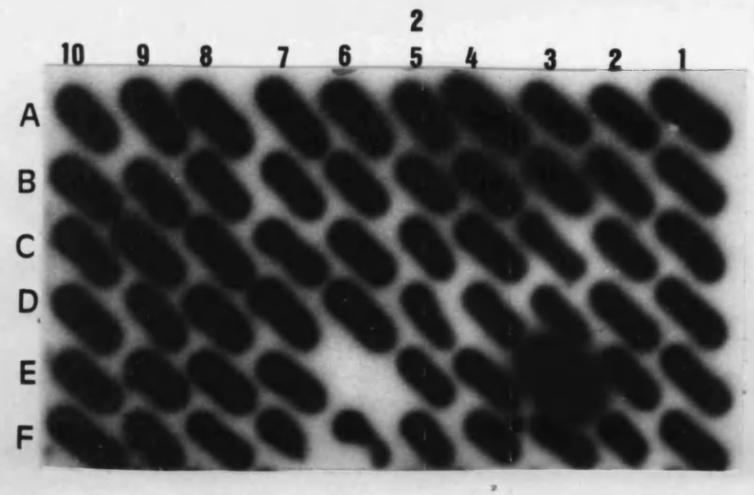
2
10 9 8 7 6 5 4 3 2 1
A
B
C
D
E
F

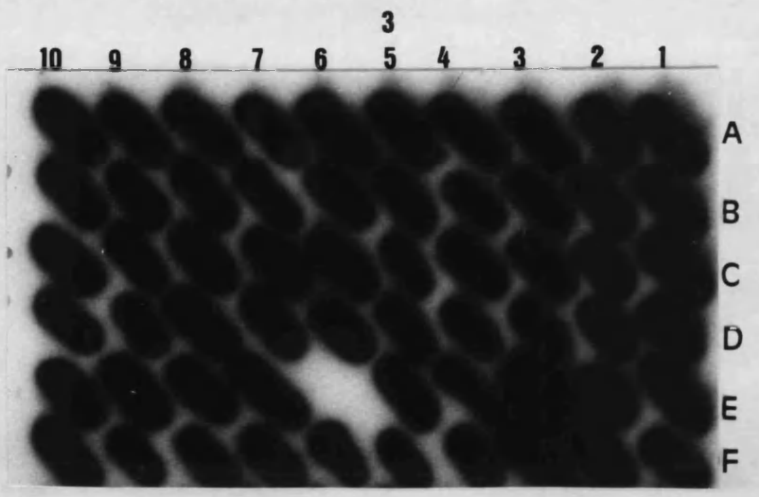
3
10 9 8 7 6 5 4 3 2 1
A
B
C
D
E
F

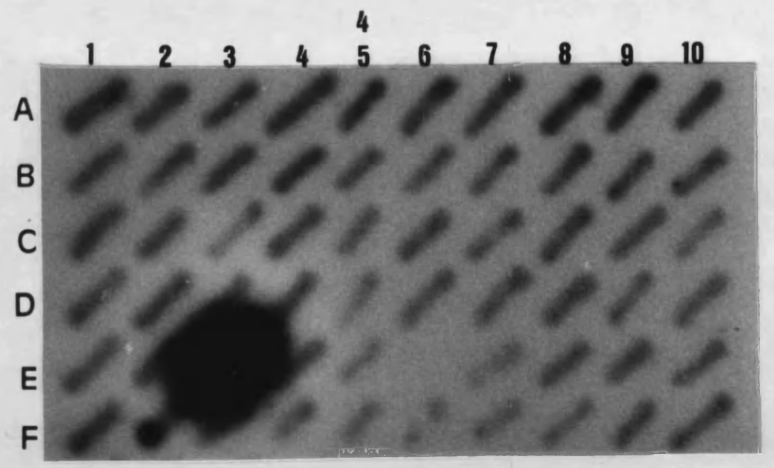
4
1 2 3 4 5 6 7 8 9 10
A
B
C
D
E
F

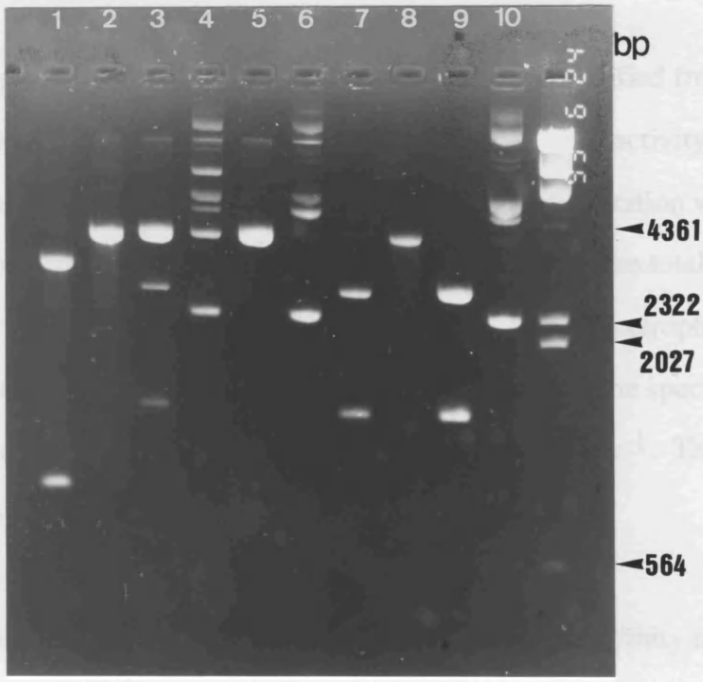

Fig 7.3: Restriction fragment analysis of 64C MDH gene in pUC19 on a 0.8% agarose gel.

Lanes: 1 to 5 are pUC64C MDH gene restricted with; (1) *Sph* I and *Hind* III; (2) *Sph* I; (3) *Hind* III and *Sal* I; (4) *Sal* I; (5) *Hind* III; (6) pUC64C MDH gene. Lanes 7 to 9 are pUCWT restricted with; (7) *Sph* I and *Hind* III; (8) *Sph* I; (9) *Hind* III; pUCWT MDH gene. The right hand lane is lambda DNA restricted with *Hind* III.

(7.2.2) Purification of pUC64C MDH.

The mutant MDH of pUC64C expressed in *E.coli* W945T1-2 was purified from the cell-free extract (Table 7.1). There is an apparent increase in the total activity during purification. The final specific activity of the 64C MDH protein preparation was 293 $\mu mol.min^{-1}.mg$ of $protein^{-1}$, corresponding to a yield of 70% of the total MDH activity. Densitometry scanning of the protein after SDS-PAGE gel electrophoresis indicated that the protein was 23% pure (Fig 7.5), which would raise the specific activity of homogeneous 64C MDH to 1274 $\mu mol.min^{-1}.mg$ of $protein^{-1}$. This value is approximately 88% of that of homogeneous wild type MDH.

Attempts to couple mutant 64C MDH to the Sepharose CL6-B thiol affinity matrix were unsuccessful. The mutant MDH would not bind, possibly indicating that cysteine 64 was not available to the coupling reagent.

(7.3.1) Screening for the substitutions of the codon for serine 222 (222C).

Plasmid from colonies were screened for the presence of the mutation by colony hybridisation (Fig 7.6). Colonies that showed strong hybridisation to the 5' [^{32}P] labelled oligonucleotide at 66°C were subjected to restriction fragment analysis with *Hind* III, *Sal* I and *Fsp* I (Fig 7.7). *Hind* III or *Sal* I restriction of pUC222C produced a linearised DNA fragment, but restriction with *Hind* III and *Sal* I excised a DNA fragment of similar size to *Hind* III restricted pUCWT. This indicated successful removal of the *Hind* III restriction site in the polylinker. *Fsp* I has two recognition sites in pUC19: one at the nucleotide position 251 and one at the nucleotide position 1919. Restriction of pUCWT with *Fsp* I will produce two DNA fragments of approximately 1000 bp and 3000 bp. Introduction of an *Fsp* I restriction site into the MDH gene at nucleotide position 666 will result in the excision of three DNA fragments of approximately 1000 bp, 1250 bp and 2100 bp. Restriction of

Fraction	Protein Concentration ($mg.ml^{-1}$)	MDH Activity (μ $mol.min^{-1}.ml^{-1}$)	Volume (ml)	Total Protein (mg)	Total Activity (μ $mol.min^{-1}$)	Specific Activity (μ $mol.min^{-1}.mg$ of $protein^{-1}$)
(1)	3	60	25	75	1500	20
(2)	23	110	1	23	110	5
(3)	3	110	25	75	2750	37
(4)		70	15		1050	
(5)	3	880				293
(6)						1274

Table 7.1: Purification of 64C MDH.

Lanes: (1) Cell-free extract; (2) Precipitate of 60% saturation ammonium sulphate dialysis; (3) 60% saturation ammonium sulphate dialysate; (4) Eluate of Procion red matrix; (5) Precipitate of 100% saturation ammonium sulphate dialysis; (6) Homogeneous MDH.

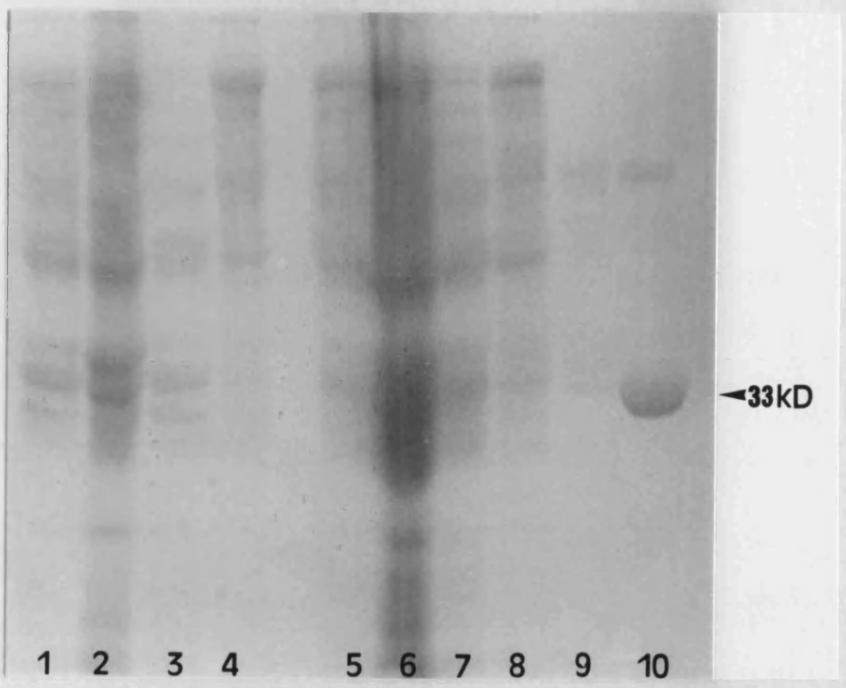

Fig 7.5: SDS-PAGE analysis of fractions from the purification of mutant 64C *E.coli* MDH by precipitation of protein with ammonium sulphate and Procion red H3-B affinity chromatography.

Lanes from left to right: (lanes 1 to 4 are of *Ecoli* W945T1-2): Cell-free extract; (2) Precipitate of cell-free extract; (3) Supernatant of 60% saturation ammonium sulphate dialysate; (4) Precipitate of 60% saturation ammonium sulphate dialysate. (lanes 5 to 9 are of *E.coli* W945T1-2 expressing plasmid 64C MDH); (5) Cell-free extract: (6) Precipitate of Cell-free extract; (7) Supernatant of 60% saturation ammonium sulphate dialysate; (8) Precipitate of 60% saturation ammonium sulphate dialysate; (9) Elution of Procion red matrix; (10) Preparation of wild type MDH. 33kD band of MDH subunit is indicated on the right hand side with ←.

Fig 7.6: Hybridisation of 222C MDH gene with 5' [^{32}P] labelled oligonucleotide-15 probe.

(1) Wash of Hybond-N membrane at 37°C for 10 minutes in 2 x SSC, SDS (0.1% w/v).

(2) Wash of Hybond-N membrane at 66°C for 2 minutes in 2 x SSC, SDS (0.1% w/v).

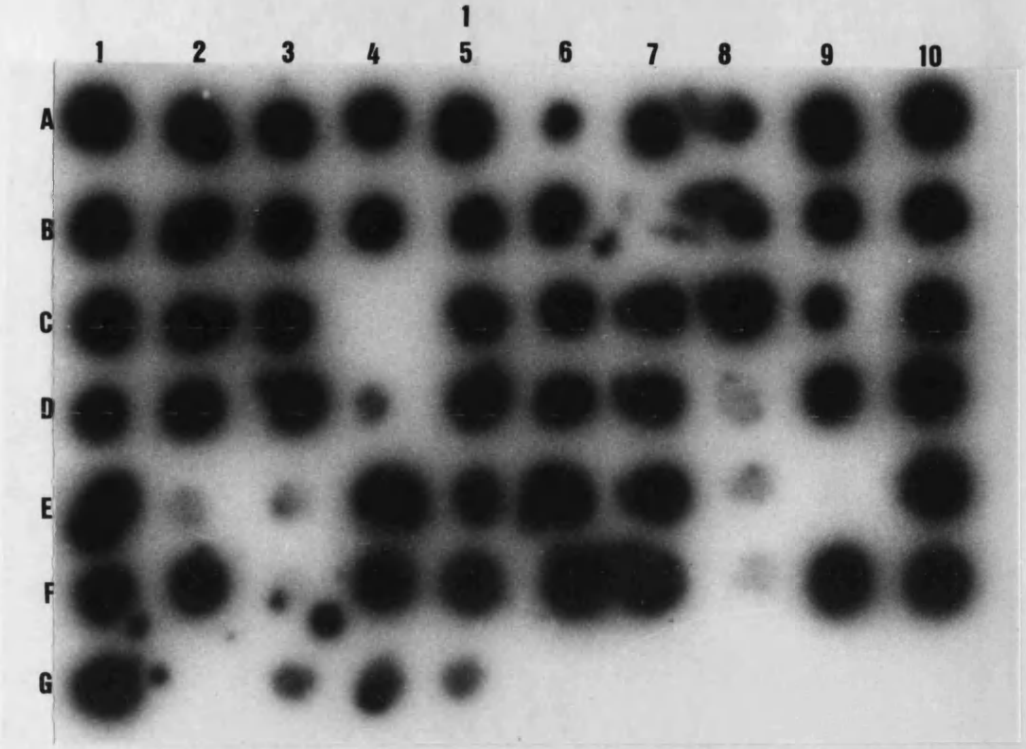
1
1 2 3 4 5 6 7 8 9 10
A
B
C
D
E
F
G

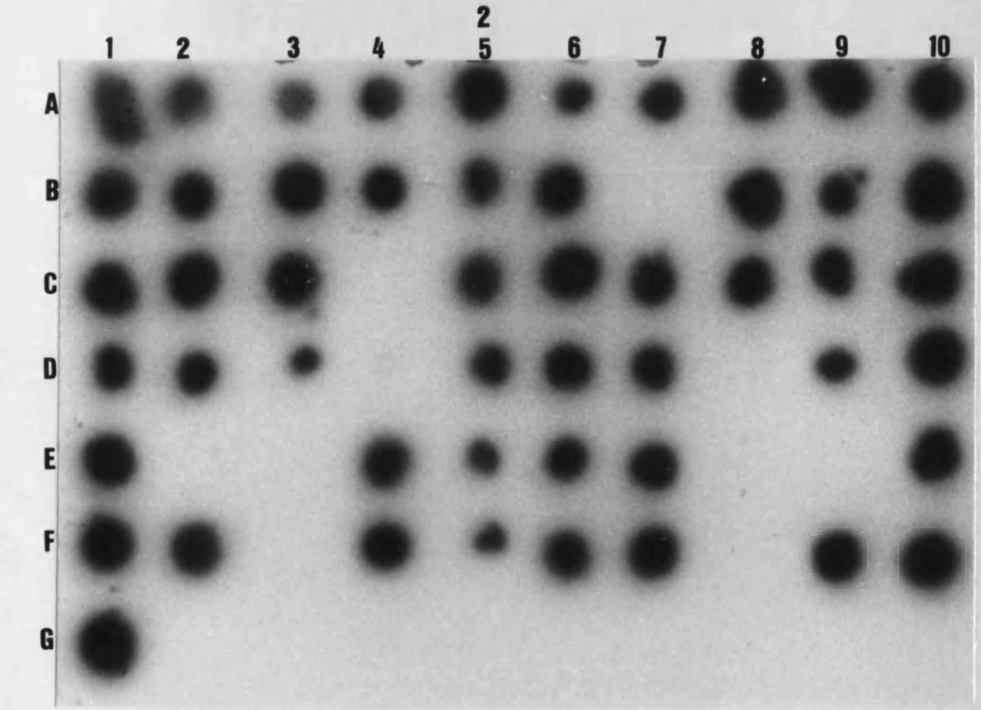
2
1 2 3 4 5 6 7 8 9 10
A
B
C
D
E
F
G

Fig 7.7: Restriction fragment analysis of wild type and 222C MDH gene in pUC19 on a 0.8% agarose gel.

Lanes: 1 to 6 are pUC222C restricted with; (1) *Fsp* I; (2) *Nhe* I; (3) *Nde* I; (4) *Hind* III and *Sal* I; (5) *Sal* I; (6) *Hind* III; (7) pUC222C; 8 to 13 are pUCWT restricted with (8) *Fsp* I; (9) *Nhe* I; (10) *Nde* I; (11) *Hind* III and *Sal* I; (12) *Sal* I; (13) *Hind* III; (14) pUCWT; (15) pUC19 restricted with *Hind* III; (16) pUC19. Right hand lane is *Pst* I restricted Lambda DNA.

pUC222C with *Fsp* I generated three DNA fragments of the predicted sizes. This confirmed the presence of a third *Fsp* I recognition site and therefore the presence of the 222C mutation. Oligonucleotide-6 which annealed between the nucleotides 747 and 767 of the MDH gene was used as a sequencing primer to confirm the nucleotide substitutions introduced into pUC222C (Fig 7.8).

(7.3.2) Purification of pUC222C MDH.

The mutant MDH of pUC222C expressed in *E.coli* W945T1-2, exhibited different characteristics to the wild type and mutant 64C MDH when purified from the cell-free extract (Table 7.2). The mutant showed a loss of 85% of activity from 1000 $\mu mol.min^{-1}$ (fraction 1) to 150 $\mu mol.min^{-1}$ (fraction 4) upon purification and a 25% loss in specific activity. This decrease in the specific activity indicated that the mutant was being inactivated during purification. The final specific activity of the MDH preparation was 30 $\mu mol.min^{-1}.mg\ of\ protein^{-1}$. Densitometric scanning of the protein after SDS-PAGE gel electrophoresis (Fig 7.9) indicated that the 222C mutant was 60% pure which would raise the specific activity of homogeneous 222C to 50 $\mu mol.min^{-1}.mg\ of\ protein^{-1}$. This value is only 3% of that observed for the wild type MDH and 9% of that observed for mutant 64C.

Attempts to couple mutant 222C MDH to the Sepharose CL6-B thiol affinity matrix were unsuccessful. The mutant MDH would not bind, possibly indicating that cysteine 222 was not available to the coupling reagent.

(7.4) **Derivatization of MDH.**

Murphey *et al*, (1967) has shown that wild type *E.coli* MDH thiols are not derivatizable with p-hydroxymercuribenzoate indicating that these residues were not accessible to this derivatizing agent. Derivatization of protein samples containing wild

Fig 7.8: Dideoxy sequence analysis of mutant 222C gene using oligonucleotide-6 as primer.

Lanes from left to right: Thymine (T); Guanine (G); Cytosine (C); Adenine (A) with corresponding codon usage. Bold uppercase indicates introduced *Fsp* I restriction site and mutations. Corresponding triple letter amino acid code is indicated above codon.

Fraction	Protein Concentration ($mg.ml^{-1}$)	MDH Activity (μ $mol.min^{-1}.ml^{-1}$)	Volume (ml)	Total Protein (mg)	Total Activity (μ $mol.min^{-1}$)	Specific Activity (μ $mol.min^{-1}.mg$ of $protein^{-1}$)
(1)	1	40	25	25	1000	40
(2)	5	2	1	5	2	
(3)	2	4	25	50	100	2
(4)		10	15		150	
(5)	1	30				30
(6)						50

Table 7.2: Purification of 222C MDH.

Lanes: (1) Cell-free extract; (2) Precipitate of 60% saturation ammonium sulphate dialysis; (3) 60% saturation ammonium sulphate dialysate; (4) Eluate of Procion red matrix; (5) Precipitate of 100% saturation ammonium sulphate dialysis; (6) Homogeneous MDH.

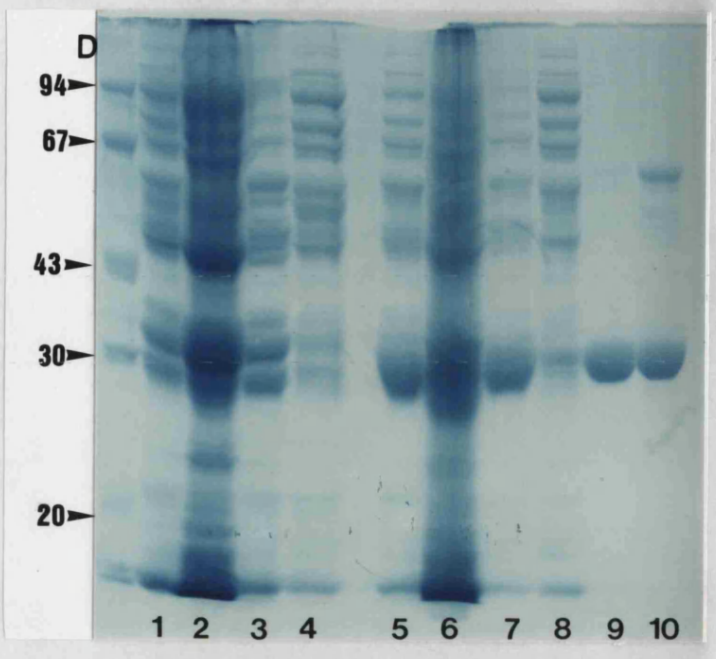

Fig 7.9: SDS-PAGE analysis of fractions from the purification of mutant 222C *E.coli* MDH by precipitation of protein with ammonium sulphate and Procion red H3-B affinity chromatography.

Lanes from left to right: (1 to 4 are *E.coli* W945T1-2); (1) Cell-free extract; (2) Precipitate of cell-free extract; (3) 60% saturation ammonium sulphate dialysate; (4) Precipitate of 60% saturation ammonium sulphate dialysate; (lanes 5 to 9 are *E.coli* W945T1-2 expressing plasmid 222C MDH); (5) Cell-free extract; (6) Precipitate of cell-free extract; (7) 60% saturation ammonium sulphate dialysate; (8) Precipitate of 60% saturation ammonium sulphate dialysate; (9) Elution of Procion red matrix; (10) Wild type preparation. Left hand lane are standard molecular weight markers.

type, mutants 113S and 109S/113S with excess DTNB or N-ethylmaleimide did not alter the activity of the enzyme. However, derivatization of a wild type MDH protein sample (~0.3 nmol MDH, 120 μg of total protein) with DTNB produced 3 nmol of NTB within 60 seconds of the addition of DTNB (Fig 7.10). This value was 40% above that calculated if all MDH thiols were derivatized, indicating that non-MDH thiols were available for derivatization. Derivatization of mutant 222C with DTNB or N-ethylmaleimide resulted in a 95% loss of activity. Derivatization of this mutant MDH (285 μg or 570 μg of total protein) with DTNB resulted in the formation of 12.5 nmol and 24 nmol of NTB respectively (Fig 7.10). If an assumption is made that the formation of NTB in the wild type MDH sample was due to the derivatization of non-MDH protein, then derivatization of mutant 222C produced an equivalent of 44% more NTB than the wild type MDH protein sample. The decrease in activity and increase in NTB upon derivatization of 222C, indicates that thiol(s) are being derivatized in the mutant MDH. Derivatization of mutant 222C (56μg) with 5 nmol of N-ethylmaleimide resulted in a 98% loss of MDH activity (Fig 7.11). Addition of 5000 nmol of N-ethylmaleimide resulted in a further 1% decrease in activity.

Initial results suggest that MDH mutant 64C protein samples did not show a decrease in activity when derivatized by DTNB or N-ethylmaleimide, or liberate NBT in a similar manner to that observed for mutant 222C protein samples. This indicated that the introduced cysteine at residue 64 was not available for derivatization with DTNB.

Protein samples of wild type, mutant 64C and 222C MDHs were electrophoresed in an iso-electric focusing gel paired with their derivatized (DTNB) counterparts. Activity staining of the gel indicated that the samples developed at approximately equal rates to produce a major and several minor bands in both derivatized and non-derivatized samples (Fig 7.12). However on several occasions (not shown) an extra band was apparent in the mutant 222C derivatized MDH sample. Coomasie blue staining of the gel did not reveal any further protein bands or alter the relative intensities in either the

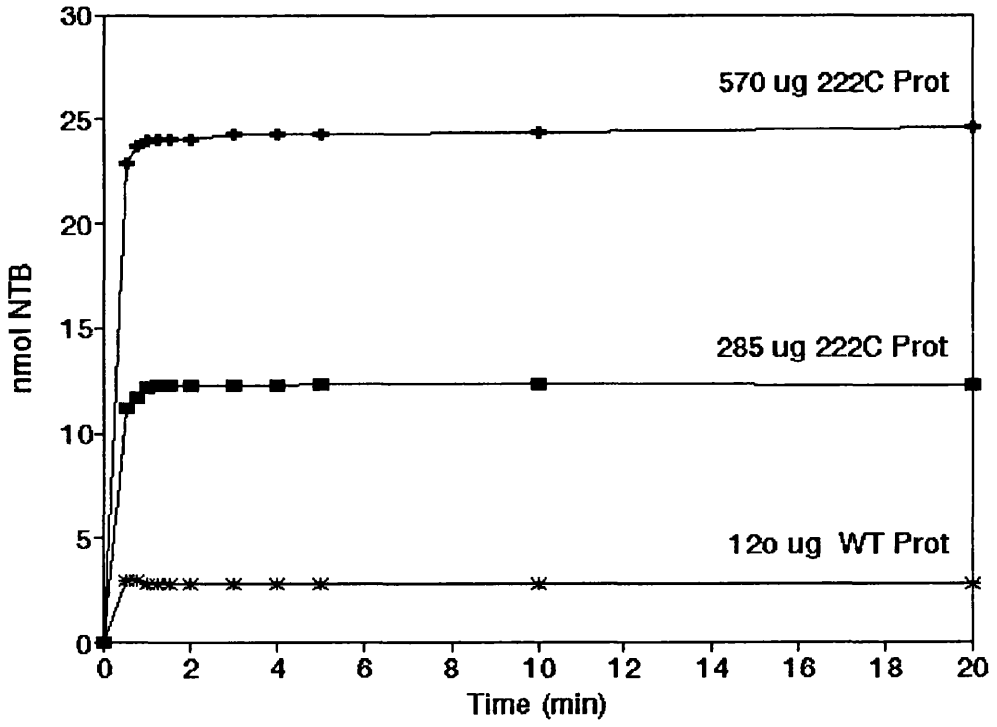

Fig 7.10: Liberation of NTB upon derivatization of wild type and mutant 222C MDHs with time.

WT Prot is protein sample containing wild type MDH; 222C Prot is protein sample containing mutant 222C MDH.

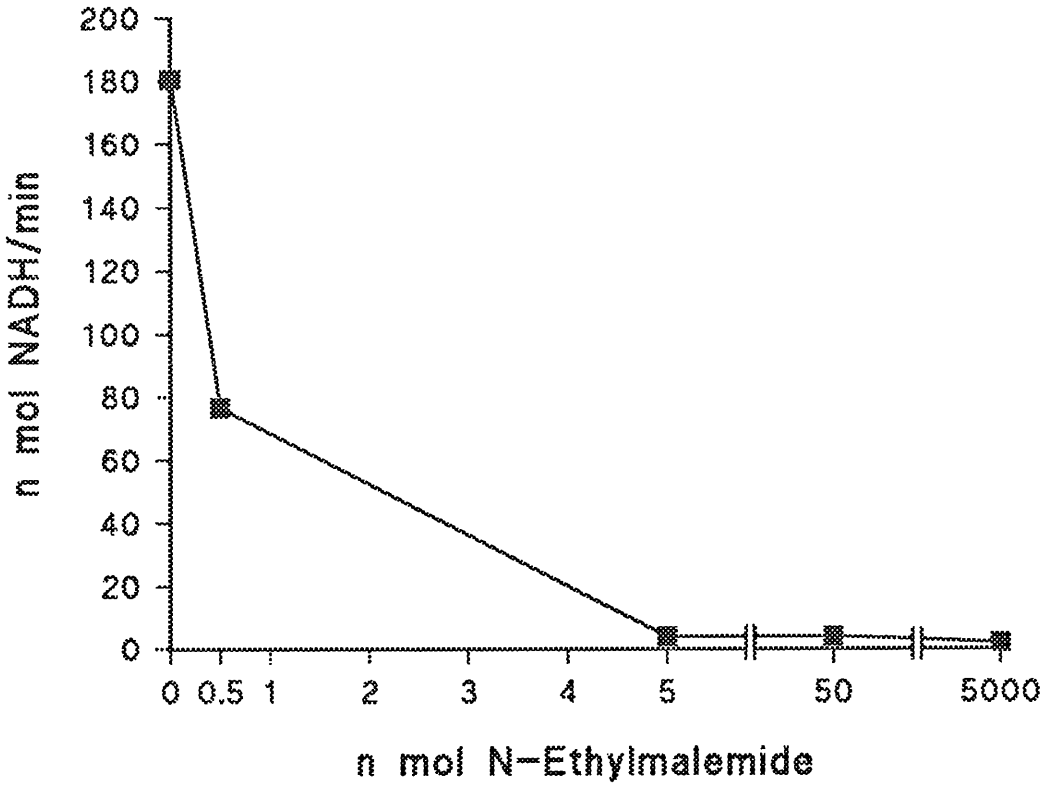

Fig 7.11: Decrease in MDH activity upon derivatization of protein sample (56 µg) containing Mutant 222C MDH with N-Ethylmaleimide.

Gel 1

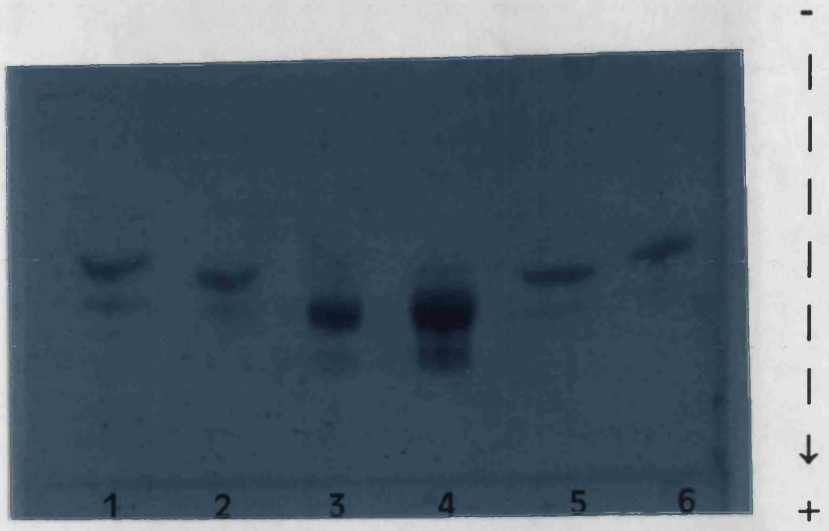

Gel 2

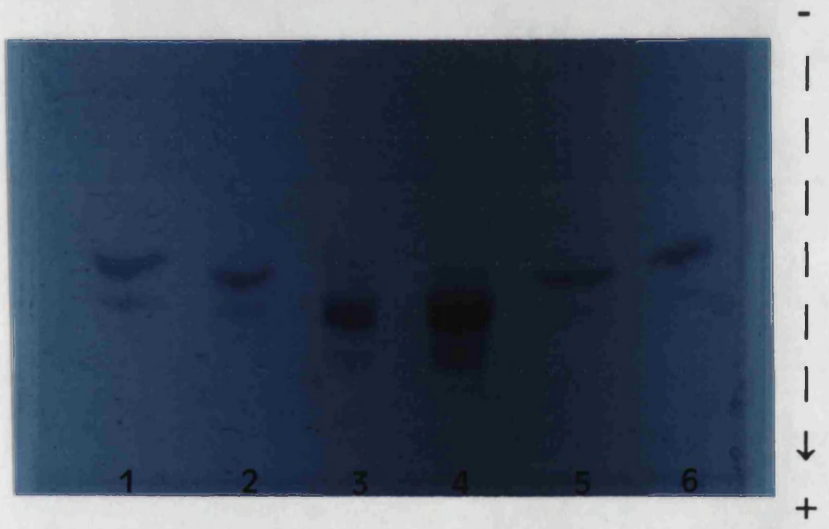

Fig 7.12: Iso-electric focussing of wild type mutants 64C and 222C MDHs.

Gel 1 is MDH activity stain, Lanes: (1) Mutant 222C derivatized with DTNB; (2) Mutant 222C; (3) Wild type MDH derivatized with DTNB; (4) Wild type MDH;(5) Mutant 64C derivatized with DTNB; (6) Mutant 64C.

Gel 2 is Coomasie blue stain, Lanes: (1) Mutant 222C derivatized with DTNB; (2) Mutant 222C; (3) Wild type MDH derivatized with DTNB; (4) Wild type MDH;(5) Mutant 64C derivatized with DTNB; (6) Mutant 64C.

wild type or mutant MDHs.

(7.5) **Kinetic studies on wild type, mutant 64C and 222C MDHs.**

Measurement of single data points of initial rates in the absence of product using NADH and oxaloacetate as coenzyme and substrate suggest that mutant 64C and 222C have different characteristics to wild type MDH. Varying the concentration of NADH at fixed concentrations of oxaloacetate, maximum wild type MDH activity was obtained at an oxaloacetate concentration of 0.1 mM (Fig 7.13). Increasing the oxaloacetate concentration to 0.26 mM did not increase the observed activity. At each fixed oxaloacetate concentration, increasing the NADH concentration did not inhibit the MDH activity. Qualitatively similar results were obtained using fixed NADH concentrations while varying the oxaloacetate concentration (Fig 7.14). Mutant 64C exhibited different characteristics to the wild type MDH. Varying the NADH concentration (0 to 0.3 mM) at fixed oxaloacetate concentrations indicated that maximum 64C MDH activity was obtained with 1 mM oxaloacetate as opposed to 0.1 mM oxaloacetate with wild type MDH (Fig 7.15). No plateau in activity was reached, possibly suggesting that the affinity of the MDH for oxaloacetate had decreased. The observed initial rates at a fixed oxaloacetate concentration of 0.1 mM, displays anomalous behaviour, having less activity than the MDH at fixed oxaloacetate concentrations of 0.07mM. At a fixed oxaloacetate concentration of 1 mM the MDH appeared to show a decrease in activity at NADH concentrations of 0.2 mM. Varying the oxaloacetate concentration at fixed NADH concentration , maximum rate was observed at approximately 0.125 mM to 0.2 mM NADH (Fig 7.16). Further increases in the concentration of NADH resulted in decreased MDH activity. Varying the concentration of NADH at several fixed concentrations of oxaloacetate, indicated that mutant 222C displayed maximum activity at an oxaloacetate concentration of 7.5 mM (Fig 7.17). At oxaloacetate concentrations above 7.5 mM no increase in activity was observed. However at NADH concentrations above 0.125 mM, the MDH displays a

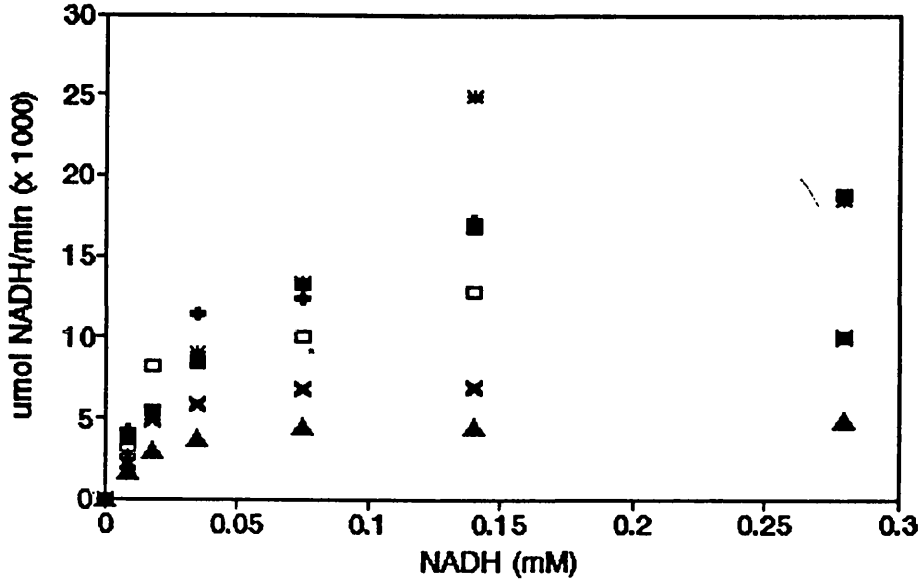

Fig 7.13: Rate concentration plot for wild type MDH of activity with varying NADH at fixed oxaloacetate concentration.

Where ■ = 0.26 mM oxaloacetate, + = 0.16 mM oxaloacetate, * = 0.10 mM oxaloacetate, □ = 0.06 mM oxaloacetate, x = 0.04 mM oxaloacetate and ▲ = 0.02 mM oxaloacetate.

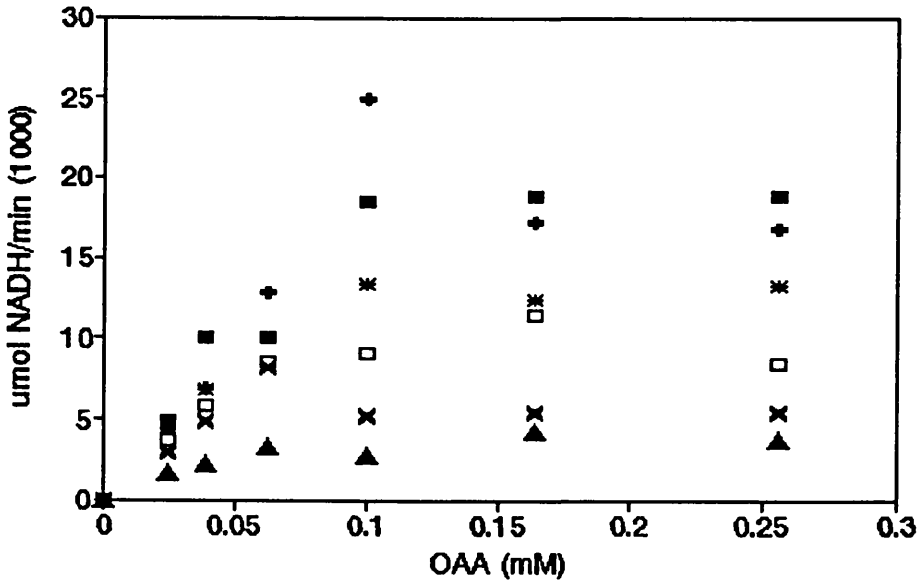

Fig 7.14: Rate concentration plot for wild type MDH of activity with varying oxaloacetate at fixed NADH concentration.

Where ■ = 0.28 mM NADH, + = 0.14 mM NADH, * = 0.08 mM NADH, □ = 0.04 mM NADH, x = 0.02 mM NADH and ▲ = 0.01 mM NADH.

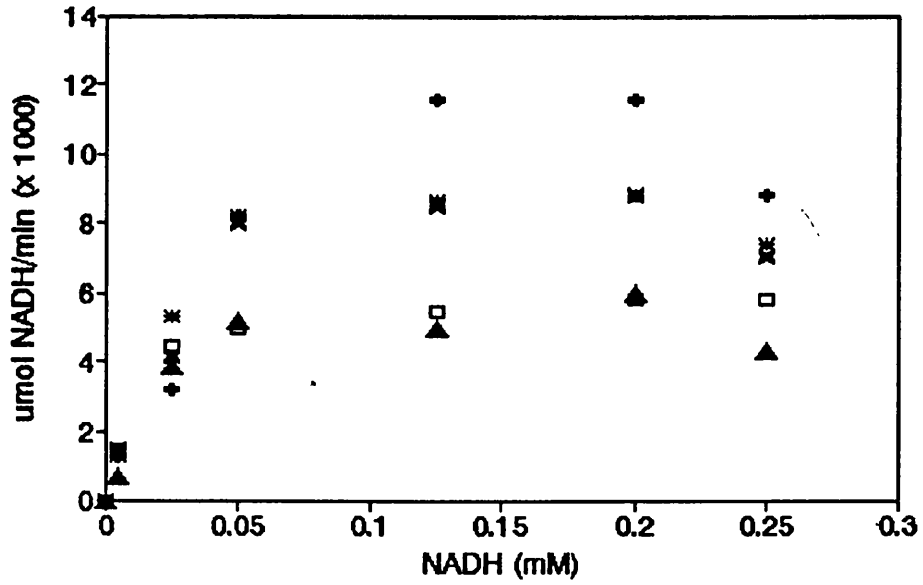

Fig 7.15: Rate concentration plot for mutant 64C MDH of activity with varying NADH at fixed oxaloacetate concentration.

Where + = 1.0 mM oxaloacetate, * = 0.30 mM oxaloacetate, □ = 0.10 mM oxaloacetate, x = 0.07 mM oxaloacetate and ▲ = 0.03 mM oxaloacetate.

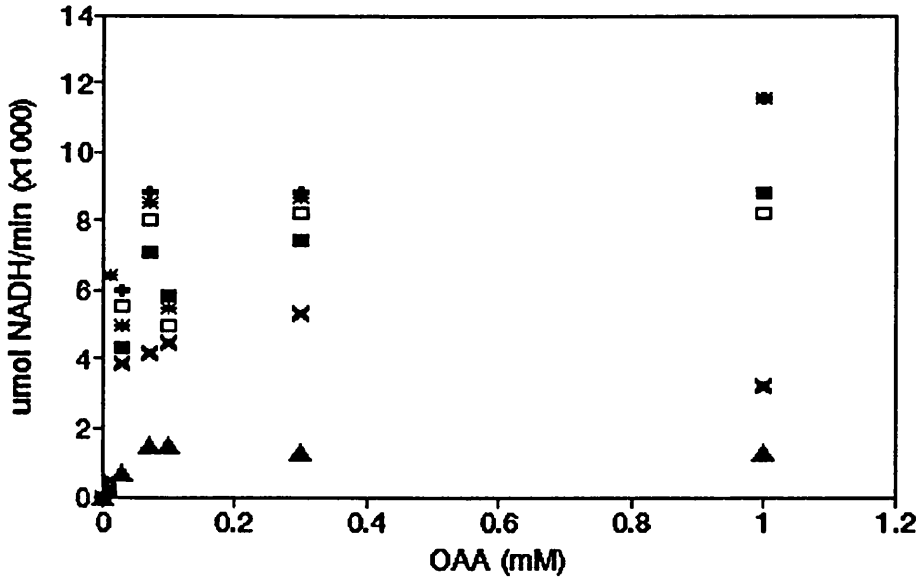

Fig 7.16: Rate concentration plot for mutant 64C MDH of activity with varying oxaloacetate at fixed NADH concentration.

Where ■ = 0.25 mM NADH, + = 0.20 mM NADH, * = 0.13 mM NADH, □ = 0.05 mM NADH, x = 0.03 mM NADH and ▲ = 0.01 mM NADH.

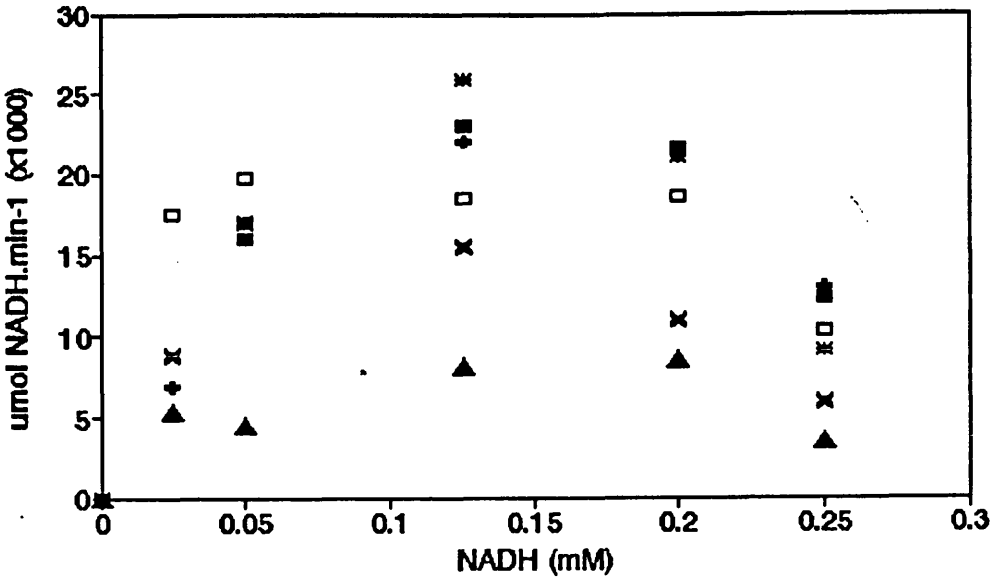

Fig 7.17: Rate concentration plot for mutant 222C MDH of activity with varying NADH at fixed oxaloacetate concentration.

Where ■ = 12.5 mM oxaloacetate, + = 10.0 mM oxaloacetate, * = 7.5 mM oxaloacetate, □ = 5.0 mM oxaloacetate, x = 1.0 mM oxaloacetate and ▲ = 0.50 mM oxaloacetate.

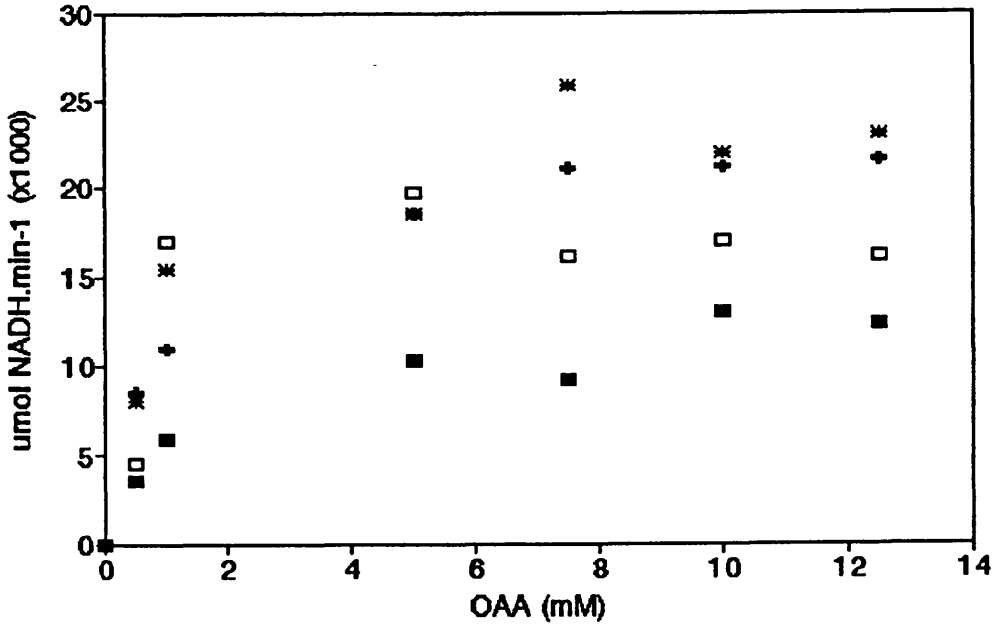

Fig 7.18: Rate concentration plot for mutant 222C MDH of activity with varying oxaloacetate at fixed NADH concentration.

Where ■ = 0.25 mM NADH, + = 0.20 mM NADH, * = 0.125 mM NADH and □ = 0.05 mM NADH.

decrease in activity. This decrease in activity appears to be more pronounced with increasing concentration of oxaloacetate. At varying concentrations of oxaloacetate and fixed concentrations of NADH maximum MDH activity was observed at 0.125 mM to 0.2 mM NADH (Fig 7.18). Increasing the NADH concentration to 0.25 mM appeared to cause inhibition of mutant 222C at the oxaloacetate concentration used. However at each fixed NADH concentration no inhibition was observed with increasing oxaloacetate. Attempts to obtain the Km and Vmax from linear and non-linear plots of the data were unsuccessful. However estimations of the Km from initial rates verses substrate concentration indicated that the Km for NADH on did not vary between the wild type and mutants, but the Km for oxaloacetate with mutant 222C had increased from 0.04 mM (wild type and mutant 64C) to 0.94 mM (Fig 7.19).

(7.6.1) Increasing the yield of mutant 222C MDH.

As mutant 222C appeared promising for use in the EMIT assay (i.e. the MDH was derivatizable) it was desirable to increase the concentration of the MDH in the cell-free extract for further characterisation. This was achieved by shuttling the 222C MDH gene into an expression vector as outlined (Fig 7.20).

(7.6.2) Screening for the substitution in 222C.

Plasmids from colonies were screened for the presence of the gene by colony hybridisation (Fig 7.21). Colonies that showed strong hybridisation to the 5' [^{32}P] labelled oligonucleotide at 47°C were subjected to restriction fragment analysis with *Eco*R I and *Hind* III. Restriction with *Eco*R I and *Hind* III excised a DNA fragment of approximately 1000bp, indicating the presence of the gene. An oligonucleotide-5 which hybridised at nucleotide positions -372 to -356 on the vector was used as a sequencing primer to confirm the truncation of the MDH gene (Fig 7.22).

MDH	Oxaloacetate Km (mM)	NADH Km (mM)	References
Wild type	0.04	0.02	
64C	0.04	0.02	
222C	0.94	0.03	
81Q	3	0.03	Nicholls *et al*, 1992
Wild type	0.04	0.05	Nicholls *et al*, 1992

Fig 7.19: Determination of the Km of wild type and mutant *E.coli* MDHs.

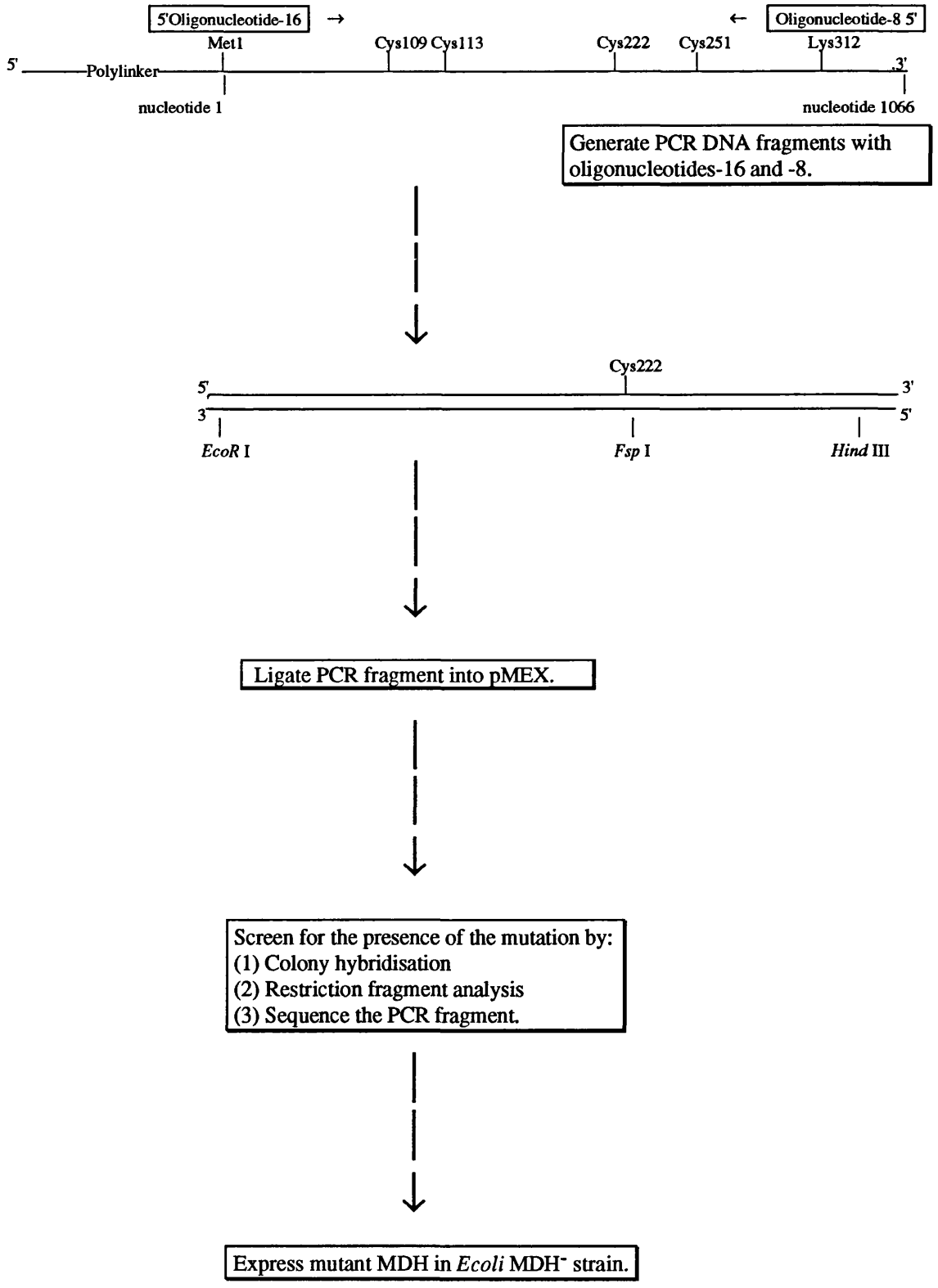

Fig 7.20: Flow diagram of steps used to generate mutant pMEX222C.

Fig 7.21: Hybridisation of 222C MDH gene in pMEX with 5' [^{32}P] labelled oligonucleotide-16.

(1) Wash of Hybond-N membrane at 37°C for 10 minutes in 2 x SSC, SDS (0.1% w/v).

(2) Wash of hybond-N membrane at 47°C for 10 minutes in 2 x SSC, SDS (0.1% w/v).

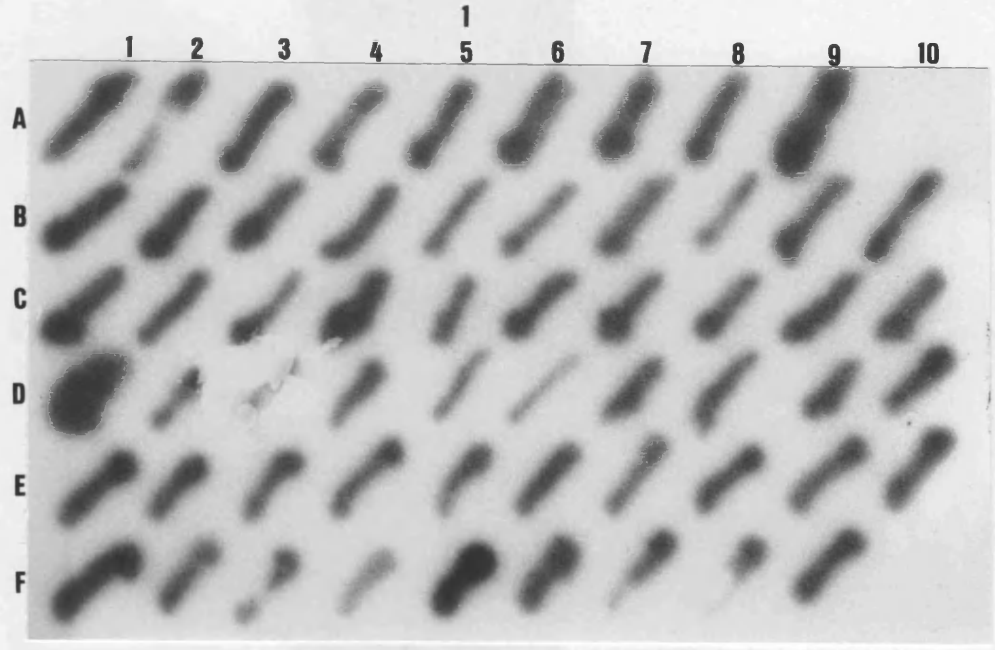
1
1 2 3 4 5 6 7 8 9 10
A
B
C
D
E
F

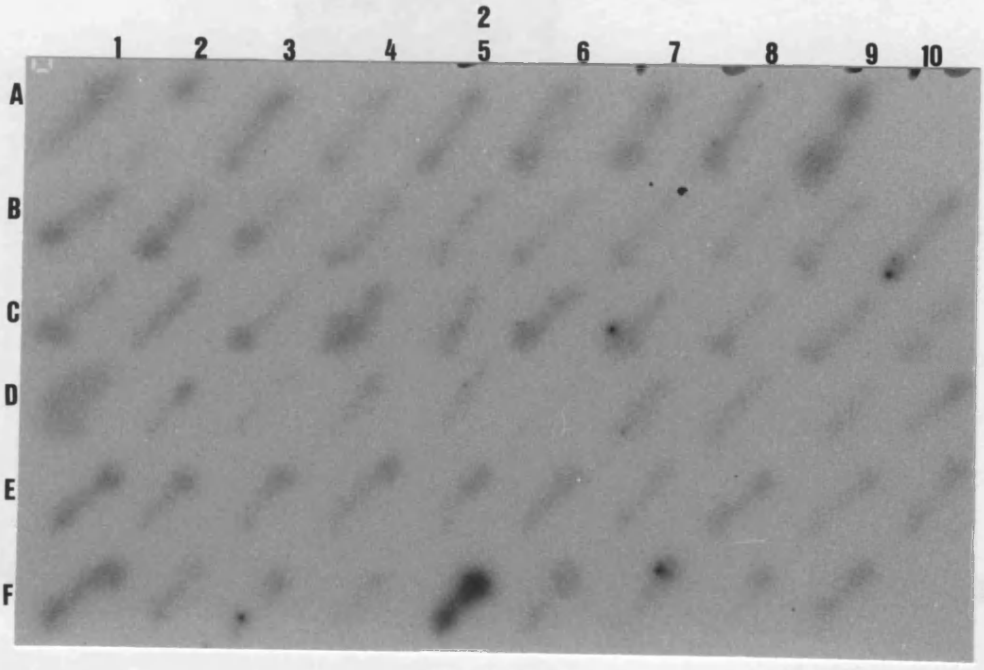
2
1 2 3 4 5 6 7 8 9 10
A
B
C
D
E
F

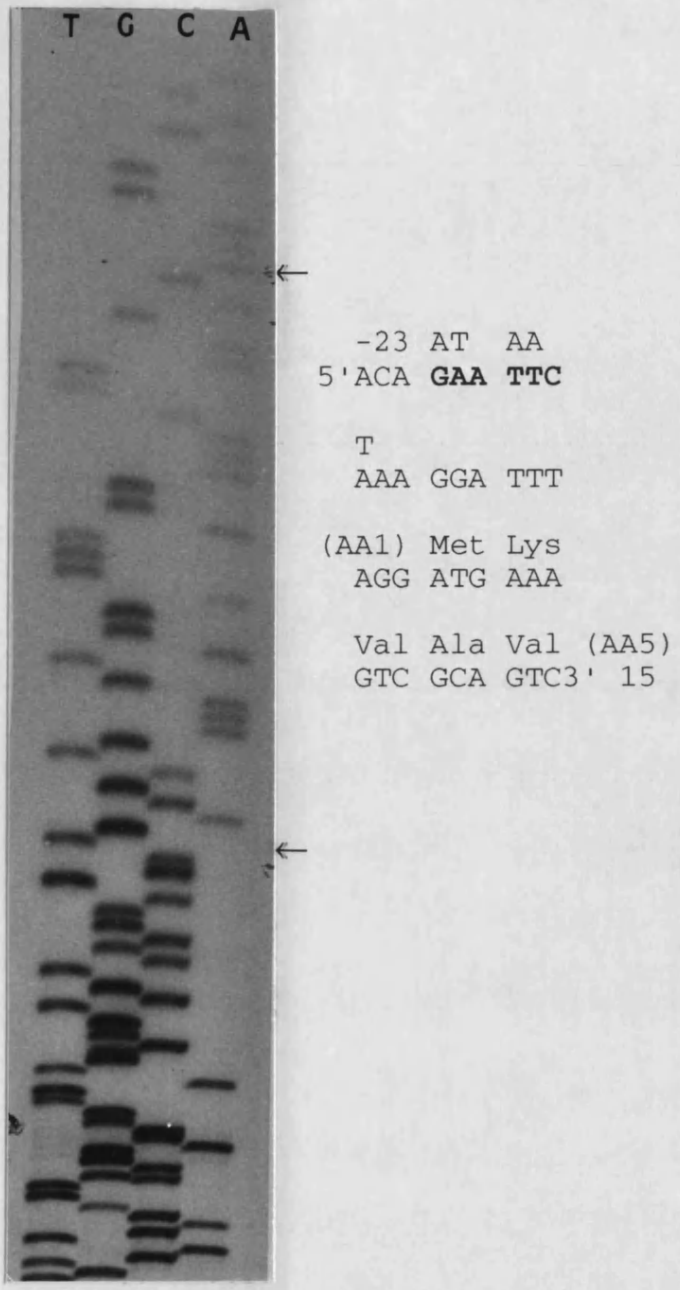

Fig 7.22: Dideoxy sequence analysis of pMEX222C using oligonucleotide-5 as primer.

Lanes from left to right: Thymine (T); Guanine (G); Cytosine (C); Adenine (A) with corresponding codon usage. Bold uppercase indicates introduced *EcoR* I restriction site and mutations. Corresponding triple letter amino acid code is indicated above codon.

(7.6.3) Purification of pMEX222C MDH.

No increase in the MDH activity was observed in the cell-free extract upon induction with IPTG (1 mM) above that of the control. Restriction digestion with *Eco*R I and *Hind* III of plasmid preparation from the culture indicated that the pMEX222C was present in the *E.coli*.

(7.7) **Discussion.**

(7.7.1) Substitution of threonine 64 to cysteine.

Expression of the gene encoding mutant 64C in *E.coli* MDH$^-$ strain W945T1-2 resulted in MDH activity in the cell-free extract of 1500 $\mu mol.min^{-1}$. This was equivalent to 9% and 2% of that of wild type and mutant 113S MDHs. The 33kD subunit of MDH was determined to be only a minor component of the cell-free extract when analysed by SDS-PAGE. Specific activity of this mutant was 1274 $\mu mol.min^{-1}.mg$ of $protein^{-1}$, which is similar to that obtained for mutant 113S and only slightly less than that of the wild type MDH. These results suggest that the substitution of threonine 64 for cysteine increased the susceptibility of MDH to degradation but did not greatly affect catalysis. Attempts to couple this mutant to a thiol affinity matrix or derivatize with a thiol specific reagent were unsuccessful. This indicated that cysteine 64 was not accessible to the thiol of the matrix or derivatizing agent.

Substitution of cysteine for threonine 64 resulted in a decrease of solvent accessible side chain surface area from 42Å^2 to 37Å^2. The surface area of a methyl group is 30Å^2 (Bordo and Argos, 1991) (Fig 7.23). It is possible that the small surface area of cysteine presented to the thiol matrix and derivatizing agent was too small to allow derivatization under similar conditions to those used for mutant 222C. However this

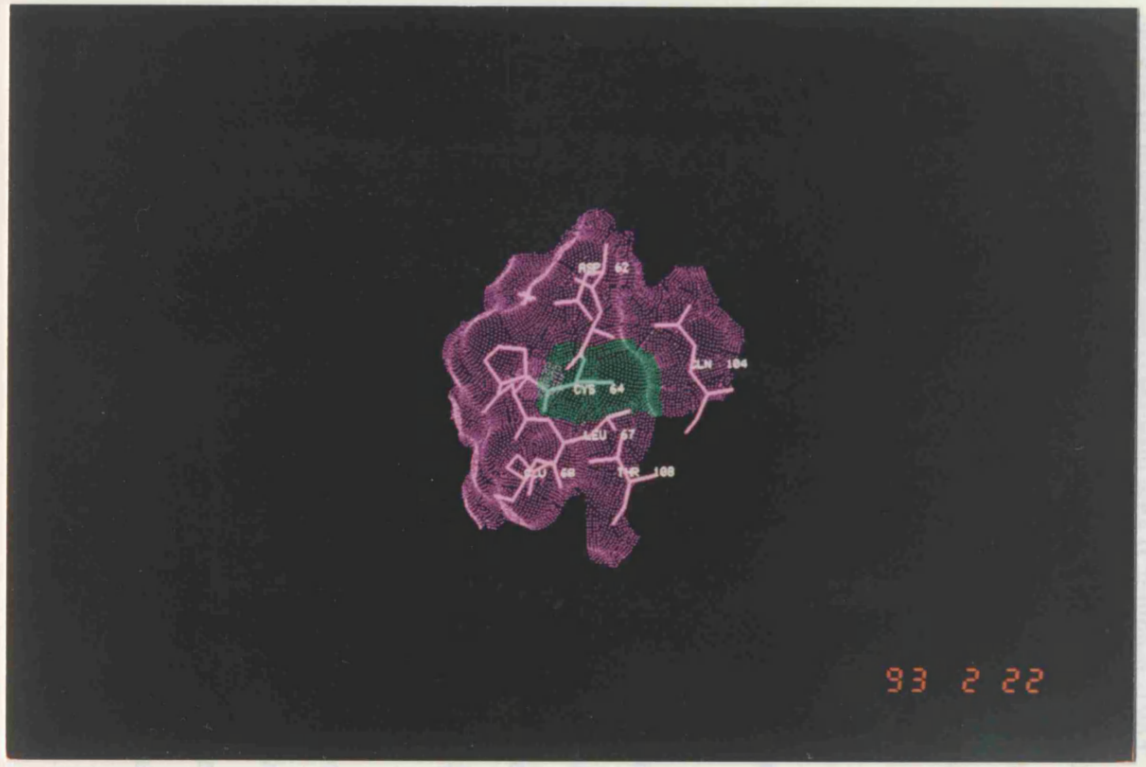

Fig 7.23: Connolly surface prediction of cysteine 64 in the *E.coli* MDH crystal structure.

Figure 7.23 is a surface view of a Connolly surface. It indicates that the side chain of cysteine 64 is solvent accessible as depicted by stippled surface (green).

does not account for the decrease in the amount of MDH observed in the cell-free extract.

Possible reasons why substitution of a residue could increase susceptibility to degradation is discussed in chapter five. Cysteine and threonine show only a small change in hydropathy and side chain area (Creighton, 1983; Kyte and Doolitle, 1982; Roseman, 1988). It is unlikely that these small changes would cause large perturbation in the secondary structure surrounding the substituted residue. However these changes in some instances have been associated with an increased susceptibility of a protein to degradation (Pakula *et al*, 1986).

The increased susceptibility to degradation could be due to a change in the folding pathway as a result of this mutation (Browning *et al*, 1986). However, this is unlikely, as cysteine 64 is greater than 20Å from cysteines 109, 113 and 251, if substituted into the *E.coli* MDH crystal structure. Any disulphide bond (~3Å) or intermediate which could form between cysteine 64 and an endogenous cysteine would be expected to cause a major perturbation of the protein structure which would disrupt the active site. This could be tested by substituting threonine 64 for valine. Valine has a similar surface area (155Å^2) to threonine (140Å^2) and has been observed in some instances to be substituted for threonine (Bordo and Argos, 1991). Provided that valine substitution does not perturb the protein secondary structure, a protein with a similar level of expression to the wild type MDH would indicate that cysteine 64 is in-fact influencing the folding pathway of the MDH.

Threonine 64 is the second residue (from the N-terminus) of the small α-helix αC' (Hall *et al*, 1992). This region of the protein has a high degree of flexibility, possibly indicating that these residues are not tightly packed (Hall *et al*, 1992). Threonine and cysteine have similar preferences to this position on α-helices (Chapter five) (Richardson and Richardson, 1988).

The *E.coli* crystal structure indicates that threonine 64 is in a region of high negative charge with its nearest neighbours being aspartate 62, glutamate 68 and glutamine 104. The crystal structure indicates that cysteine could take part in similar hydrogen bonding as threonine 64. However, substitution of cysteine might alter the charge in that region. Roseman (1988) has indicated that the charge on an individual residue in a protein is determined by the environment that the residue is found. This is amply illustrated with the observed differences in the pK of histidine in different proteins. Therefore introduction of cysteine 64 could result in two forms of residue; -SH and $-S^-$ (The pK of cysteine in water is ~8.3). If the predominant form of this residue is -SH, then substitution of this residue should not perturb the local secondary structure surrounding the substitution. If the cysteine is in the $-S^-$ form then it would increase the negative charge in the region of the substitution. To minimise this charge effect αC' could possibly re-orientate in the protein, minimising the effect of the negative charge, but increasing the susceptibility of the MDH to degradation. However, as αC' is a small helix at the extremities of the coenzyme binding domain, the disruption associated with αC' might not affect catalysis. This could be tested by substituting threonine 64 for a positive and a negative charged residue. Substitution of the lysine which is positively charged at physiological pH and has a surface area of 170$Å^2$ should enhance stability of the protein. Whereas substitution of aspartic acid which is negatively charged at physiological pH and surface area of 150$Å^2$ should destabilise the MDH increasing susceptibility to degradation.

(7.7.2) Conclusion.

Mutant 64C appeared to be more susceptible to degradation than the wild type MDH. The inability to derivatize this mutant under similar conditions to mutant 222C suggests that substituted residue 64 was not accessible to the derivatizing agent. This is likely to be due to a local change in conformation surrounding residue 64. This change in local conformation making this residue more susceptible to degradation.

(7.7.3) Substitution of serine 222 to cysteine.

The MDH gene containing cysteine 222 when expressed in *E.coli* W945T1-2 produced a similar level of the 33kD subunit in the cell-free extract as wild type and mutant 113S MDH when analysed by SDS-PAGE. Mutant 222C could be derivatized by thiol specific derivatizing agents but could not be bound to a thiol affinity matrix, when the matrix free thiol group was bound to a "short" linker arm. This suggests that although cysteine 222 was solvent exposed it was not predominant on the protein surface. The specific activity of this MDH was only 3.5% and 4.0% of that observed for the wild type and 113S MDH. Kinetic data suggests that the reduced specific activity is due to a reduced affinity for substrate (oxaloacetate).

The *E.coli* crystal structure indicated that serine 222 is located at the entrance of the active site cleft. Substitution of serine 222 for cysteine in the crystal structure indicated that the cysteine side chain could be accomodated without perturbation of the active site (Fig 7.24 and 7.25). The -SH group displayed a small movement of 0.2Å and 0.1Å away from the C^3 carbon of malate and the NAD ribose unit. This residue is shielded from the catalytically important histidine and aspartate (Hall *et al*, 1992) by malate (Fig 7.26). Residue 222 is 9Å and 12Å from this histidine and aspartate making direct perturbation of these residues by the substitution unlikely (Fig 7.26). Nicholls *et al*, (1992) has substituted arginine 81 of *E.coli* MDH for glutamine. This arginine participates in a salt bridge with the C^4 carboxy moiety of malate upon βD/αD loop closure, while the glutamine participates in a weaker hydrogen bond (Hall *et al*, 1992; Nicholls *et al*, 1992). Kinetic data suggests that this mutant MDH has a reduced affinity for oxaloacetate, but the affinity for coenzyme remains undiminished (Nicholls *et al*, 1992). This decrease in affinity for substrate is similar in magnitude to that observed for mutant 222C and has been attributed to the loss of the salt bridge between arginine 81 and malate and the large hydration potential of arginine which excludes water from the active site upon interaction with the

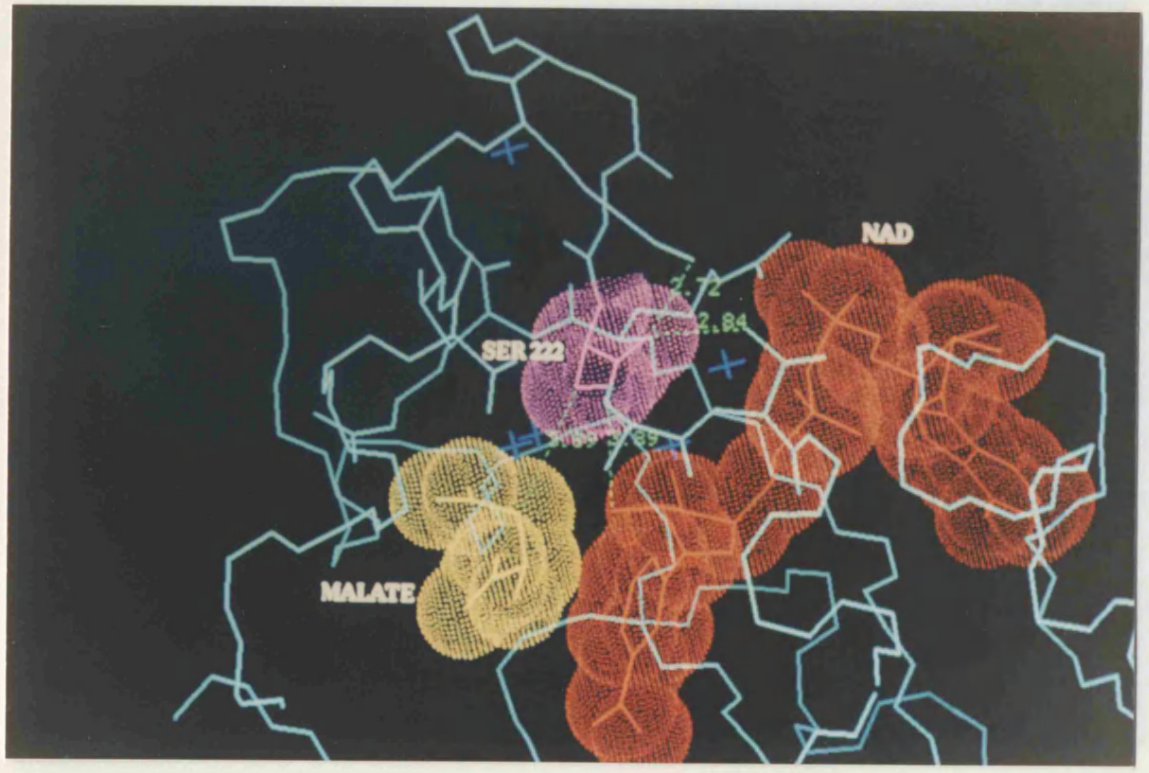

Fig 7.24: Space filled model of *E.coli* MDH crystal structure active site.

Figure 7.24 indicates that L-malate (yellow), coenzyme (orange) and serine 222 (magenta) are in close proximity to each other. The distance of serine 222 from the closest point of coenzyme, substrate and adjacent residues is indicated in green and distance given in Å.

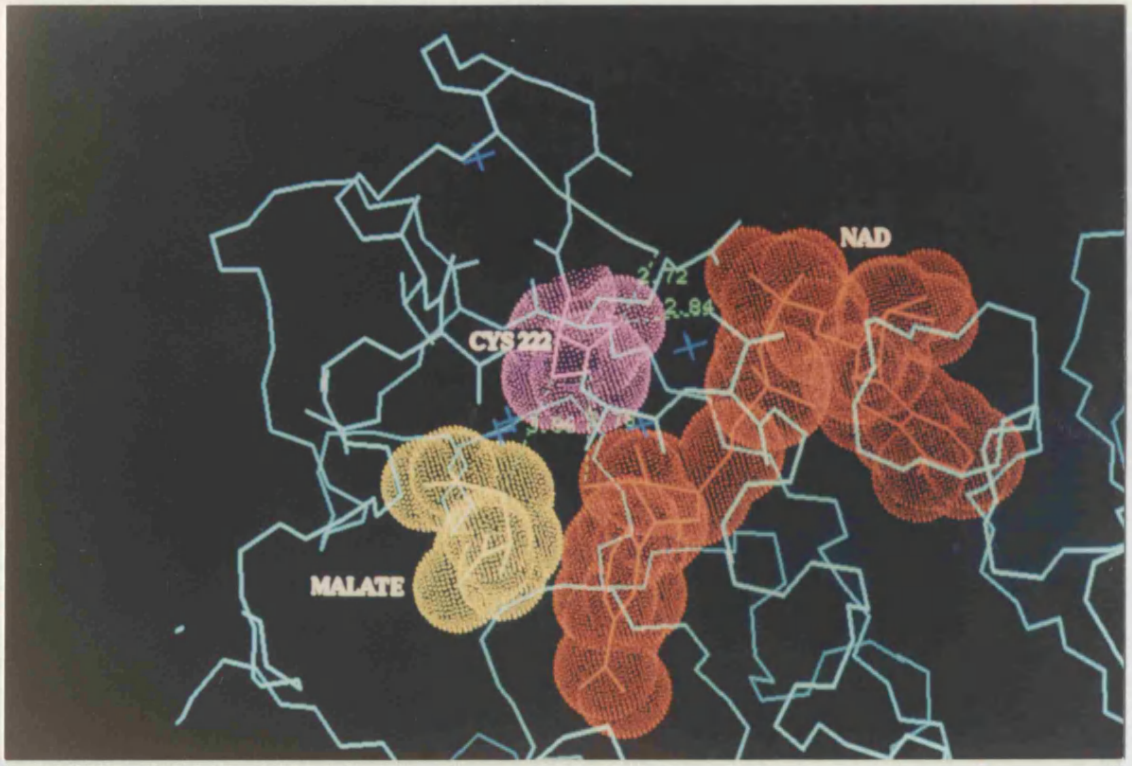

Fig 7.25: Space filled model of *E.coli* MDH crystal structure active site with serine 222 substituted for cysteine.

Figure 7.25 indicates that L-malate (yellow), coenzyme (orange) and cysteine 222 (magenta) are in close proximity to each other. The distance of cysteine 222 from the closest point of coenzyme, substrate and adjacent residues is indicated in green and distance given in Å.

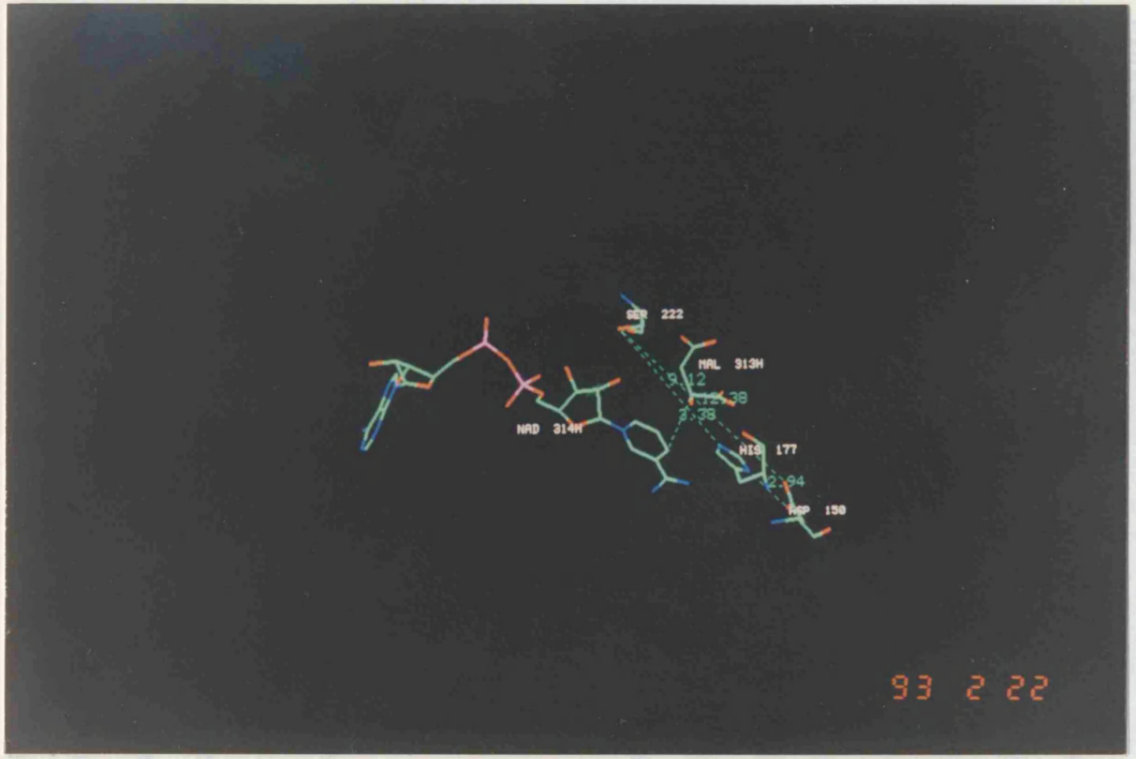

Fig 7.26: Spatial orientation of serine 222 in *E.coli* MDH active site in relation to coenzyme, substrate, histidine 177 and aspartate 150.

Figure 7.26 indicates that L-malate and coenzyme interject between serine 222 and the catalytically important histidine 177 and aspartate 150. The distances of serine 222 from the closest point of the histidine and aspartate are indicated in green and distances given in Å.

substrate. Exclusion of water from the active site is thought to increase the electrostatic interactions between substrate and substrate binding residues.

If the cysteine is in the $-S^-$ form in the active site, the extra negative charge could result in a hydration shell surrounding exposed cysteines. If upon loop closure this extra water due to the hydration of cysteine is not removed from the active site, it may result in weaker interactions between the substrate and the substrate binding residues. This will manifest in a lower substrate affinity. It is possible that substitution of serine 222 reduces the affinity for substrate by preventing removal of water from the active site upon loop closure. If the pertubation of the affinity for oxaloacetate is due to the $-S^-$ form in the active site it would be expected that substitution of glutamate which is negatively charged for serine 222 would decrease the enzymes affinity for substrate. However, substitution of serine 222 for threonine which represents a similar side chain area increase as the cysteine substitution would not affect substrate binding in the active site.

(7.7.4) Conclusion.

Substitution of serine 222 for cysteine did not increase the susceptibility of this mutant to degradation when compared to the wild type MDH. This mutation did however alter the affinity of the enzyme for oxaloacetate. This decrease in affinity could be due to the enzymes inability to exclude water from the active site upon βD/αD loop closure. The introduced negative charge in the active site hinders expulsion of water which in turn decreases the interaction of the substrate with the substrate binding residues.

CHAPTER EIGHT:
IMPLICATIONS OF RESULTS ON EMIT

(8.1) Implications of results on EMIT.

The ability to express plasmid encoded wild type *E.coli* MDH in *E.coli* and purify this enzyme made this MDH ideal candidate to ascertain the potential of modified MDHs in EMIT. The lack of non solvent accessible cysteines per MDH made cysteine a suitable residue to investigate the coupling of ligands to the surface of the MDH. Initially it was planned to remove the endogenous cysteines from the wild type MDH (to ensure that endogenous cysteines could not interact with introduced cysteines, altering the folding pathway), then substitute cysteines into the βD/αD surface loop. However, results indicate that MDHs with endogenous cysteines removed were less prevalent in the cell-extracts. This inability to generate a mutant devoid of cysteines restricted the potential of this MDH for use in EMIT. Introduction of cysteine into the βD/αD surface loop of a mutant with cysteines 109 and 113 substituted for serine resulted in no MDH being present in the cell-extracts. However, substitution of residues 64 and 222 for cysteines in the wild type MDH resulted in active MDHs. Only the mutant bearing the 222C substitution was capable of derivatization. This enzyme had a diminished specific activity when compared to the wild type enzyme, which was attributed to a reduced affinity for oxaloacetate. Attempts to covalently bind this enzyme to a thiol on a short linker arm of a thiol affinity matrix were unsuccessful indicating that this cysteine was not predominant on the protein surface. The *E.coli* crystal structure confirms that cysteine 222 is not directly solvent accessible and is situated in the active site cleft. For an antibody to form an antibody-ligand enzyme complex, the ligand bound to cysteine 222 would have to be on a linker arm which would allow the ligand to protrude out of the active site cleft. This linker could block the active site cleft preventing the movement of substrate into and out of the active site, or prevent collapse of the βD/αD surface loop over the active site. Therefore

MDH mutant 222C is not suitable for use in EMIT. The *E.coli* crystal structure (Hall *et al*, 1992) indicates that glycine 220 is on the surface of the MDH at the apex of α2G/α3G turn. Provided that the change in hydrophobicity and surface area upon substitution of cysteine does not perturb the structure, or influence the folding pathway, it might be possible to produce a modified MDH suitable for use in EMIT. Native thermophilic enzymes are less susceptible to degradation than their mesophilic counterparts (Menendez.-Arias and Argos, 1989) and as such are more able to tolerate mutations. An alternative approach would be to substitute cysteine residues into a wild type thermophilic MDH. The gene encoding the dimeric MDH of *Thermus aquaticus* B has been cloned (Nicholls *et al*, 1990). This protein contains a unique cysteine and has a high sequence identity to porcine cytoplasmic MDH. Substitution of this cysteine will produce a mutant devoid of cysteine. Further introduction of cysteine into this mutant will not be influenced by disulphide bond intermediates. This mutant when expressed in *E.coli* can be rapidly purified by the method of Nicholls *et al*, (1990). The high sequence identity with the cytoplasmic MDH enables accurate modelling of the *T. aquaticus* B MDH.

REFERENCES.

C. Abad-Zapatero, J. P. Griffith, J. L. Sussman and M. G. Rossmann, (1987), J. Mol. Biol., **198**, 445-467.

A. Atkinson, J. E. McArdell, M. D. Scawen, R. F. Sherewood and D. A. P. Small, (1982), in "Affinity chromatography and related techniques", pp 399-410, Eds T. C. T Gribnau, J. Visser, R. J. F. Nivard, Elsevier, New York.

R. Axen, H. Drevin and J. Carlsson, (1975), Acta. Chemica. Scandinavia, **29**, 471-474.

S. J. Barnes and P. D. B. Weitzman, (1986), FEBS., **201**, 267-270.

S. Beeckmans and L. Kanarek, (1981), Eur. J. Biochem., **117**, 527-535.

L. H. Bernstein, M. B. Grisham, K. D. Cole and J. Everse, (1978), J. Biol. Chem., **253**, 8697-8701.

L. H. Bernstein and J. Everse, (1978), J. Biol. Chem., **253**, 8702-8707.

J. J. Birktoft, R. T. Fernley, R. A. Bradshaw and L. J. Banaszak, (1982), PNAS., **79**, 6166-6170.

J. J. Birktoft and L. J. Banaszak, (1983), J. Biol. Chem., **258**, 472-482.

J. J. Birktoft, Z. Fu, G. E. Carnaharn, G. Rhodes, S. L. Roderick and L. J. Banaszak, (1989), Biochem. Soc. Trans., **17**, 301-304.

J. J. Birktoft, G. Rhodes and L. J. Banaszak, (1989b), Biochemistry, **28**, 6065-6081.

D. M. Bleile, R. A. Schulz, E. M. Gregory and J. H. Harrison, (1977), J. Biol. Chem., **252**, 755-758.

D. Bordo and P. Argos, (1991), J. Mol. Biol., **217**, 721-729.

M. M. Bradford, (1976), Anal. Biochem., **72**, 248-254.

J. F. Browning, R. J. Mattaliano, E. P. Chow, S.-M. Liang, B. Allet, J. Rosa and J. E. Smart, (1986), Analyt. Biochem., **155**, 123-128.

L. Bülow and K. Mosbach, (1991), TIBTECH, **9**, 226-231.

J. Chang, S. Gotcher and J. B. Gushaw, (1982), Clin. Chem., **28**, 361-367.

A. R. Clarke, C. J. Smith, K. W. Hart, H. M. Wilks, W. N. Chia, T. V. Lee, J. J. Birktoft, L. J. Banaszak, D. A. Barstow, T. Atkinson and J. J. Holbrook, (1987), Biochem. and Biophys. Res. Comm., **148**, 15-23.

A. R. Clarke , H. M. Wilks, D. A. Barstow, T. Atkinson, W. N. Chia and J. J. Holbrook, (1988), Biochemistry, **27**, 1617-1622.

R. Cleeland, J. Christeinson, M. U-Gomez, J. Heveran, R. Davis and E. Grunberg, (1976), Clin. Chem., **22**, 712-725.

M. L. Connolly, J. of Appl. Crystal., (1983), **16**, 548-558.

J. B. Courtright and U. Henning, (1970), J. Bacteriol., **102**, 722-728.

T. E. Creighton, (1980), J. Mol. Biol., **144**, 521-550.

T. E. Creighton, (1983), in "Proteins: Structure and Molecular Properties", W. H. Freeman and company, NewYork.

S. Daopin, T. Alber, W. A. Baase, J. A. Wozniak and B. W. Matthews, (1991), J. Mol. Biol, **221**, 647-667.

A. Datta, J. M. Merz and H. O. Spivey, (1985), J. Biol. Chem., **260**, 15008-15012.

D. D. Davies, A. Teixera and P. Kenworthey, (1972), Biochem. J., **127**, 335-343.

D. R. Davies and E. A. Padlan, (1990), Ann. Rev. Biochem., **59**, 439-473.

M. O. Dayhoff, W. C. Barker and L. T.Hunt, (1983), Methods in Enzymol., **91**, 524-545.

G. L. Ellman, (1959), Arch. Biochem. Biophys, **2**, 70-77.

R. T. Fernely, S. R. Lentz and R. A. Bradshaw, (1981), Bioscience Report, **1**, 497-507.

J. L. Gelpi, A. Dordal, J. Montserrat, A. Mazo and A. Cortes, (1992), Biochem. J. **283**, 289-297.

D. V. Goeddel, D. G. Kleid, F Bolivar, H. L. Heyneker, D. G. Yanusura, R. crea. T. Hirose, A. Kraszewski, K. Itakura and A. D. Riggs, (1979), PNAS., **76**, 106-110.

U. M. Grau, W. E. Trommer and M. G. Rossmann, (1981), J. Mol. Biol., **151**, 289-307.

C. T. Gray, J. W. T. Wimpenny and M. R. Mossman, (1966), Biochim. et Biophys. Acta, **117**, 33-41.

S. M. Green, A. K. Meeker and D. Shortle, (1992), Biochemistry, **31**, 5717-5728.

M. D. Hall, D. G. Levitt and L. J. Banaszak, (1992), J. Mol. Biol., **226**, 867-882.

W. G. J. Hol, (1985), Prog. Biophys. Molec. Biol., **45**, 149-195.

J. J. Holbrook, A. Lodola and N. P. Illsley, (1974), Biochem. J., **139**, 797-800.

E. Honika, S. Fabry, T. Niermann, P. Palm and R. Hensel, (1990), Eur. J. Biochem., **188**, 623-632.

S. Ihara and T. Takahashi, (1982), Biopolymers, **21**, 131-145.

S. Iijima, M. J. Oh, T. Saiki and T. Beppu, (1986), J. Biochem., **99**, 1667-1672.

W. Kabsch and C. Sander, (1983), Biopolymers, **22**, 2577-2637.

M. Karplus, (1987), in "Protein engineering", pp 35-44, Eds D. L. Oxender and C. F. Fox, A. R. Liss, Inc, New York.

H. Kawasaki, C. J. Carrera and D. A. Carson, (1992), Anal. Biochem., **207**, 193-196.

G. B. Kitto and N. O. Kaplan, (1966), Biochemistry, **5**, 3966-3980.

Y. Konishi, T. Ooi and H. A. Scheraga, (1981), Biochemistry, **20**, 3945-3955.

J. Kyte and R. F. Doolittle, (1982), J. Mol Biol., **157**, 105-132.

J. Lindel, H. E. Taylor, M. D. Feldman, E. B. Woodward, C. R. Ayers, M. L. Ripley, S. Iflah and A. Patel, (1992), Anal. Biochem., **201**, 246-254.

T. Maniatis, E. F. Fritsch and F. Sambrook, (1982), Molecular Cloning: A Laboratory Manual. Cold Spring Harbour Laboratory.

L. McAlister-Henn, M. Blaber, R. A. Bradshaw and S. J. Nisco, (1987), NAR., **15**, 4993.

L. Menendez-Arias and P. Argos, (1989), J. Mol. Biol., **206**, 397-406.

C. Mitchinson and J. A. Wells, (1989), Biochemistry, **28**, 4807-4815.

W. H. Murphey, C. Barnaby, F. J. Lin and N. O Kaplan, (1967), J. Biol. Chem., **242**, 1548-1559.

F. C. Neidhardt, J. L. Ingraham, K. B. Low, B. Magasanik, M. Schaechter and H. E. Umbarger, (1988), in "Escherichia coli and Salmonella Typhimurium, Cellular and Molecular Biology", Vols I and II, American Society for Micro Biology, Washington, D. C..

D. J. Nicholls, N. P. Minton, T. Atkinson and T. K. Sundaram, (1989), Appl. Microbiol. Biotechnol., **31**, 376-382.

D. J. Nicholls, T. K. Sundaram, T. Atkinson and N. D. Minton, (1990), FEMS. Microbiology letters, **70**, 7-14.

D. J. Nicholls, J. Miller, M. D. Scawen, A. R. Clarke, J. J. Holbrook, T. Atkinson and C. R. Goward, (1992), Biochem. and Biophys. Res. Comm., **189**, 1057-1062.

E. G. Norman and B. Colman, (1991), Arch. Microbiol., **156**, 28-33.

J. F. Novotny and J. J. Perry, (1990), Arch. Microbiol, **154**, 304-307.

B. E. Noyes, B. E. Glatthaar, J. S. Garavelli and R. A. Bradshaw, (1974), PNAS., **71**, 1334-1338.

W. D. Odell, J. Griffin and R. Zahradnik, (1986), Clin. Chem., **32**, 1873-1878.

A. R. Pakula, V. B. Young and R. T. Sauer, (1986), PNAS., **83**, 8829-8833.

C. Papadea, I. J. Check and C. B. Reimer, (1985), Clin. Chem., **31**, 1940-1945.

M. Persson, G. M. Bergstrand, L. Bülow and K. Mosbach, (1988), Anal. Biochem., **172**, 330-337.

M. Persson, L. Bülow and K. Mosbach, (1990), FEBS., **270**, 41-44.

M. D. Portis, D. G. Griffiths and G. C. Roberts, (1983), J. Pro. Chem. **2**, 263 to 277.

D. N. Raval and R. G. Wolfe, (1962), Biochemistry, **1**, 263-269.

J. F. Reidhaar-Olson and R. T. Sauer, (1988), Science, **241**, 53-57.

J. S. Richardson and D. C. Richardson, (1988), Science, **240**, 1648-1652.

J. B. Robinson, L. Inmam, B. Sumegi and P. A. Srere, (1987), J. Biol. Chem., **262**, 1786-1790.

S. L. Roderick and L. J. Banaszak, (1986), J. Biol. Chem., **261**, 9461-9464.

M. A. Roseman, (1988), J. Mol. Biol., **200**, 513-522.

M. G. Rossmann, A. Liljas, C.-I. Branden and L. J. Banaszak, (1975), The Enzymes, Ed P. D. Boyer, 3rd Edn.,Vol XI, pp 61-102, Academic press, New York.

G. L. Rowley, K. E. Rubenstein, J. Huisjen and E. F. Ullman, (1975), J. Biol. Chem., **250**, 3759-3766.

R. K. Saiki, D. H. Gelfand, S. Stoffel, S. J. Scharf, R. Higuchi, G. T. Horn, K. B. Mullis, H. A. Erlich, (1988), Science, **239**, 487-491.

J. S. Sandhu, (1992), Clin. Rev. Biotech., **12**, 427-462.

B. D. Sanwal, (1969), J. Biol. Chem., **244**, 1831-1837.

F. Sanger, S. Niklen, and A. R. Coulson, (1977), PNAS., **74**, 5463-5467.

K. R. Shoemaker, et al, (1985), PNAS., **82**, 2349-2353.

K. R. Shoemaker, P. S. Kim, E. J. York, J. M. Stewart and R. L. Baldwin, (1987), Nature, **326**, 563-567.

E. Silversteine and G. Sulebelele, (1969), Biochemistry, **8**, 2543-2550.

I. Smith, (1976), in "Chromatographic and Electrophoretic Techniques, Vol II, Zone Electrophoresis", pp 195-209, Heinemann, London.

K. Smith, T. K Sundaram, M. Kernick and A. E Wilkinson, (1982), Biochemica et Biophysica Acta, **708**, 17-25.

K. Smith and T. K. Sundaram, (1988), Biochemica et Biophysica Acta., **955**, 203-213.

W. E. Trommer and K. Glöggler, (1979), Biochemica et Biophysica Acta., **571**, 186-194.

B. K. Van Weemen and A. H. W. M Schuurs, (1971), FEBS., **15**, 232-236.

P. M. G. F. Van Wezenbeek, T. J. M. Hulsebos and J. G. G. Schoemakers, (1980), Gene, **11**, 129-148

R. F. Vogel, K. D. Entian and D. Mecke, (1987), Arch. Microbiol., **149**, 36-42.

A. Voller, A. Bartlett and D. E Bidwell, (1978), J. Clin. Pathol., **31**, 507-520.

A. D. B. Waldman, K. W. Hart, A. R. Clarke, D. B. Wigley, D. A. Barstow, T. Atkinson, W. N. Chia and J. J. Holbrook, (1988), Biochem. and Biophys. Res. Comm., **150**, 752-759.

L. E. Webb, E. J. Hill and L. J. Banaszak, (1973), Biochemistry, **12**, 5101-5109.

M. Weininger, J. J. Birktoft and L. J. Banaszak, (1977) in "Pyr. Nuc. Dep. Dehyd"., pp 87-100, Ed., H. Sund.

J. A. Wells and D. B. Powers, (1986), J. Biol. Chem., **261**, 6564-6570.

R. Wetzel, L. J. Perry, W. A. Baase and W. J. Becktel, (1988), PNAS., **85**, 401-405.

H. M. Wilks, K, M, Morton, D. J. Halsall, K. W. Hart, R. D. Sessions, A. R. Clarke and J. J. Holbrook, (1992), Biochemistry, **31**, 7802-7806.

E. L. Winnacker, (1987), in "From Genes to Clones: Introduction to Gene Technology", pp 451-477, V. C. H. Verlagsgesellschaft, Weinheim, Germany.

G. Winter and C. Milstein, (1991), Nature, **349**, 293-299.

I. P. Wright and T. K. Sundaram, (1979), Biochem. J., **177**, 441-445.

S. E. Zale and A. M. Klibanov, (1986), Biochemistry, **25**, 5432-5444.

A. Zhiri, H. A. Mayer, V. Michaux, M. Wellman-Bednawska and G. Siest, (1986), Clin. Chem, **32**, 2094-2097.

‡ Prepared by S. Searle of Bath University, Dept of Biochemistry, Claverton Down, Bath BA2 7AY.

ABBREVIATIONS.

Å	Angstrom
ATP	Adenosine 5'-triphosphate
BSA	Bovine serum albumin
bp	Base pairs
Ci	Curie
CoA	Coenzyme A
dATP	2'-Deoxyadenosine 5'-triphosphate
[α-^{32}P]dATP	[α-^{32}P] 2'-Deoxyadenosine 5'-triphosphate
[γ-^{32}P] ATP	[γ-^{32}P] 2'-Deoxyadenosine 5'-triphosphate
[α-^{35}S]dATP	[α-^{35}S] 2'-Deoxyadenosine 5'-triphosphate
ddATP	2' ,3' -Dideoxyadenosine 5'-triphosphate
dCTPαS	2'-Deoxycytidine 5'-(αthio) triphosphate
dCTP	2'-Deoxyctidine 5'-triphosphate
ddCTP	2' ,3' -Dideoxyctidine 5'-triphosphate
dGTP	2'-Deoxyguanosine 5'-triphosphate
ddGTP	2' ,3' -Dideoxyguanosine 5'-triphosphate
dNTP	2' -Deoxynucleotide 5'-triphosphate
ddNTP	2' ,3' -Dideoxynucleotide 5'-triphosphate
DSSP	Directory of secondary structure prediction
dTTP	2'-Deoxythymidene 5'-triphosphate
ddTTP	2' ,3' -Dideoxythymidene 5'-triphosphate
DTT	Dithiothreitol
DTNB	5, 5'-Dithio-bis-(2-nitrobenzoic acid)
3D	3-Dimensional
DNA	Deoxyribonucleic acid
E.coli	*Escherichia coli*
EcoR I	Restriction endonuclease from *E.coli*

EDTA	(Disodium) ethylenediaminetetraacetate
EIA	Enzyme inmmunoassay
EMIT	Enzyme multiplied immunoassay technique
Fsp I	Restriction endonuclease from *Fischeralla ssp*
g	Gravity
X-gal	5-bromo-4-chloro-3-indolyl-β-D-galactoside
Hind III	Restriction endonuclease from *Haemophilus influenza*
IPTG	Isopropyl-β-D-thiogalactoside
kb	1000 bases
kD	1000 Daltons
Km	Michaelis constant
Kpn I	Restriction endonuclease from *Klebsiella pneumonia*
LB	Luria Bertani (Broth)
LDH	Lactate dehydrogenase
LMP	Low melting point
M13	Filamentous bacteriophage (M13)
MDH	Malate dehydrogenase
MOPS	4-Morpholinepropanesulphonic acid
MSE	Measuring and scientific equipment
Nae I	Restriction endonuclease from *Nocardia aerocolonigenes*
NAD	Nicotinamide-adenine dinucleotide
NAD^+	Nicotinamide-adenine dinucleotide (oxidised form)
NADH	Nicotinamide-adenine dinucleotide (reduced form)
NBT	Nitro blue tetrazolium
Nci I	Restriction endonuclease from *Neisseria cinarea*
Nde I	Restriction endonuclease from *Neisseria denitrificans*
Nhe I	Restriction endonuclease from *Neisseria mucosa heidelbergensis*
OD	Optical density

PCR	Polymerase chain reaction
PAGE	Polyacrylamide-gel electrophoresis
PEG	Polyethylene glycol
pH	= -log [Proton]
pK	= log [dissociated acid/undissociated acid]
pMEX222C	Expression vector (pMEX) containing 222C MDH gene
PMS	Phenazine methosulphate
Pst I	Restriction endonuclease from *Providencia stuarti*
pUC19	Plasmid of pUC19
pUCWT	Plasmid of pUC19 containing wild type MDH gene
pUC64C	Plasmid of pUC19 containing 64C MDH gene
pUC113S	Plasmid of pUC19 containing 113S MDH gene
pUC109S/113S	Plasmid of pUC19 containing 109S/113S MDH gene
pUC109S/113S/81C	Plasmid of pUC19 containing 109S/113S/81C MDH gene
pUC109S/113S/84C	Plasmid of pUC19 containing 109S/113S/84C MDH gene
pUC109S/113S/90C	Plasmid of pUC19 containing 109S/113S/90C MDH gene
pUC109S/113S/251S	Plasmid of pUC19 containing 109S/113S/251S MDH gene
pUC251S	Plasmid of pUC19 containing 251S MDH gene
PVP	Polyvinylpyrollidone
RF	Replicative form
RIA	Radioimmunoassay
RMS	Root mean square
RNA	Ribonucleic acid
RNAse	Ribonuclease A
Sal I	Restriction endonuclease from *Streptomyces albus* G
SDS	Sodium dodecyl sulphate
Sph I	Restriction endonuclease from *Streptomyces phaeochromogenes*
SSC	0.15 M sodium chloride and 15 mM sodium citrate

TBE	Tris base-boric acid-EDTA
TCA	Tricarboxylic acid cycle
TE	Tris-EDTA
TEA	Triethylamine
TEMED	N ,N ,N',N' tetramethylethylene diamine
TG1	*E.coli* strain TG1: genotype K12 Δ(*lac, pro) sup*E, *thi, hsd*D5/F'*tra*D36, *pro*AB^{+}, *lac*I^{q} *lac*ZΔM15
TNB	Thionitrobenzoate
Tris-HCl	2-Amino-2-hydroxymethylpropane-1,3-diol. hydrochloric acid
UV	Ultraviolet
v/v	Volume/volume
Vis	Visible
w/v	Weight/volume
W945T1-2	*E.coli* strain W945T1-2: genotype (*thi thr leu lac gal trp mtl str*^{R}, F^{-})

Restriction endonuclease	Recognition site
EcoR I:	5'GAATTC3' 3'CTTAAG5'
Fsp I:	5'TGCGCA3' 3'ACGCGT5'
Hind III:	5'AAGCTT3' 3'TTCGAA5'
Kpn I:	5'GGTACC3' 3'CCATGG5'
Nae I:	5'GCCGGC3' 3'CGGCCG5'
Nde I:	5'CATATG3' 3'GTATAC5'
Nhe I:	5'GCTAGC3' 3'CGATCG5'
Sal I:	5'GTCGAC3' 3'CAGCTG5'
Sph I:	5'GCATGC3' 3'CGTACG5'

Appendix A : Restriction endonucleases with restriction endonuclease recognition sites.Positions of "nick" sites on 5' and 3' DNA are indicated by ▼ and ▲.

Appendix B: Restriction map of pUC19 and location of restriction endonuclease sites.

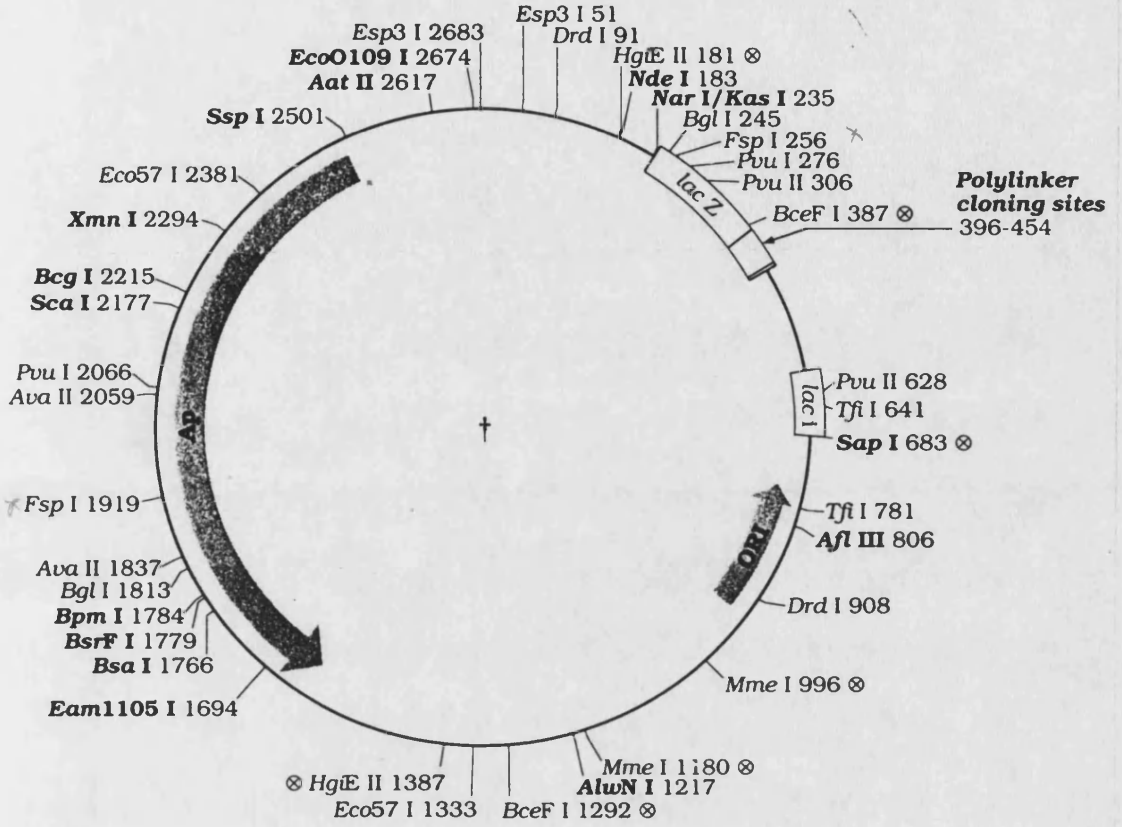

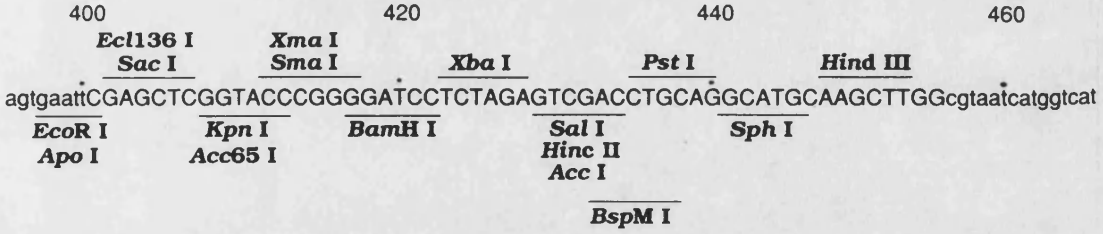

Appendix C: Sense and anti-sense codon table.

Amino acid		Sense codon	Anti-sense codon	Amino acid		Sense codon	Anti-sense codon	Amino acid		Sense codon	Anti-sense codon	Amino acid		Sense codon	Anti-sense codon
Phe	F	UUU	AAA		S	UCU	AGA	Tyr	Y	UAU	AUA	Cys	C	UGU	ACA
	F	UUC	GAA		S	UCC	GGA		Y	UAC	GUA		C	UGC	GCA
Leu	L	UUA	UAA		S	UCA	UGA	Ter	*	UAA	UUA	Ter	*	UGA	UCA
	L	UUG	CAA		S	UCG	CGA		*	UAG	CUA	Trp	W	UGG	CCA
	L	CUU	AAG	Pro	P	CCU	AGG	His	H	CAU	AUG	Arg	R	CGU	ACG
	L	CUC	GAG		P	CCC	GGG		H	CAC	GUG		R	CGC	GCG
	L	CUA	UAG		P	CCA	UGG	Gln	Q	CAA	UUG		R	CGA	UCG
	L	CUG	CAG		P	CCG	CGG		Q	CAG	CUG		R	CGG	CCG
Ile	I	AUU	AAU	Thr	T	ACU	AGU	Asn	N	AAU	AUU	Ser	S	AGU	ACU
	I	AUC	GAU		T	ACC	GGU		N	AAC	GUU		S	AGC	GCU
	I	AUA	UAU		T	ACA	UGU	Lys	K	AAA	UUU	Arg	R	AGA	UCU
Met	M	AUG	CAU		T	ACG	CGU		K	AAG	CUU		R	AGG	CCU
Val	V	GUU	AAC	Ala	A	GCU	AGC	Asp	D	GAU	AUC	Gly	G	GGU	ACC
	V	GUC	GAC		A	GCC	GGC		D	GAC	GUC		G	GGC	GCC
	V	GUA	UAC		A	GCA	UGC	Glu	E	GAA	UUC		G	GGA	UGG
	V	GUG	CAC		A	GCG	CGC		E	GAG	CUC		G	GGG	CCC

Appendix D: Table of oligonucleotides.

Number	Number of nucleotides	Sense/anti-sense	Function	Oligonucleotide
1	26	sense	Introduce *Nhe* I restriction site and substitute cysteine 113 for serine.	G T (326) 5'GC CCG AAA **GCT AGC** ATT GGT AAT ATC3' (351) Cys (AA107) Thr Cys Pro Lys Ala **Ser** Ile Gly Asn Ile Thr Asn (AA119)
2	17	sense	Sequencing oligonucleotide	(243) 5'AAA CCG GGT ATG GAT CGT3' (261)
3	36	sense	Remove polylinker *Hind* III restriction site.	*Hinc* II *Acc* I *BamH* I *Sal* I *Sph* I GC (-314) 5'GATC CTCTAGAGTC GACCTGCAGG CATGCAAATT TC3' (-279) *Xba* I *Pst* I *Hind* III
4	29	anti-sense	Introduce *Nhe* I restriction site and substitute cysteines 109 and 113 for serines.	A C A (347) 5'TT ACC AAT **GCT AGC** TTT CGG **GCT** GGT TTT3' (319) Cys Cys (AA118) Thr Ile Asn Gly Ile **Ser** Ala Lys Pro **Ser** Thr Lys Ala Val (AA105)
5	17	sense	Sequencing oligonucleotide.	(-372) 5'GTTTTCCCAGTCACGAC3' (-356)
6	21	anti-sense	Introduce *Nde* I restriction site and substitute cysteine 251 for serine.	G G C (767) 5' CC TTC AAC **ATA TGC AGA** TTC G3' (747) Cys (AA258) Gly Asp Gly Glu Val Tyr Ala **Ser** Glu Val Val Gly (AA 247)
7	21	sense	Introduce *Nde* I restriction site.	C C (747) 5'C GAA TGT **GCA TAT** GTT GAA GG3' (767) (AA247) Gly Val Val Glu Cys Ala Tyr Val Glu Gly Asp Gly (AA258)
8	16	anti-sense	Sequencing oligonucleotide.	(1066) 5'AACAGCTATGACCATG3' (1051)

9	59	anti-sense	Introduce *Nae* I restriction site and substitute arginine 81 and or glycine 84 for cysteine(s).	(291) 5' GAT GCC GGC GTT AAC GTT AAA CAG GTC GGA (AA99) Lys Val Ile Gly Ala Asn Val Asn Phe leu Asp Ser C G ACG ATC CAT ACA CGG TTT ACA CCG TAC GC3' (233) Gly Arg Arg Asp Met Cys Pro Lys Cys Arg Val Gly Ala Ser (AA76)
10	32	anti-sense	Introduce *Nae* I restriction site and substitute leucine 90 for cysteine.	CAG (294) 5'CAC GAT GCC GGC GTT AAC GTT AAA GCA GTC GG3' (263) Leu (AA100) Asn lys Val Ile Gly Ala Asn Val Asn Phe Cys Asp Ser Arg Asp (AA86)
11	36	sense	Remove polylinker *Hind* III and *Sph* I restriction sites.	*Hinc* II *Acc* I *BamH* I *Sal* I *Sph* I GC (-314) 5'GATC CTCTAGAGTC GACCTGCAGG GATGCAAATT TC3' (-279) *Xba* I *Pst* I C *Hind* III
12	22	anti-sense	Introduce *Sph* I restriction site and substitute threonine 64 for cysteine.	AGT C (200) 5' AG CGC CGG GCA TGC ATC TTC AC3' (179) Thr (AA69) Gly Glu Leu Ala Pro Cys Ala Asp Glu Gly Ser Phe (AA58)
13	22	sense	Introduce *Sph* I restriction site and substitute threonine 64 for cysteine.	G ACT (179) 5' GT GAA GAT GCA TGC CCG GCG CT3' (200) Thr (AA58) Phe Ser gly glu Asp Ala Cys Pro Ala Leu Glu Gly (AA69)
14	20	anti-sense	Introduce *Fsp* I restriction site and substitute serine 222 for cysteine.	AG (675) 5' CAC GGT TGC GCA CCC GCC AC3' (656) Ser (AA227) Met Ser Leu Thr Ala Cys Gly Gly Gly Ala Lys (AA217)

15	19	sense	Introduce *Fsp* I restriction site and substitute serine 222 for cysteine.	CT (658) 5'GGC GGG **TGC GCA** ACC CTG T3' (676) Ser (AA218) Ala Gly Gly Gly **Cys** Thr Leu Ser Met Gly (AA228)
16	29	sense	Truncate MDH gene and introduce *EcoR* I restriction site.	AT AA T (-26) 5'GT TTA TCA **GAA TTC** AAA GGA TTT AGG ATG3' (3) (AA1)Met Lys Val (AA3)

Restriction endonuclease sites and substituted nucleotides are indicated in bold, while corresponding residues to codons are indicated in triple letter code.

Appendix E: Properties of Amino acids.

Amino acid	Accessible surface area ($Å^2$)	Side chain pK	Structure of amino acid
Ala (A)	115		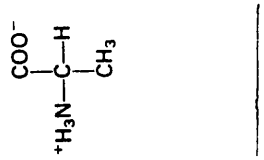
Arg (R)	225	12.5	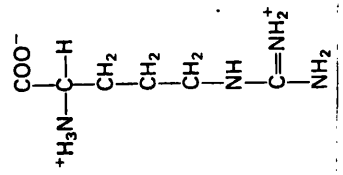
Asn (N)	160		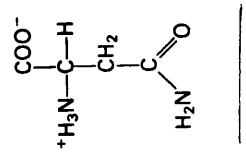
Asp (D)	150	3.9	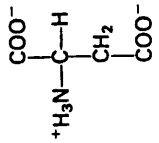
Cys (C)	135	8.3	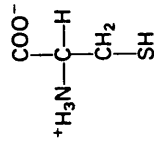
Gln (Q)	180		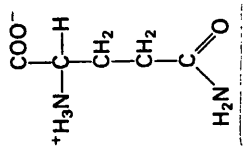
Glu (E)	190	4.3	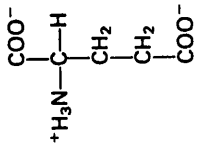

Gly (G)	75		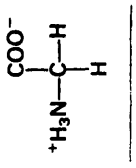
His (H)	195	6.0	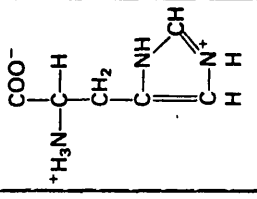
Ile (I)	175		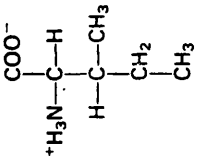
Leu (L)	170		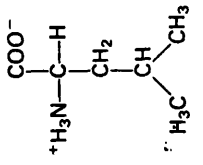
Lys (K)	200	10.8	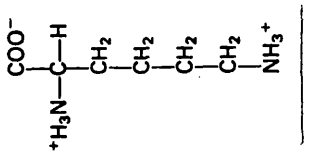
Met (M)	185		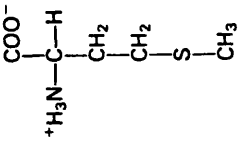
Phe (F)	210		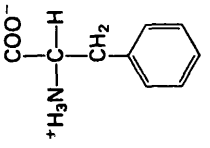
Pro (P)	145		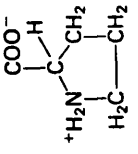
Ser (S)	115		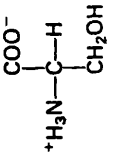

Thr (T)	140		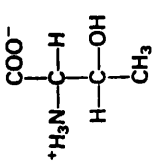
Trp (W)	255		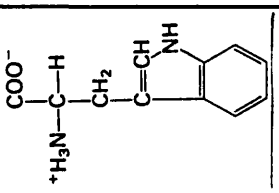
Tyr (Y)	230	10.9	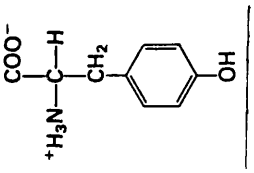
Val (V)	155		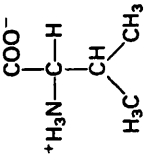

Appendix F: Ammonium sulphate addition table.

Initial concentration of ammonium sulphate, % saturation at 0°C	Final concentration of ammonium sulphate, % saturation at 0°C																
	20	25	30	35	40	45	50	55	60	65	70	75	80	85	90	95	100
	Grams of solid ammonium sulphate to add to 100 ml of solution																
0	10.6	13.4	16.4	19.4	22.6	25.8	29.1	32.6	36.1	39.8	43.6	47.6	51.6	55.9	60.3	65.0	69.7
5	7.9	10.8	13.7	16.6	19.7	22.9	26.2	29.6	33.1	36.8	40.5	44.4	48.4	52.6	57.0	61.5	66.2
10	5.3	8.1	10.9	13.9	16.9	20.0	23.3	26.6	30.1	33.7	37.4	41.2	45.2	49.3	53.6	58.1	62.7
15	2.6	5.4	8.2	11.1	14.1	17.2	20.4	23.7	27.1	30.6	34.3	38.1	42.0	46.0	50.3	54.7	59.2
20	0	2.7	5.5	8.3	11.3	14.3	17.5	20.7	24.1	27.6	31.2	34.9	38.7	42.7	46.9	51.2	55.7
25		0	2.7	5.6	8.4	11.5	14.6	17.9	21.1	24.5	28.0	31.7	35.5	39.5	43.6	47.8	52.2
30			0	2.8	5.6	8.6	11.7	14.8	18.1	21.4	24.9	28.5	32.3	36.2	40.2	44.5	48.8
35				0	2.8	5.7	8.7	11.8	15.1	18.4	21.8	25.4	29.1	32.9	36.9	41.0	45.3
40					0	2.9	5.8	8.9	12.0	15.3	18.7	22.2	25.8	29.6	33.5	37.6	41.8
45						0	2.9	5.9	9.0	12.3	15.6	19.0	22.6	36.3	30.2	34.2	38.3
50							0	3.0	6.0	9.2	12.5	15.9	19.4	23.0	26.8	30.8	34.8
55								0	3.0	6.1	9.3	12.7	16.1	19.7	23.5	27.3	31.3
60									0	3.1	6.2	9.5	12.9	16.4	20.1	23.9	27.9
65										0	3.1	6.3	9.7	13.2	16.8	20.5	24.4
70											0	3.2	6.5	9.9	13.4	17.1	20.9
75												0	3.2	6.6	10.1	13.7	17.4
80													0	3.3	6.7	10.3	13.9
85														0	3.4	6.8	10.5
90															0	3.4	7.0
95																0	3.5
100																	0